The Role of iRhoms and RAIDD in Innate Immunity

Inaugural dissertation

for the attainment of the title of doctor
in the Faculty of Mathematics and Natural Sciences
at the Heinrich Heine University Düsseldorf

presented by

SATHISH KUMAR MANEY
02-09-1984, Tirunelveli, India

From the institute of Molecular Medicine II,
Heinrich Heine University

Published by the permission from Mathematics and Natural Sciences Faculty at Heinrich Heine University (HHU), Düsseldorf.

I. Supervisor: Prof. Dr. med. Philipp Lang,
Director of Molecular Medicine II, HHU.

II. Supervisor: Prof. Dr. Thomas Klein,
Institute of Genetics, HHU.

Day of the Oral Examination: 26.04.2017

DECLARATION BY CANDIDATE

I **Sathish Kumar Maney**, hereby declare that this thesis is my own work and effort and that it has not been submitted anywhere for any award. Where other sources of information have been used, they have been acknowledged and indicated.

ABSTRACT

The innate immune response provides the first line of defense against an invading pathogen. Innate immune cells recognize conserved molecular determinants of common pathogens and initiate the production of innate immune effector molecules such as TNF or IFN-I to control the invading pathogen [12-14]. The TNF and IFN-I signal transduction is controlled by the recruitment of one or several adaptor molecules [1-10]. This thesis characterizes adaptor proteins namely iRhoms1, iRhom2 and RAIDD and these adaptor proteins are shown to regulate the signal transduction mediated by TNF and IFN-I, respectively.

TNF is a potent inflammatory cytokine, which controls infection as well as acting as a key mediator of septic shock under excessive production. TNF can trigger signaling response in cells expressing TNFR1 and/or TNFR2. TNF converting enzyme (TACE, also known as ADAM17) cleaves a variety of transmembrane proteins, including TNF and TNF receptors. Shedding of TNF receptors from cell surfaces can block responses to TNF. We have found that iRhom1 and 2 WT and iRhom1 and 2 lacking the N-terminal cytoplasmic domains interact with ADAM17. In turns, the deletion mutants of iRhom1 and 2 confer resistance to TNF induced cell death via constitutively shedding of cell surface TNF receptors.

IFN-1 is one potent anti-viral defense mechanism during the innate immune response. We found that the adaptor protein RAIDD is a critical component in Type I interferon production. RAIDD showed interaction with the IFN-I transcription factor, IRF7 and its potent phosphorylating kinase IKKε. RAIDD knockdown showed reduced IKKε and IRF7 mediated Type I Interferon activation. We have identified the adaptor molecule RAIDD to coordinate IKKε and IRF7 driven IFN-I expression. Overall, the functional regulations of adaptor proteins, iRhom1 & iRhom2 and RAIDD during innate immune response have been investigated.

TABLE OF CONTENT

TABLE OF FIGURES

TABLE OF SUPPLEMENTARY FIGURES

ABBREVIATION

ADAM10	ADAM metallopeptidase domain 10
ADAM17	ADAM metallopeptidase domain 17
IFN4a	Type I Interferon 4 alpha
IKKe	Inhibitor Of Kappa Light Polypeptide Gene Enhancer In B-Cells, Kinase epsilon
KitL2	Kit ligand 2
NFkB	Nuclear Factor Kappa light-chain-enhancer' of activated B-cells
TNFR1	Tumor necrosis factor receptor 1
5'PPP RNA	5' triphosphate double stranded RNA
7-AAD	7-aminoactinomycin D
AP1	Activator protein 1
APOBEC	Apolipoprotein B mRNA Editing Enzyme
APOBEC3	Apolipoprotein B mRNA Editing Enzyme 3
ATPase	ATP monophosphates
c-FLIP	FADD-like IL-1β-converting enzyme
CARD9	Caspase activation and recruitment domains 9
CARDIF	CARD Adapter Inducing Interferon Beta
cIAP1	caspase-Inhibitor of protein
CPR Screen	cyclical packaging rescue Screen
ELISA	enzyme-linked immunosorbent assay
ER	Endoplasmic Reticulum
ERK	Extracellular Signal-Regulated Kinase
FADD	Fas-Associated protein with Death Domain
FITC	Fluorescein isothiocyanate
FLIP	FADD-like IL-1β-converting enzyme
GAPDH	Glyceraldehyde 3-phosphate dehydrogenase
HIV	Human immunodeficiency virus
IFIT	Interferon Induced Protein With Tetratricopeptide Repeats
IFITM	Interferon Induced Transmembrane Protein
IFN	Interferon
IFN b	Type I Interferon Beta
IFN-I	Type I Interferon
IFNAR	Interferon alpha Receptor
IFNGR1& 2	Interferon gama Receptor 1 and 2
Ig	Immunoglobulin
IL-1	Interleukin 1
IPS1	IFN Promoter Stimulator 1
IRAK4	Interleukin 1 Receptor Associated Kinase 4
IRF10	Interferon Regulatory Factor 10
IRF3	Interferon Regulatory Factor 3
IRF7	Interferon Regulatory Factor 7
IRF9	Interferon Regulatory Factor 9
iRhom1	Inactive Rhomboid Protease 1
iRhom1-ΔN	Inactive Rhomboid Protease, lack cytoplasmic tail 1
iRhom2	Inactive Rhomboid Protease 2
iRhom2-ΔN	Inactive Rhomboid Protease, lack cytoplasmic tail 2
iRHOMs	Inactive Rhomboid Protease 1 and 2
ISGF3	Interferon-stimulated gene factor 3
ISRE	Interferon-sensitive response element

JAK1	Janus Kinase 1
JNK	C-Jun N-Terminal Kinase
kDa	Kilo Dalton
LPS	Lipopolysaccharide
MAP kinase	Mitogen-Activated Protein Kinase
MAP3K7	Mitogen-Activated Protein Kinase Kinas Kinase 7
MAP3K7	Mitogen-Activated Protein Kinase Kinas Kinase 8
MAVs	Mitochondrial antiviral-signaling protein
MDA5	Melanoma Differentiation-Associated protein 5)
MHC	Major Histo Compatability Complex
mTNF	Membrane TNF
MyD88	Myeloid differentiation primary response gene 88
NDV	New Castle Disease Virus
NFAT	Nuclear factor of activated T-cells
NK	Natural Killer cells
NLRS	Nucleotide-binding oligomerization domain Receptors
NOD	Nucleotide-binding oligomerization domain
OAS	2'-5'-Oligoadenylate Synthetase 1
PAMP	Pathogen-associated molecular patterns
PCR	Polymerase chain reaction
PKR	Protein kinase RNA
PMA	Para-Methoxyamphetamine
PRR	Pattern recognition receptors
RHBDF1	Rhomboid Family Member 1
RHBDF2	Rhomboid Family Member 2
RICK	RIP-Like-Interacting CLARP Kinase
RIG1	retinoic acid-inducible gene 1
RIPK1	Receptor-interacting serine/threonine-protein kinase 1
RIPK3	Receptor-interacting serine/threonine-protein kinase 3
RLR	RIG-I-Like Receptor 1
RNA	Ribonucleic acid
STAT1	Signal Transducer And Activator Of Transcription 1
STAT2	Signal Transducer And Activator Of Transcription 2
TAB2	TGF-Beta Activated Kinase 2
TAB3	TGF-Beta Activated Kinase 3
TACE	TNF Alpha Converting Enzyme
TAK1	TGF-Beta Activated Kinase 1
TBK1	TANK-Binding Kinase 1
TCR	T cell Receptor
TGFb	Transforming Growth Factor Beta
TLR3	Toll Like Receptor 3
TLR4	Toll Like Receptor 4
TNF	Tumor Necrosis Factor
TNFR1	TNF Receptor 1
TNFR2	Tumor necrosis factor receptor 2
TOC	Tylosis cancer
TRADD	TNFRSF1A Associated Via Death Domain
TRAF3	TNF Receptor Associated Factor 3

TO APPA- AMMA- GURU & TAMIL

ACKNOWLEDGEMENT

First and foremost, I like to thank Prof. Dr. Philipp Lang for choosing and allowing me to explore the research on my own way and taught me this is the phenomenon of science. I extend my gratitude for being active and available guru (24x7), for being inspiration barcode, for supporting and protecting me. Philipp, without genetic manipulation, you brought me the big transformation on my views towards science and you edit me to see the science with deeper knowledge but with bigger application. With eternal gratitude, I will leave his lab by this year (2016) with lots of lovable memories and with career-leading tricks.

Next, I would like to thank Dr. David R Mcilwain for being the best bench mate and for showing me the principal of planning and effective way to execute the results. I always admire your sportiveness and scientific debates. You are one of the worthy person, who I meet and you always earn my trust and friendship.

Next, I extend my gratitude to all my lab mates and neighboring colleagues, for extending their support in experiments, discussion, queries, and technical tricks and for lending reagents and collecting supernant. Definitely for being motivating shoulders and off course for the making me to listen all the awesome music mix of Asian, Russian, German and Electronic music's. And very special thanks to Dr. Haifeng C. Xu (Chris), the first person who I meet in Germany. Chris thanks a lot for your all support and showing me various techniques. I always admire your multitasking skills, professional ethics and poker skills too. In the near future, I love to see you driving your own Porsche 911 and lot of success in science.

Then I extend my special gratitude to Dr. Melanie Grusdat, Eugen Becker and Vitaly I Pozdeev, we had lot of laughs, and fun parties gave me really good companion ship and being awesome friend. I extend my best thanks to Prashant, Bala, Jun, Aleks, Christian, Renan, Dr. Albert, Dr. Bode, Dr. Carsten, Dr. Hiscott, Dr. Dirk, Yuang, Dr. Karl Lang for your entire relaxed and helpful attitude. I extend my heartily gratitude to my friends, who always helped in my critical time and cheering up to be active researcher, Dr. Sankari, baba, Ayyappan, Dr. Suji, Vishal, Prashant, George, Bala, Robin, Piyush and many more. I wish every one of you to achieve the best, which you desire and you always earn by friendship forever.

Last, I would like to thank my, lovable family members, who are always very close to me and always ready to take the hardness and leave me with sweetness. The, Divya (wife), Saghanaa (daughter), Dr.Sasi (sister), Kumar (brother) and Dr.Samu, Subbulakshmi, Selvaraj, Vasanatha, Rakesh (In laws) and many more. On my views, thanks is not enough to show my gratitude to my parent, rather I wish to hold the hereditary code forever.

Chapter 1 - INTRODUCTION

Pathogens

The human body is a thriving ecosystem consisting of complex cellular networks that frequently encounter invading pathogens. The human body is made up of 10^{13} host cells and 10^{14} microbial species such as bacteria, fungi, and protozoans [11]. Generally, these regular microbial inhabitants remain beneficial in maintaining the host metabolic rhythms. However, these microorganisms may become harmful upon gaining access to other sterile compartments of the body. For example, the movement of gut microbes to the peritoneal cavity can lead to peritonitis or cause serious trouble in an immune compromised situation [12].

Pathogens, which are usually distinct from normal microbial flora, can potentially breach the anatomical defensive barrier and cause severe infection. Although pathogen genomes are comparatively simple and tiny to the human genome, they are evolutionarily dynamic [13]. They have evolved to procreate and exploit the host's nutrition, while evading or subverting the host's immune defense response for its biological establishment [14]. Pathogens fall into distinct species such as bacteria, viruses, fungi, protozoan, and parasites. However, the most common pathogens are viruses and bacteria [11]. The body has evolved a vital defense network responsible for the recognition and protection against invading pathogens. This is known as the immune system. The immune system is a vital defense network that recognizes molecular determinants of deadly pathogens (nucleic acid or membrane components), ultimately protecting the host against infection [15] (Figure 1).

Figures 1- Pathogen Types and its Sensors

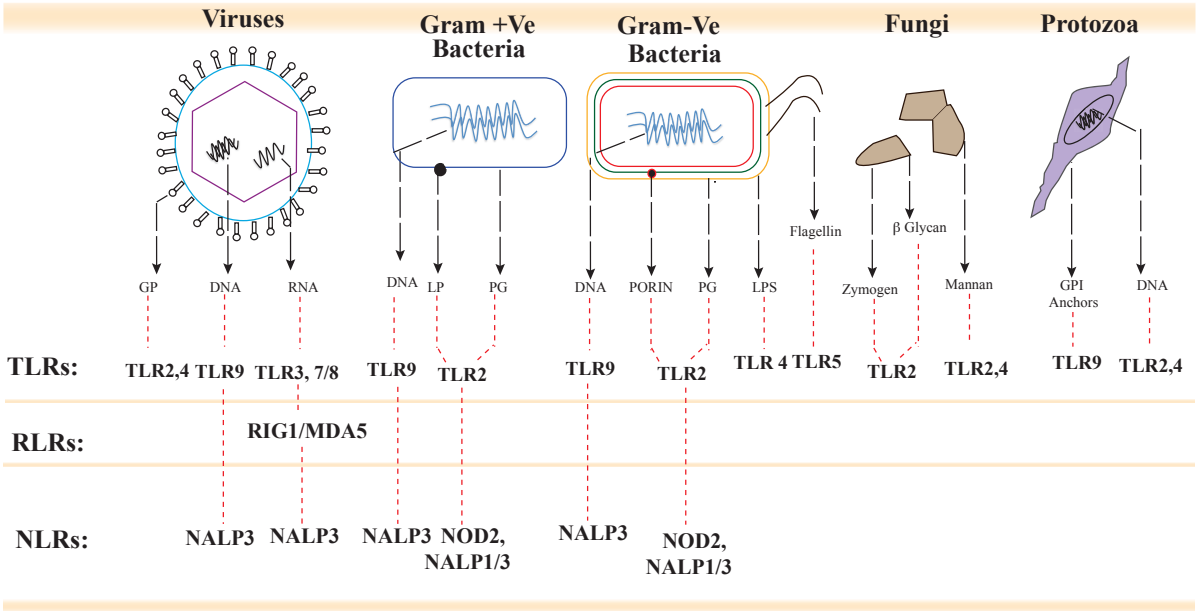

Figures 1- Pathogen Types and its Sensors

The invading microbes are recognized by their molecular structure. The immune system reads them as Pathogen Associated Molecular Patterns (PAMPs) sequence from different classes of microbial pathogen. Viruses, bacteria, fungi, and protozoa display several different PAMP sequences; few are shared between the pathogens. Major PAMPs are membrane components (peptidoglycans [PG], lipoteichoic acid [LTA], LPS, and GPI anchors) and surface glycoproteins (GP), lipoproteins (LP) as well as nucleic acids, including DNA, dsRNA, ssRNA, and 5 - triphosphate RNA. These PAMPs are recognized by different families of PRRs receptors such as TLRs, RLRs, NLR.

Adapted from Trine H. Mogensen, Clin Microbiol Rev. 2009 Apr; 22(2): 240–273.

A defective or compromised immune system can lead to the onset and pathogenesis of diseases resulting in increased morbidity and mortality [15-18].

The Immune System

In the steady state, the individual is often challenged by the dreadful pathogens but these infectious agents cause disease only occasionally. To protect itself from the challenging pathogens, the human body has developed the most skillful system called the immune system. The immune system occupies roughly 1% of our total blood cell population and is coordinated by lymphatic organs, the thymus, and bone marrow followed by lymph nodes and the spleen [11].

Briefly, in vertebrates, the level of specificity classifies the immune system into innate immunity and adaptive immunity. It is mainly composed of three major cellular components: granulocytes, monocytes, and lymphocytes [19]. The innate immune system is comprised of granulocytes and monocytes and the adaptive immune system is comprised of lymphocytes. Specifically, cellular components of innate immunity include phagocytic macrophages, the antigen presenting DCs, granulocytes, and cytotoxic NK cells. In turn, the adaptive immunity consists of T and B-lymphocytes [15]. The main difference between innate and adaptive immunity lies in the mechanism and the receptor used for the immune recognition. In adaptive immunity, the response has an extremely diverse repertoire of T and B cell receptors [20]. Together, these diverse repertoires of receptors increase the frequency of adaptive immunity to detect the possible invading antigen. These TCRs or BCRs are generated by random somatic mutation and lymphocytes bearing beneficial receptors that are clonally expanded and maintained throughout their lifetime. Even though the adaptive immune responses are long lasting, they are

delayed in their initiation [20, 21]. In addition, these are receptors that are not germline encoded; irrespective of how beneficial their role, they need to be reinvented by every generation. Therefore, adaptive immunity requires the innate immune system to ensure both the immediate and long-term protection against pathogenic invasion [15, 17, 18, 22].

In contrast to the adaptive immune response, innate immunity sensing is mediated by germline-encoded receptors. The strategy of the innate immune sensing is not to recognize every possible antigen, rather it is to recognize the few highly conserved structures that appear in the large family of microorganisms [17, 18]. These molecular structures are known to as pathogen-associated molecular patterns. In the case of bacteria the LPS, peptidoglycan or bacterial DNA molecular structures act as the PAMP sequence. These PAMP sequences are recognized by the family of receptors called Pathogen Recognition Receptors (PRRs) in which TLR4 recognizes the LPS [23, 24].

The engagement of PAMPs (e.g., LPS) to the PRR (e.g., TLR4) activates diverse signaling pathways. A family of adaptor proteins mediates the signaling cascade initially, which in part regulates the specificity of the response [1, 2]. The recruitment of one or several adaptors results in the activation of downstream signal transduction pathways through the sequential reaction of ubiquitination, phosphorylation, or protein – protein interaction. Ironically, it culminates in the activation of genes involved in the inflammation and antimicrobial host defense regulation [25]. The PRR mediated signaling are known to mediate the two major signaling pathways, NFκB and IRFs [17, 25, 26]. NFκB plays a vital role in induction of proinflammatory cytokines such as TNF [25, 26] and IRFs are

essentials for IFN-I production [17, 25, 27, 28]. The production of TNF and IFN-I is essential for the specific pathogen recognition and precisely modulating the effector function in innate and adaptive immunity. The defects in the production of these molecules or its regulatory function result in impaired innate and adaptive immune response [29-32].

The Immune Response

The immune response has an excellent ability to recognize the healthy and infected cells in the host environment. The immune response against invading pathogens can be summed up within three different phases—the first two steps occur under the tight supervision of innate immunity, which does not rely on the clonal expansion of antigenic specific lymphocytes. The third phase usually appears in the later stage of infection and is controlled by an adaptive immune response, which relies on the clonal expansion of antigenic specific lymphocytes [11] (Figure 2). All the three phases of immune response are evolved to distinguish the beneficial microsymbionts from the pathogens.

Phase I & II - The Innate Immune Response

During innate immunity, the primary response relies on soluble molecules and secreted proteins to defend against the pathogens. The soluble molecules present in blood, extracellular fluid, and epithelial secretions can either destroy or weaken the invading pathogens [11]. These classes of molecules include antimicrobial enzymes such as lysozyme, antimicrobial peptides, and complement system, etc. The lysozymes selectively cleave to the linkage between the sugar molecules exposed in the bacterial cell wall of gram- positive bacteria [33-37]. Antimicrobial peptides such as defensins

Figures 2- Overview of Immune System

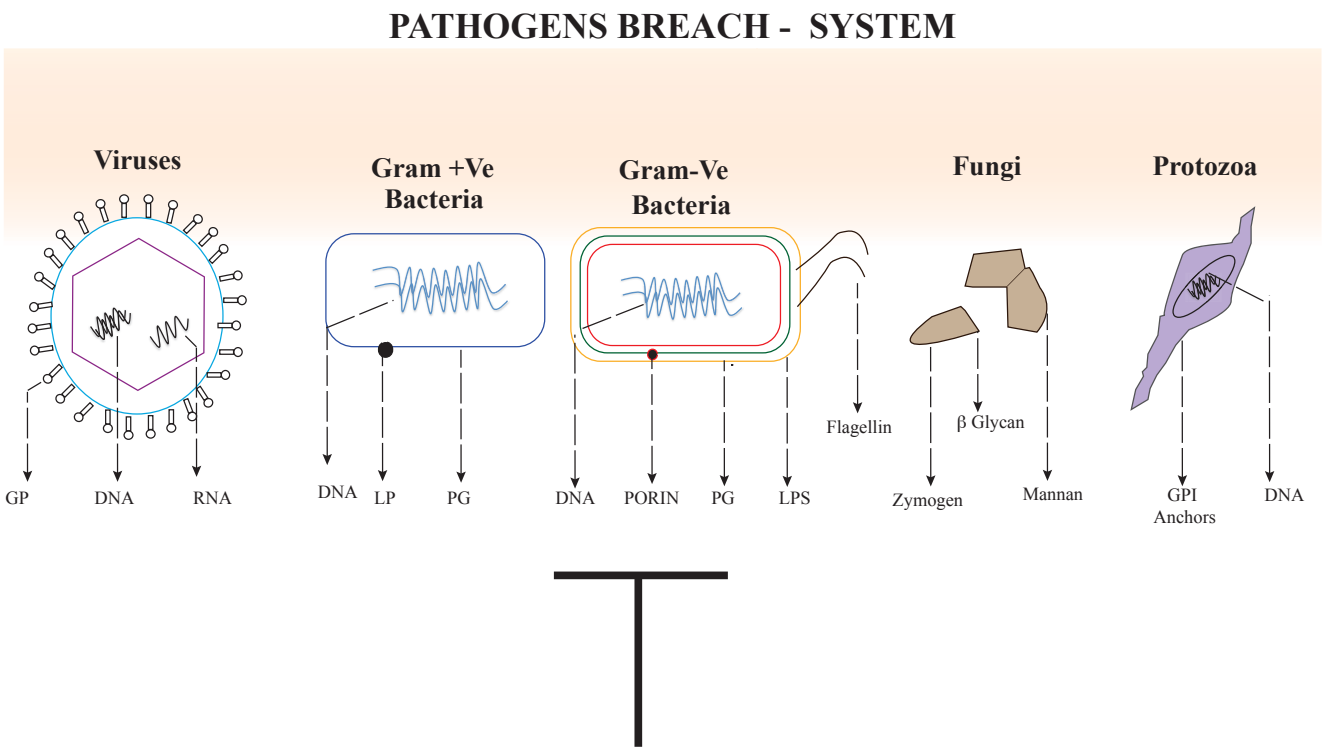

Figures 2 - Overview of Immune System

Principles in innate and adaptive immune response. The microbes are recognized through the conversed molecular patterns such as nucleic acid or cell membrane components. This event triggers the immune response for the invading microbes and can be summed up within three different phases - The first two peroids are govenred by the tight supervision of innate immune components. The third phase usually appears in the later stages of infection and is controlled by an adaptive immune response.

Adapted from Trine H. Mogensen, Clin Microbiol Rev. 2009 Apr; 22(2): 240–273.

respond in minutes via insertion and formation of pores in the membrane bilayer of bacteria, fungi, and some viral infections [38-42]. The complement system is a primary innate defense mechanism comprised of plasma proteins, which can be activated directly by pathogens or pathogen-bound antibody complexes. Complement activation [43] results in a sequential cascade of cleavage reactions on plasma proteins. The cleaved products are covalently linked to the pathogen surface, contributing to the activation of membrane attacking pore complexes on pathogens and enhancing the phagocytosis [43-45]. Antigen-presenting cells recognize the pathogens that have been flagged by the complement destruction signal and initiate more specific innate immune responses.

Sequentially in Phase II, the innate immune cells recognize the pathogens specifically for their PAMP sequence expressed in microbes and not shared by host cells [23, 46-51]. The innate encoded germline receptors have an inherent capacity to discriminate infectious non-self ligands from the host called as PRRs [15] (Illustration #3). The PAMP binding to PRRs triggers an intracellular signaling cascade, which includes adaptor molecules, kinases, and transcription factors [1, 25]. Overall, PRR signaling orchestrates the early host response to control the infection by releasing pro-inflammatory cytokines (TNF) and IFN-I at the site of infection [13, 17, 31, 52, 53]. Meanwhile, innate immune responses act together to remove the infection and promote adaptive immunity [23, 24, 30, 50, 52, 54, 55].

Phase III - Adaptive immune Response B and T cells

In the third step, the adaptive immune response utilizes lymphocytes, B and T cells, to effectively remove a wide variety of pathogens. B cells are critical mediators of humoral immunity. They express immunoglobulins (Ig) that have the potential to

distinguish between the host and antigenic peptides. The membrane-bound forms of Ig are known as the B-cell receptors (BCR) that serve as the cell receptor for antigens [56-65]. Terminally differentiated B cells, known as plasma cells, produce secreted immunoglobins, which bind to pathogens or toxic products in the extracellular spaces of the body.

In the case of T cells, solely membrane-bound proteins known as MHC molecules make antigenic recognition of T-cells. They are transmembrane glycoproteins encoded in the large clusters of genes known as major histocompatibility complexes (MHC), which are polymorphic expressed within the population. T cell receptors can recognize MHC molecules bound with antigenic peptide. In the case of intracellular pathogens, the B cells and T cells can recognize the antigenic peptide expressed on the infected cell surface [61, 64, 66-75]. Adaptive immunity has evolved to recognize large repertories using TCR and BCR to recognize the diversity of antigens from bacteria, viruses, and other disease-causing agents [20, 21]. The site-specific somatic recombination generates the antigenic specific receptor on T and B lymphocytes [76]. These pathogenic-specific lymphocytes are clonally selected and maintained throughout life to encounter the pathogen. Overall, the processes of the immune system are tightly regulated to achieve a balanced state in the elimination or neutralization of pathogens (Figure 2).

Specifically, the effector cytokines such as TNF [79-83] and interferon [29, 30, 52, 84-86], produced during the innate immune response, play vital roles in promoting the adaptive immune response and in the eradication of invading pathogens [87-89]. The current understanding of the immune response helps in eradicating many

dreadful diseases such as measles and smallpox or remedies against highly infectious diseases such as hepatitis C and the Ebola infection [90-96]. However, a deeper understanding of the intricate mechanisms governing the innate immune response will undoubtedly facilitate the identification of novel therapeutic targets for the prevention of a variety of dreadful diseases. In order to fully understand the innate immune response, it is imperative to gain an insight into innate immune cell pathogen recognition, signaling pathways involved in the production of effector molecules.

Pathogen Recognition Receptors.

Antigen presenting cells (APCs) including dendritic cells (DCs), macrophage and granulocytes recognize and control microbial infection. The granulocytes and macrophages play a prominent role in phagocytosis of pathogens, while dendritic cells (DCs) play a vital role in presentation of processed antigens to cells of the adaptive immune system. They are responsible for the initiation and modulation of the primary adaptive immune response [15, 20, 30, 97]. DCs are equipped abundantly with non-clonal but germline-encoded pattern recognition receptors (PRRs), which recognize molecular patterns expressed by various infectious organisms [16, 98-101]. Further, PRRs are classified as the nucleotide binding and oligomerization domain (NOD)—like receptors (NLRS), the retinoic acid-inducible gene I (RIG)-like receptors (RLRs) and TLRs [15, 54, 55, 77, 98, 99] (Illustration #1&2).

NOD Like Receptor

NLRs compose one of a large family of intracellular PRRs, all bearing a conserved NOD domain. NLRs include NOD1 and NOD2, and they recognize the synthesis or degradation of peptidoglycans [102-107]. Mechanistically, ligand engagement on leucine-rich-repeat (LRR) motifs of NODs leads to the recruitment of RICK and CARD9 adaptors. This is followed by TAK1-mediated activation of the IKK complex, which results mainly in NFκB, MAP kinase, ERK, and JNK pathway activation. Overall activation of NOD receptors culminates in the production of pro-inflammatory cytokines such as TNF [108-112].

RLRs—Retinoid acid—inducible gene I-like (RIG-I) receptors

RLRs are cytosolic PRRs that are activated by intracellular cytosolic pathogens via recognition of 5'PPP RNA and dsRNA [113-116]. RLRs include RIG-I and the Melanoma differentiation-associated gene 5 (MDA5). RLRs are composed of two N-terminal caspase recruitment domains (CARDs), a central DExD/box helicase/ATPase domain, and a C-terminal regulatory domain (RD), the latter of which confers ligand specificity [114, 116-118] (Figure 3). conformational change of the CARD domain and enhances the polyubiquitin modification mediated by TRIM25 and Riplet [123, 124]. This results in the formation of an oligomeric complex. It consists of four RIG1 with four ubiquitin chains, [125, 126] and in the case of MDA5, it forms the polar filamentous oligomers around a long dsRNA [127, 128]. The formation of an oligomeric complex results in the aggregation of MAVs/IPS1/CARDIF in the mitochondrial membrane and it eventually enhances the molecular interaction with oligomers of RIG 1 and/or MDA5 [5, 113, 118, 129-131]. RLRS and MAVs/IPS1/CARDIF association culminates in the massive production of IFN-I through the activation of IRF3 and IRF7 [22].

Figures 3- RLR Signaling Cascade

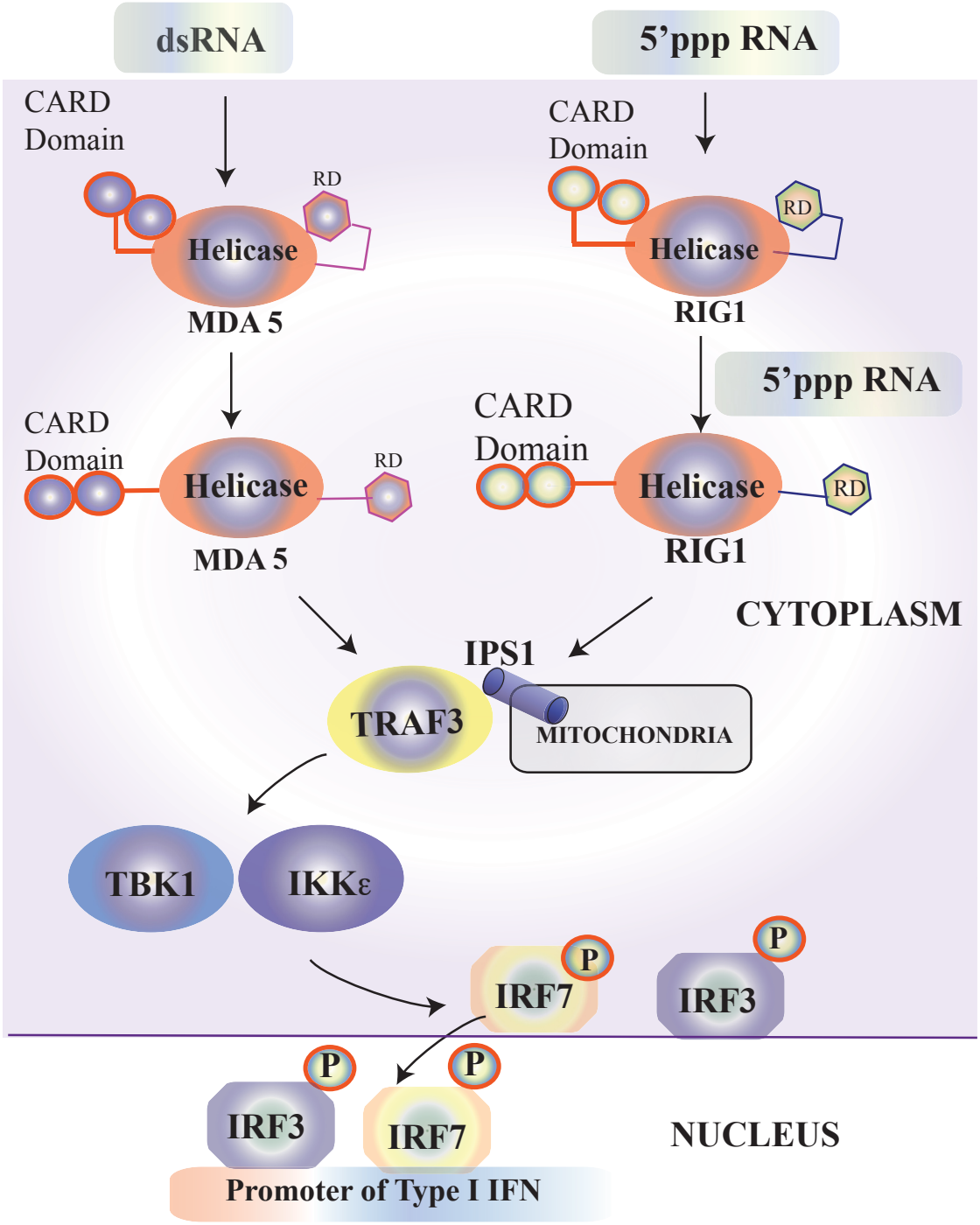

Figures 3 - RLR Signaling Cascade

Binding to dsRNA or 5ppp-RNA ligand binding to RIG-I or MDA5 induce the oligomerization. Oligomerized CARD domains of RIG-I and MDA5 interact with the functional domain of IPS1. This interaction promotes the polymerization of IPS1 CARD and leads to the activation of TBK1 and IKKε via TRAF3. In turn, it activate interferon transcription factor IRF3&7 and culiminates in production of the type I interferon. (Abbreviations: CARD -caspase activation and recruitment domain, RD- recruitment domain, dsRNA- double-stranded RNA, MDA5, melanoma differentiation associated gene 5, RLR, RIG-I-like receptor; TM, transmembrane domain.)

Adapterd from Wu J and Chen ZJ, Annu Rev Immunol. 2014;32:461-88

Toll – Like Receptors

The TLRs are type I transmembrane proteins and 13 TLR receptors have been reported. TLRs 1-9 are conserved between human and mouse. Murine TLR 10 is not functional due to a retrovirus insertion. TLRs 12 and 13 are absent from the human genome [30, 99, 101, 132]. The localization of TLRs is necessary for the ligand accessibility and tolerance to host molecules such as nucleic acids [15, 23, 77, 97-99, 101, 133].

According to their cellular localization and respective PAMP ligands, TLRs are classified into two groups, Plasma membrane-bound and intracellular TLRs. The cell surfaces of TLRs include TLR1, 2,4,5,6 and 11 that recognize microbial components such as proteins, lipids, and lipoproteins. The intracellular TLRs 3,7,8 and 9 are expressed exclusively in intracellular vesicles such as the endosomes, lysosomes, and endolysosomes [17, 134-136] (Figure 4).

The engagement of TLRs by their cognate PAMPs results in the activation of MyD88-dependent pathways or TRIF-dependent pathways. Myd88 recruits the IL-1 receptor-associated kinases IRAK4 and TRAF6 [8-10] whereas TRIF recruits TRAF3 [137-139]. Downstream signaling results in the activation of NF-κB and IRF3/7 transcription factors. The NF-κB activation [140] results in the production of inflammatory cytokines such as TNF [46]. TBK1 and/or IKKε-driven IRF3/7 activation [141, 142] leads to the production of IFN-I [132, 137-140, 143] (Figure 5).

Figures 4- Cellular Localisation of TLRs

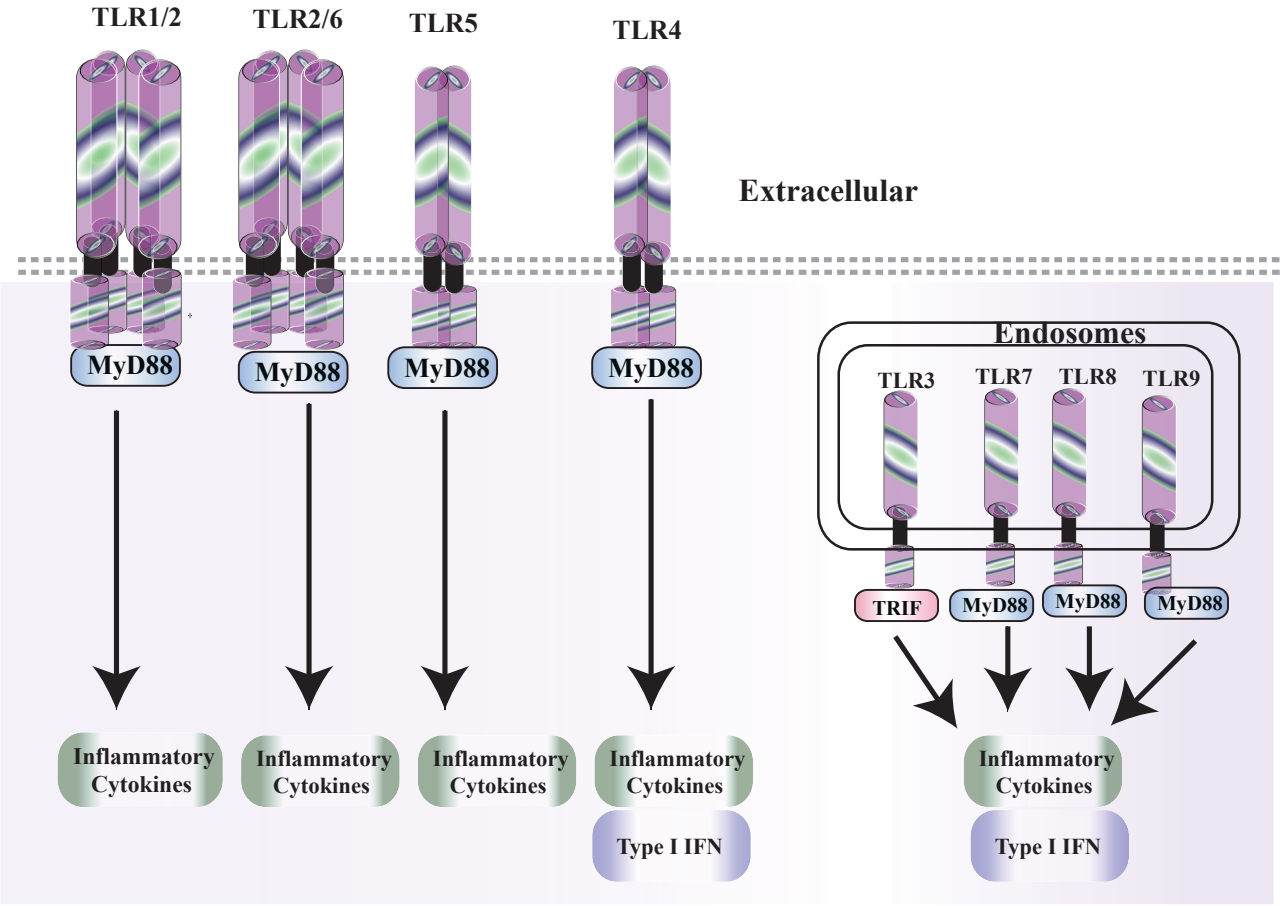

Figures 4 - Cellular Localisation of TLRs

The TLR are expressed in the different cellular localisation. TLR1/2, TLR4, TLR5 are localised in cell Membrane and activate MyD88 depdentent signaling. Whereas TLR3 is dependent on TRIF and TLR, -7, -8, and -9 have MyD88 for signaling and all localised in endosomal vesicles. Both MyD88- dependent and TRIF-dependent signaling culiminates in activation of both inflammatory and type I IFN response.

Adapted from Trine H. Mogensen, Clin Microbiol Rev. 2009 Apr; 22(2): 240–273.

Figures 5-TLR Signaling Cascade

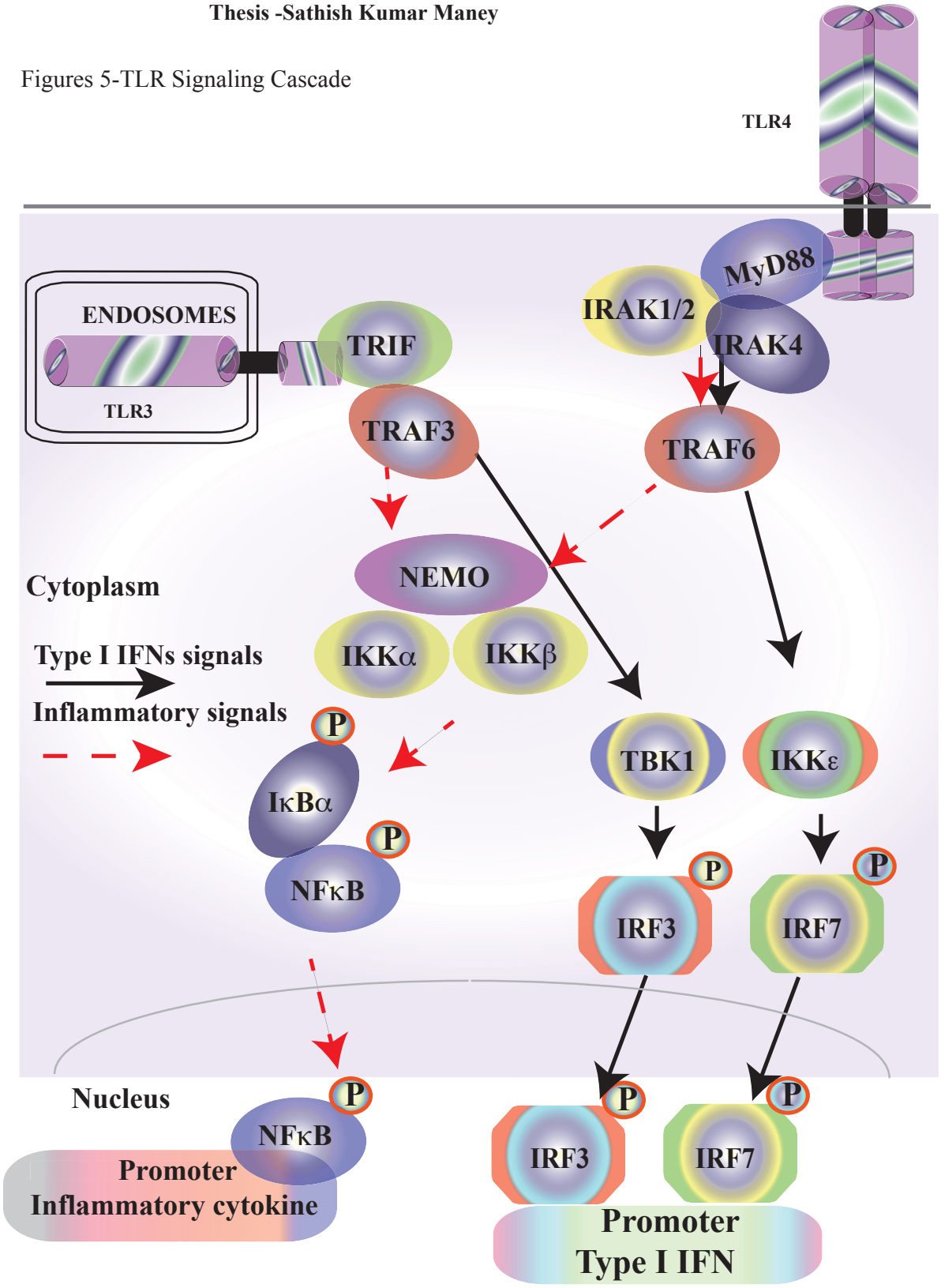

Figures 5 - TLR Signaling Cascade

TLR3 ligand dsRNA and TLR4 ligand LPS induces signaling casdade which mediate interaction with the adaptor molecule MyD88, IRAKS, TRAF6 activate NFκB and IRF3/7 through phophorylation via IKK and TBK/IKKε respectively. Overall activation resutls in the production of inflammatory cytokines such as TNF and Type I interferon.

Tumor Necrosis Factor (TNF) –Central Player of Immunity

TNF is mainly produced by activated monocytes/macrophages, dendritic cells, NK, and T cells. In addition, a marginal expression of TNF is observed in various non-immune cells such as endothelial cells, fibroblast, microglia cells, and other cells in the nervous system [80-82, 144-147]. TNF was initially identified as an endotoxin-inducible molecule that induces necrosis of tumor cells. Later, extensive research on TNF revealed an important function of TNF in innate and adaptive immune responses [79, 148, 149]. In addition, TNF is known to regulate bacterial and viral infection, cancer, cardiovascular, pulmonary, neurologic, and metabolic disorders [79].

The TNF ligand binding to the TNFRs receptors results in the activation of NF-κB or cell death signaling. Almost every mammalian cell type expresses TNFR1. TNFR2 expression is observed in immune cells and endothelial cells [152]. But the intracellular domains of TNFR1 and 2 are strikingly different. The TNFR1 cytoplasmic death domain recruits, TRADD, whereas TNFR2 lacks this cytoplasmic death domain and shows association with TRAF1 and 2. However, the TNFR1 or 2 result in NF-κB activation [31, 79]. It is shown that TNF- TNFR2 –TRAF1 and 2 signaling enhances cell survival. The TNF-TNFR1–TRADD signaling complex results either in the activation of cells or leading to the cell death signaling cascades [148] (Figure 6). The ubiquitination level of RIPK1 consisder as a molecular switch between cell death and cell survival. The presence of K63 RIPK1 ubiquitination leads to pro-survival signaling, and the absence of RIPK1 ubiquitylation facilitates the activation of programmed cell death.

Figures 6- TNF Signaling Cascade

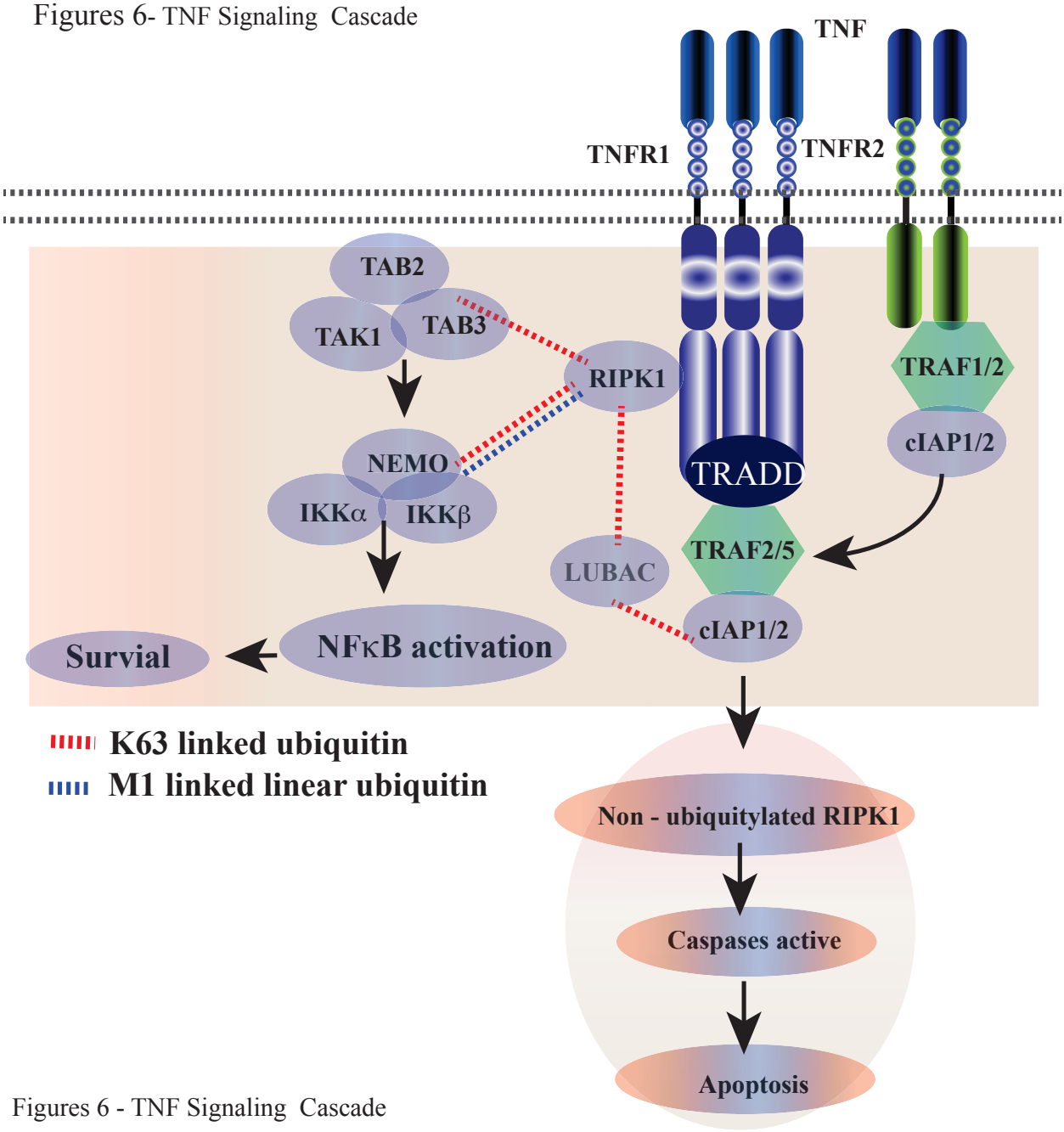

Figures 6 - TNF Signaling Cascade

TNF binding to TNF receptor 1 (TNFR1) recruit the TNFR1-associated death domain protein (TRADD), which associate with receptor-interacting serine/threonine-protein kinase 1 (RIPK1), TRAF5 or TNFR-associated factor 2 (TRAF2) and cellular inhibitor of apoptosis protein 1 (cIAP1) or cIAP2 to form TNFR1 signalling complex I. In case of TNFR2 - TNF binding recruit TRAF1 or TRAF2 cIAP1 or cIAP2. Both cIAP1 and 2 add K63-linked polyubiquitin chains to RIPK1. K63-polyubiquitylated RIPK1 recruits MAP3K7-binding protein 2 (TAB2), TAB3, TGFβ-activated kinase 1 (TAK1), which activate the IκB kinase (IKK) complex. The IKK complex then activates nuclear factor-κB (NF-κB) signalling, that promote cell survival. In contrast between the non and ubiquintylated RIPK1 results in activation of cell death.

Adapted from Dirk Brenner et al. Nat Rev Immunol. 2015 Jun;15(6):362-74

Furthermore, higher levels of RIPK1 ubiquitylation result in the recruitment of the cellular inhibitor of apoptosis (cIAP1) or cIAP2, which acts as an inhibitor for TNF-induced cell death. Both TNFR1 and 2 signaling complexes converge at the activation of TGFβ activated kinase 1 (TAK1) and MAP3K7, binding protein 2 (TAB2) and (TAB3). In turn, it can also activate the IκB kinase (IKK) complex. The activated IKK complex phosphorylates the NF-κB and activates the TNF induced pro-survival signaling cascade (Figure 7). In contrast, the non-ubiquitylated RIPK1 assembles with FADD, procaspase8, FLIP, and RIPK3 and eventually activates caspase 8-driven programmed cell death [258].

Shedding of TNF, TNFR1 and 2 from the cell surface.

In the steady state, TNF is expressed as a 26 KDa trimeric type II transmembrane protein. During inflammation or exposure to endotoxin (LPS), transmembrane TNF (mTNF) is liberated from the cell surface into a 17KDa soluble form, sTNF. sTNF is subsequently released into the blood stream and it confers a potent endocrine function through the TNFR1 or TNFR2. Metalloproteinase ADAM17 is known to cleave both TNF and its receptors from the cell surface. Thus, ADAM17 controls TNF-mediated cell fates ranging from cell proliferation, survival, and differentiation to apoptosis, which is crucial during the immune defense function against bacterial or viral infection [158]. ADAM17 belongs to the protein family of a disintegrin and metalloproteinase. Humans have 21 ADAM proteins, out of which 13 possess proteolytic activity while the rest are considered as inactive ADAMs. The latter are predicted to be involved in intracellular communication. One of the most prominent and well-studied ADAM enzymes is ADAM17 [158, 159].

ADAM17

Black *et, al* and Moss *et, al* reported in 1997 about ADAM17 or the tumor necrosis factor converting enzyme (TACE) sheddase action on membrane-bound TNF during inflammation [155, 157]. Later, ADAM17 was reported to have ectodomain shedding properties toward the epidermal growth factor ligands, TNF receptor 1 and 2, proinflammatory cytokines, cell adhesion molecules, and amyloid precursor proteins [159].

ADAM 17 is expressed in the spleen, lymph nodes, bone marrow, heart, brain, and kidneys [158, 159]. ADAM17 is a multidomain protein, which consists of 824 amino acids (aa). ADAM17 has various domains, short signaling sequence (1-17aa), and a prodomain (18-214aa), followed by a catalytic domain (215-473aa) with typical HEXXHXXGXXH (X could be any amino acid sequence), a disintegrin domain (474-572aa), a cysteine-rich domain (603-671aa), an EGF-like domain, and a transmembrane domain (672-694aa) and ends with the cytoplasmic tail (695-824aa) [160] (Figure 7). Furthermore, the golgi-localized protein Furin is reported to control the release of the ADAM17 prodomain and production of the ADAM17 active protease [161, 162, 166]. Moreover, an inactive rhomboid protein iRhom2 interacts with ADAM17 and this interaction was essential for ADAM17 trafficking towards the cell surface [153]

iRhoms

iRhoms belong to inactive rhomboid proteinases. There are two versions of iRhoms— iRhom1 and iRhom2, also called as RHBDF1 and RHBDF2, respectively [167]. iRhoms have two hallmark features: first, the loss of the catalytic site of rhomboids, because serine or histidine residues were replaced with a proline

Figures 7- ADAM17 Domins and its Fucntion

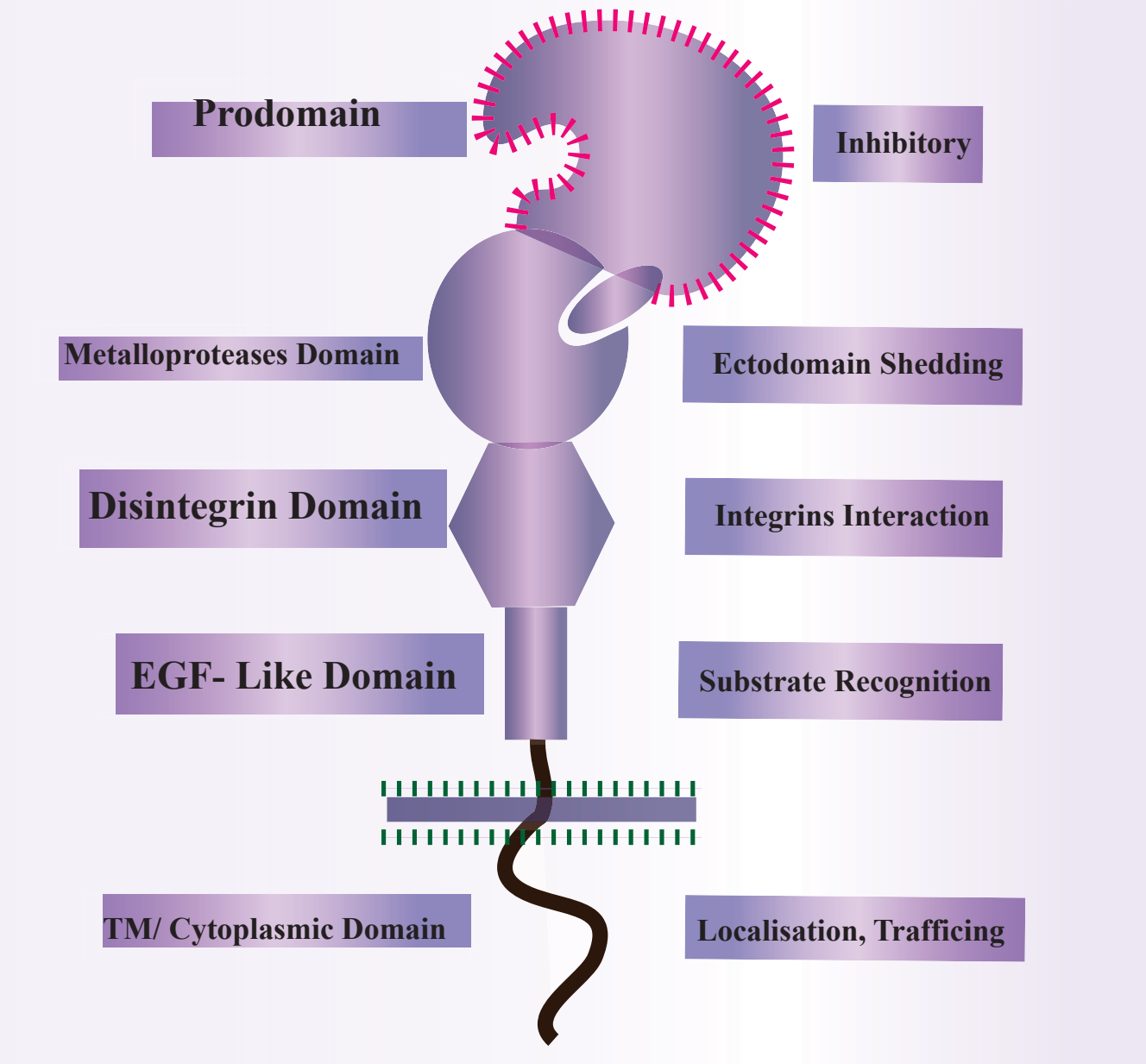

Figures 7- ADAM17 Domains and its Fucntion

The systematic representation of ADAM17/ TACE function domains and its regulation.

Adapted from Jürgen Scheller et al., Trends in Immunology, Volume 32, Issue 8, p380–387, August 2011

residue; and second, they have an extended cytoplasmic amino terminus with a highly conserved Cys-rich luminal loop and are considered as the iRhom homology domain [167-169].

However, the importance of the domain is not clear. A recent study has shown that mutation in the cytoplasmic tail of human iRhom2 could lead to tylosis syndrome, which is associated with esophageal cancer (TOC) [170]. In our experiment, iRhom2 retained its ability to interact with the type 1 transmembrane protein TACE/ADAM17 [153] and a similar finding were supported by other groups [83, 171-173]. iRhom 2 plays a vital role in trafficking TACE from the ER to the cell membrane. iRhom2 deficiency attenuated TACE-mediated TNF shedding, and it had significant effects on the innate immune response against bacterial infection [83, 153]. We have utilized the unbiased cyclic rescue screening methods to aid the detection of novel negative regulators of TNF signaling, resulting in the identification of iRhom1 and iRhom2 that lack the conserved cytoplasmic tails. These truncated versions of iRhom1 (IR1ΔC) and iRhom2 (iR2ΔC) showed promising target for the prevention of septic shock and inflammation. Mechanistically, we found that both full-length and ΔC forms of iRhoms interacted with ADAM17/TACE. (Figure 8)

Figures 8-Role of iRhom2 in TNF Signaling

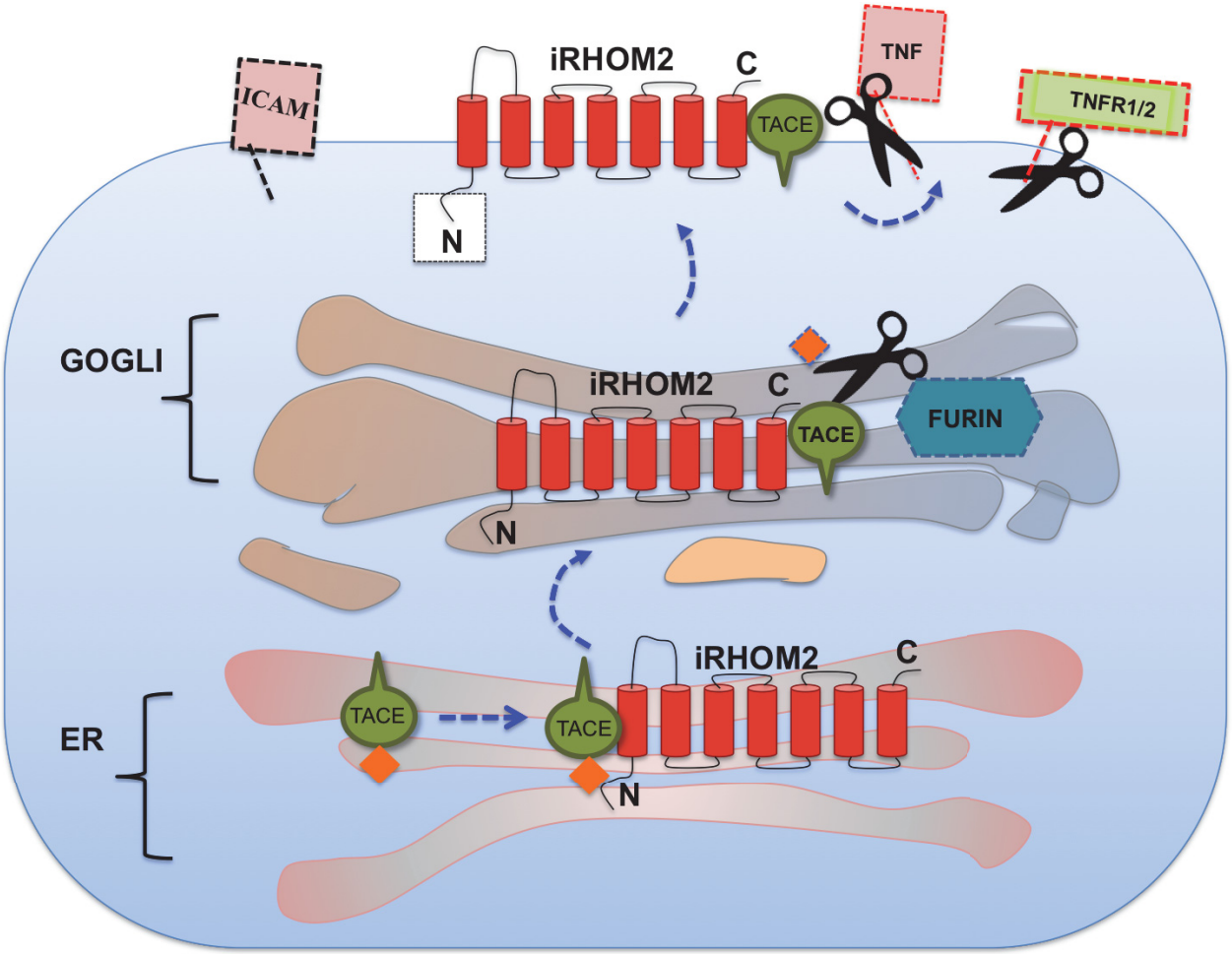

Figures 8- Role of iRhom2 in TNF Signaling

TNF is synthesized as a membrane- bound precursor and is liberated from the cell surface by the TNF converting enzyme (TACE, also known as ADAM17). ADAM17 traffic from ER, gogli apparatus to cell membrane to catalyzes the shedding of a variety of transmembrane proteins TNF, TNF receptors ICAM etc.

Type I Interferon Regulation

The virus-infected cells secrete polypeptides known as Type I Interferon (IFN-I). They execute the very essential functions in the innate immune response against the infection [85]. IFN-I also regulates the innate immune response to enhance the antigen presentation and activate natural killer cell cytotoxic functions. And IFN-I activates the adaptive immune system, thus promoting the development of high-affinity antigen-specific T and B cell responses and immunological memory. IFN-I is mainly known to be protecting against viral infection.

IFNs-I are produced after PRR recognition of microbial products [84, 176, 177] (Figure 6). IFN-I bind to the hetrodimeric transmembrane receptor termed the IFNα receptor (IFNAR), which is composed of IFNAR1 and IFNAR2 subunits [85, 174, 175]. Engagement of IFNs toward IFNAR activates the receptor-associated protein tyrosine kinase Janus kinase 1 (JAK1) and tyrosine kinase 2 (TYK2), which leads to phosphorylation of signal transducer and activator of transcription 1 (STAT1) and (STAT2) [178, 179].

Subsequently, STAT1 and STAT2 dimerize and translocate to the nucleus. As they dimer they interact with IRF9 to attain the trimolecular complex called IFN-stimulated gene factor 3 (ISGF3). The IFN-I signaling culminates in the activation of cell intrinsic factors such as myxovirus resistant 1 (MX1), IFN inducible double-stranded RNA-dependent protein kinase (PKR), 2'-5'-oligioadenylate synthetase (OAS), IFN-induced transmembrane proteins (IFITMs), apolipoprotein B mRNA-editing enzyme catalytic polypeptide (APOBEC), and interferon-induced proteins with tetratricopeptide repeats (IFIT) family proteins, etc. [29, 78].

MX1 resides in the nucleus in a mouse and cytosol in humans. In mouse models, studies have shown that MX1 blocks the replication of early influenza virus. In contrast, MX1 is known to prevent the late phase of influenza replication in human influenza [182-184]. OAS and PKR target the broad spectrum of the virus by modulating the protein translation [185-188]. Dengue and West Nile Viral infection are sentinels by IFITMs [189]. APOBECs, specifically APOBEC3, are reported to act against HIV infection [190]. IFITs have the ability to distinguish between the host and viral RNA through the the absence or lack of 2′-O-methylation in viral RNA [191-193]. However, most of the viral genome pave the mechanism to destabilize the IFNs and thereby illustrate the importance of this cytokine in the protection against viral infection [194-196].

In addition to IFN-I, innate immunity also comprises two additional interferon's such as IFN γ and IFN λ [197]. The IFN γ is genetically unrelated to IFN-I and functions through its receptors IFNGR1 and 2. IFNGR1 (90kDa) has primary ligand binding and IFNGR2 (60kDa) has minimal ligand binding [86, 197-200]. IFN λs signals through its own receptor, the IFN –λ receptor, and is also known as IL-28A and B and IL29 [201, 202]. Nevertheless, IFN-I production is activated immediately after the sensing of microbial nucleic acid by PRRs and most cells synthesize IFNβ. The hematopoietic cells, particularly conventional and plasmacytoid dendritic cells, significantly produce IFNα [203]. The production of IFN-I is mainly dependent on the IRF3 and 7 that mediated the IFN-I transcription [204]. Any defects in IRF3/7 itself or in the signaling cascade involved in the activation of IRF3/7 are reported to have a detrimental impact on the innate immune response against viral infections [27, 32].

Interferon Regulatory Factor – IRF

IRFs belong to a family of transcription factors and play an important role in host defense. Moreover, IRFs have a pivotal role in immune cell development and oncogensis [27, 32, 205, 206]. In mammalian cells, an expression of nine members of IRF is reported. The IRFs proteins consist of a conserved N-terminal DNA binding domain (DBD) with a tryptophan repeats that is essential for DNA recognition and binding [208]. IRF that lacks tryptophan residues fails to bind to the DNA [209, 210]. Furthermore, IRF comprises the IRF association domain, a nuclear export sequence, an autoinhibitory domain, and a signal responding domain with serine residue that is sensitive to the pathogen and agonist-induced phosphorylation [32, 203]. IFN-I genes are reported to be transcribed by IRF3, and IRF7. IRF3 and IRF7 are highly homologous and considered as principal factors for Type I IFN gene expression elicited after PRR recognitions and activation of viral infection [211, 212]. In the steady state, IRF3 is constitutively expressed. Unlike IRF3, IRF7 is expressed in small quantities and is strongly upregulated after IFN-I or PRR activation. Both IRF3 and IRF7 reside in the cytosol [27, 213-215]. PRR activation induces the phosphorylation of IRF3 and 7, which results in nuclear translocation [27, 213-216]. TBK1 (TANK-binding kinase 1) and IKKε (inhibitor of NF-κB kinase ε) are known to phosphorylate IRF3/7 results in the IFN-I gene transcription [141, 142, 217, 218]. IRF3 is a potent activator of IFNβ genes, when compared to IFNα. IRF7, on the other hand, efficiently activates both IFNα and IFN β genes [28, 204, 212, 219]. After the initial induction of IFN-I, IRF7 mediated positive feedback loop amplifies IFN-I production [28, 204]. Overall, kinase and adaptor molecules govern the activation of IRF3 and IRF7 [1, 2, 17, 18]. In our study, we

found that RAIDD interacts specifically with IRF7 but not IRF3 and is essential for IRF7-induced IFN-I production.

RAIDD

The adaptor protein RIP associated ICH-1/CED-3-homologous protein with a death domain (RAIDD) is abundantly expressed in most all cell types [224]. RAIDD has two functional domains, a death domain (DD) at its C- terminus and a caspase activation and recruitment domain (CARD) at the N- terminus [224, 225]. Its functional domains regulate apoptosis and inflammation [224-229]. RAIDD is known to interact with RIP1 through the death domain. The CARD domain is known to interact with caspase-2 [228, 229]. Additionally, recent findings suggested that RAIDD limits NF-κB signaling in T cells by sequestering B cell lymphoma 10 (BCL10) [227]. Nevertheless, the involvement of RAIDD during PRR activation has not been described. In this present, we report that RAIDD is critical for Type I interferon production after TLR activation, specifically for TLR3 activation (Figure 9).

Figures 9 - Role of RAIDD in TLR 3 Signaling Cascade

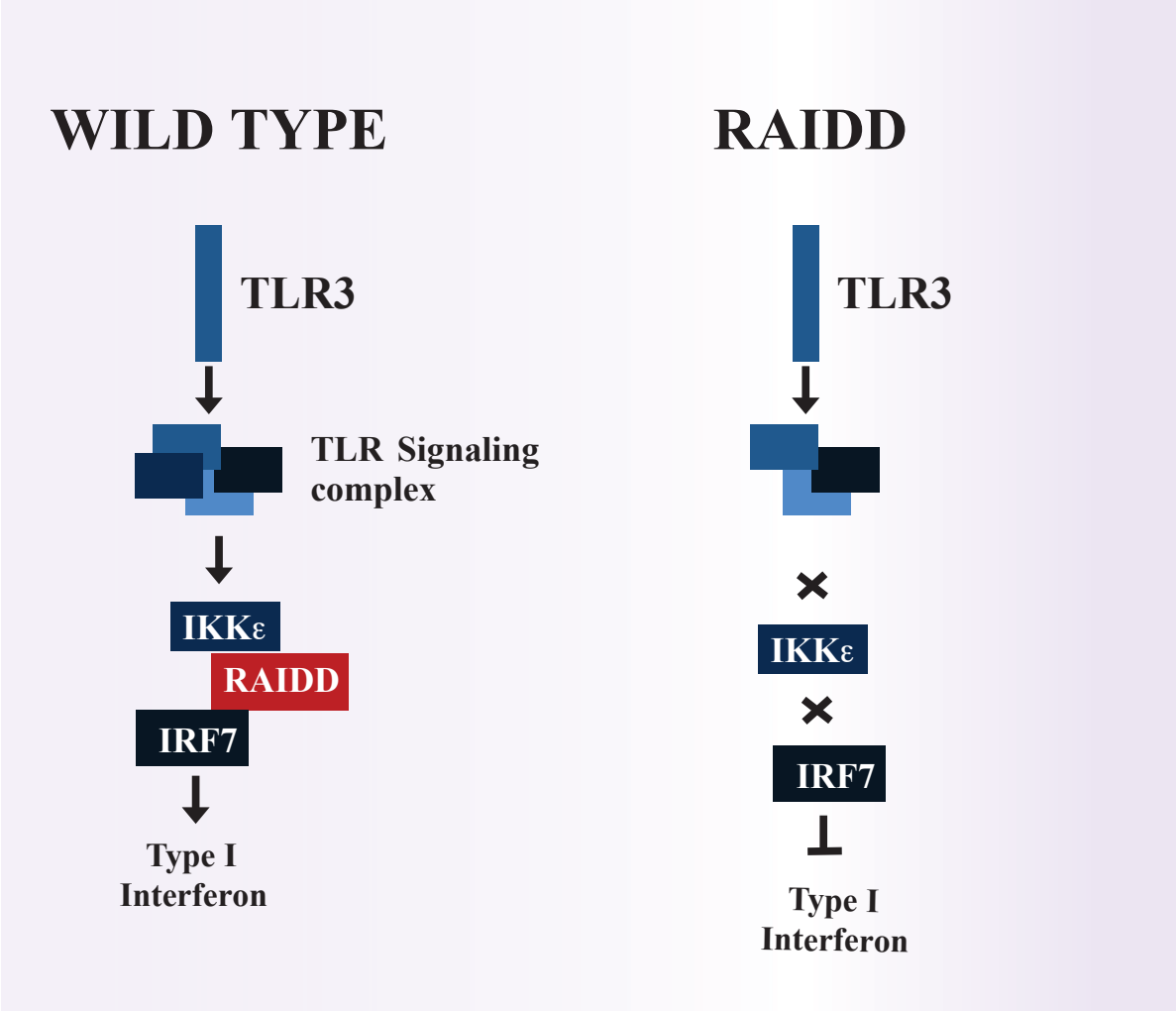

Figures 9- Role of RAIDD in TLR 3 Signaling Cascade

The adaptor protein (CRADD/ RAIDD) is a critical component in TLR3 driven type I interferon production. RAIDD interacts with interferon regulatory factor 7 (IRF7) and its potential phosphorylating kinase IKKε. Consequently, RAIDD knockdown largely abrogated IKKε and IRF7 mediated Type I Interferon production via TLR3 stimulation

Chapter 2 - AIM OF THE THESIS

Topic I - Truncated iRhoms Promote shedding of TNF receptors

TNF is known as the master regulator of immune responses and its defensive role against bacterial infections is highly indispensable. The excessive production of TNF is often associated with various inflammatory disorders [31]. The primarily focus of this doctoral thesis is to find a novel factor that potentially inhibits the dreadful effects of TNF caused during inflammation. The unbiased genetic screen reveals two novel genes, truncated iRhom1 and 2, which induce the shedding of TNF receptors and inhibit the TNF response.

Topic II – RAIDD affects the IFN-I Production

The next objective of the doctoral research is to investigate the role of adaptor protein RAIDD in IFN-I production. IFN-I is the most potent anti viral defense. Deficiency of RAIDD reveals the existence of the defects in IFN-I production. Specifically, RAIDD controls the TLR3 and IRF7-driven IFN-I production.

Chapter 3 - MATERIALS

Instrument Details	Manufacture
Centrifuge (Eppi)	Eppendorf
Centrifuge	Themo Fisher
ECL Developer Curix 60	AGFA
ELISA plate 96-well	Nunc
ELISA-Reader	Thermo Fisher
FACS tubes	BD
Amersham Hyperfilm ECL	**GE Healthcare**
Cell skretcher, steril	BD Falcon
Cell-Observer (Microscope)	Zeiss
Elyria	Zeiss
Freezer -20°C	Samsung
Freezer -80°C	Thermo Fisher
Fume hood	Vinitex
Gel chamber Novex Mini Cell	Thermo Fisher
Heating block Thermostat 5320	Eppendorf
Pasteur Pipettes	Welabo
Petri Plates 6 cm	Nunc,
Immersol	Zeiss
Incubator	Thermo Fisher
Luciferase Reader	Promega
Microscope, convex	VWR International
GmbH	
Nanodrop ND-1000	Peqlab
Nitrocellulose membrane	GE Healthcare
NuPAGE 4-12% Bis-Tris Gel	Thermo Fisher
Pipetboy	VWR International
GmbH	
Pipettes 1000 µL, 200 µL, 20 µL, 10 µL	Brand
Plastic Pipettes 5 ml, 10 ml, 25 ml	Costar
Power supply power pack 200	BioRad

Vaccum Pump	Welch
Reaction vessels 0.2 ml, 1.5 ml, 2 ml	Eppendorf
Roller Mixer	Progen Scientific
Shaker (rocking shaker)	Edmund Bühler
Sterile Bench	Welabo
Steril filter-bottle	Nalgene
Test tubes	VWR International
GmbH	
Tips 1000 µl, 200 µl, 20 µl	Star Lab
Tissue	Wep
Tubes, 15 ml, 50ml	BD Falcon
Vortex	Scientific Industries
Waterbath	Medingen
Whatman Paper	GE Healthcare
FACS Canto/Aria	BD Science

Chemicals	**Manufactures**
1,10-Phenanthroline	Sigma
2N sulfuric acid	VWR
Annexin Binding Buffer 10x	BD Bioscience
Bradford	Cytoskeleton Inc.
BSA	GE Healthcare
Surface Biotinylation Kit	Thermo Fisher
Crystal violet	Serva
Dimethylsulfoxide	Sigma
Dual Luciferase	Promega
EDTA	Merck KGaA
Ethanol	VWR
Sample Buffer x4	life technologies
Sodium chloride	Merck KGaA
Super Signal Western Blot Enhancer	Thermo Scientific
TNFα recombinant Mouse	R&D Systems
Trypsin/ EDTA	Pan Biotech
Tween®-20	Merck KGaA

TX-100	Roth
β-Mercaptoethanol	Sigma
FACS clean	BD Biosciences
FACS flow	BD Biosciences
FACS shutdown	BD Biosciences
Fetal Bovine Serum	Biochrome
Formaldehyde	Sigma
Chloromethylketone (FCI)	Enzo life science
GI254023X	Sigma
Glycerol	Merck
GW280264X	Glaxo Smith Kline
L-Glutamine–Penicillin–Streptomycin solution	Sigma
Marimastat (BB-2516)	Tocris Bioscience
Methanol	VWR
NuPage MOPS Buffer	Invitrogen
PBS Pulver (10 L)	Panbiotech
Phostop	Roch
Protease Inhibitor cocktail	Sigma
Protein marker	life technologies

Chapter 4A - METHODS

Topic I - Truncated iRhoms Promote shedding of TNF receptors

The Method section was adapted from the published manuscript in Science Signaling. 2015 Nov 3;8(401): ra109. doi: 10.1126/scisignal.aac5356 and it is entitled as

Deletions in the cytoplasmic domain of iRhom1 and iRhom2 promote shedding of the TNF receptor by the protease ADAM17

Sathish K. Maney,[#] David R. McIlwain,[#] Robin Polz,[#] Aleksandra A. Pandyra,[#] Balamurugan Sundaram, Dorit Wolff, Kazuhito Ohishi, Thorsten Maretzky, Matthew A. Brooke, Astrid Evers, Ananda A. Jaguva Vasudevan, Nima Aghaeepour, Jürgen Scheller, Carsten Münk, Dieter Häussinger, Tak W. Mak, Garry P. Nolan, David P. Kelsell, Carl P. Blobel, Karl S. Lang[+], and Philipp A. Lang[+],

- [+,#] equally contributed

Sathish K. Maney (SKM) contributed almost 18% to this study with experiments and manuscript preparation.

CPR Screening:

L929 are murine fibrosarcoma cell lines generated with plasmids expressing mCAT1 (murine cationic amino acid transporter, mediating ecotropic retrovirus infection) and hCAR (human coxsackievirus and adenovirus receptor). They were selected for their high infectivity towards ecotropic retrovirus and human adenovirus, and high susceptibility to TNF.

Phoenix ecotropic packaging cells were transfected with retroviral mouse 3T3 cell cDNA library by using calcium phosphate precipitation. Retroviral supernatants were obtained 48hours after transfection and used to transduce the selected l929 cells. After stable integration, cells were treated with 2 ng/ml TNF for 24 hours. Surviving cells were allowed to recover from TNF stress and expand for 72hours. Followed by, cells were infected with adenoviruses expressing gag-pol and env (amounts of adenoviruses were determined empirically) and rescued the integrated gene. Rescued viral particles were harvested after 24h and used to transduce new batches of selector cells. Genomic DNA was extracted form a fraction of the surviving cells at each round of screening. A portion of cDNA inserts were amplified by PCR using primers 5'-AGCCCTCACTCCTTCTCTAG-3'and5'-CTACAGGTGGGGTCTTTCATTCCC and sequenced.

Generation and maintenance of cells expressing iRhom isoforms:

Phoenix ecotropic packaging cells (ATCC) were used to prepare the retroviral particles for CPR identified cDNAs (of iRhom1-WT & iRhom1-ΔN, iRhom 2-WT & iRhom2-ΔN) into MSCVpuro (Clontech) containing a C-terminal T7 tag vector. Stable L929 cells were generated using puromycin (10 μg/ml) selection. Unless

otherwise indicated, cells were cultured in DMEM containing 10% FCS, L-Glutamine, Penicillin, and Streptomycin. Mouse embryonic fibroblasts were isolated from E13.5 wild type, ADAM17$^{-/-}$ [156], iR2$^{-/-}$ iR1$^{-/-}$ and iR1/2$^{-/-}$ [153, 173, 230] embryos head and viscera were removed. Followed by trypsin treatment for 15 min at 37 °C, cells were harvested and cultured for 24hours. Further cells were transduced with plasmid expressing simian virus 40 (SV40) large T antigen and maintained in (DMEM) supplemented with antibiotics and 10% FCS.

Immunofluorescence:

L-929 cells stably expressing indicated version of T7 tagged iRhoms were grown on glass cover slips. For intracellular staining, cells were fixed with 4% Formalin and where permeabilized with 1% Triton X-100. In case of surface immunofluorescence staining of T7-iRhom2 and T7-iRhom2-ΔN cells was performed after fixation with 4% formalin. The indicated iRhom versions were detected using a T7-Tag rabbit primary monoclonal antibody (mAb) at 1:300 (abcam) and donkey anti-rabbit Cy3-labelled secondary Ab (Jackson Immunolabs). Further cells, were stained with phalloidin FITC (Sigma) and hoechst 34580 (Invitrogen). Images were captured using confocal microscopy (Zeiss ELYRA).

Stable Knockdown of ADAM17

Lentiviral particles were prepared using calcium phosphate transfection methods. The sub-confluent (50-60%) 293TV cells were transiently transfected with 10μg transADAM17 expressing shRNA/ scramble (origene) including viral packing plasmids such as pRSV-Rev and pMDLg/pRRE constructs. After 48 hours, collected supernatant was filtered through a 0.45 μm filter and stored at -80°C.

L929 cells were infected with lentiviral particles containing the indicated shRNAs and cells were selected with puromycin selection (48h).

TNFR Shedding

To analyze the TNFR shedding in L929 cells overexpressing T7-iRhom2, T7-iRhom2-ΔN, T7-iRhom1, T7-iRhom1-ΔN and control vector cells were seeded (10^5) in 24-well plates. The supernatant was harvested after 24h and used for ELISA measurement according to the manufacturer's instructions. To inhibit ADAM 17 cells were incubated with marimastat (BB2516). In addition to inhibit ADAM10 and ADAM17 cells were treated for 6h with GI or GW (Sigma) culture medium containing FCS free DMEM containing 3μM of the inhibitors.

Ectodomain Shedding assay for AP-tagged KitL2

iRhom2 deficient fibroblasts cells were transiently transfected with AP-tagged KitL2 and the mutant irhom1&2 construct using lipofectamine 2000. 24 hours post-transfection cells were incubated with marimastat, overnight followed by three brief washes. Constitute shedding was measured after 24h of subsequent incubation. Quantification of AP activity in culture supernatant and cell lysate were performed by colorimetric assays

Viability Assay

10^5 l929 cells expressing T7-iRhom2, T7-iRhom2-ΔN, T7-iRhom1, T7-iRhom1-ΔN and control vector were seeded in 24 well plates. Cells were treated with recombinant mouse TNF (R&D Systems), with or without 20μM of MM (Tocris Bioscience) or with ADAM17 shRNA/scrRNA. Viability was accessed at indicated time points using Annexin V -7AAD staining according to the manufacture's (eBioscience) instruction.

Clonogenic Assay

24-well plates were seeded with 10^5 L929 cells expressing T7-iRhom2, T7-iRhom2-ΔN, T7-iRhom1, T7-iRhom1-ΔN and control vector. After 24h were treated with recombinant mouse TNF (R&D Systems) at the indicated concentrations. After 48h, cells were washed and stained with crystal violet at RT for 1hr. The remaining crystal violet was dissolved with methanol and measured using colorimetric assays.

ELISA:

10^5 L-929 cells overexpressing T7-iRhom2, T7-iRhom2-ΔN, T7-iRhom1, T7-iRhom1-ΔN and control vector were seeded in 24-well plates. After indicated points supernatant was harvested and subjected to ELISA [DuoSet ELISA (R&D Systems)] that was performed according to the manufacturer's instructions. In case of ADAMs inhibition studies, cells were co-cultured with marimastat (20 μM, MM, Tocris Bioscience) or with 3 μM of GI or GW (Sigma) culture medium without FCS for 6 hours. Similarly, $2x10^5$ cells from TOC patient derived keratinocytes were seeded into 24-well tissue culture plates.

After indicated time points supernatant was harvested and used for ELISA, performed according to the manufacturer's instructions (as above). To block ADAM17, cells were co-cultured with TMI-005 (500 nM) or vehicle (DMSO). This medium was then collected and ELISA measured the TNRF1 concentration. All experiments were carried out in triplicate or more.

Reverse transcription PCR

RNA was extracted using RNeasy kit (Qiagen). The taqman primers (applied biosystem) were used to measure indicated mRNA expression using reverse

transcription PCR (Bio rad). The relative expression of the indicated mRNA was normalized to beta actin or GAPDH expression. Furthermore, relative expression values were then calculated on the RTpr method. Relative quantities (RQ) were determined with the equation: $RQ = 2^{n}\text{-}\Delta\Delta^{et}$

Cell surface protein isolation

Cell surface proteins from L929 cells expressing T7-iRhom2, T7-iRhom2ΔN were isolated using a sulfo-NHS-SS-biotin-based Cell Surface Protein Isolation Kit (Pierce) according to the manufacturers' instructions, after addition of 20mM BB-2516 (Tocris Bioscience) and 1,10-phenanthroline (Sigma) to the lysis and wash buffers.

Flow Cytometry

Single cell suspensions from cultured cells were prepared after trypsin treatment and stained for 20 min at 4°C with anti-T7 in PBS containing 1% FCS and 5mM EDTA The staining of anti-TNFR1-biotin and anti-TNFR2-biotin (eBioscience) was performed in PBS containing 1% FCS and 5mM EDTA for 1hr at RT, followed by washing and incubation with streptavidin tagged PE/APC antibody (eBioscience) for 30min at 4°C.

Immunoprecipitation & Immmunoblotting

Cells were lysed in PBS containing 1% TX-100 (Sigma), EDTA-free protease inhibitor cocktail (Roche), Phospho stop (1 tablet/10mL), and the inhibitors BB-2516 (20μM; Tocris Bioscience) and 1,10-phenanthroline (10mM; Sigma). To analyze PARP-cleavage, Phospho-p65 or phospho-IκBα the cells were exposed to 2.5ng recombinant mouse TNF (R&D Systems) for indicated time points and activation was determined by harvesting cells from 60mm dishes. Immunoprecipitation was performed using mouse mAbs recognizing the T7 tag

(millipore) or anti-ADAM17 (Abcam).

Statistical Analysis

Data are expressed as mean ± S.E.M. Statistical significance between two groups was analyzed using students t-test. For experiments involving analysis of multiple time points, two-way ANOVA with an additional Bonferroni post-test was used. p-values < 0.05 were considered statistically significant.

Chapter 4B - METHODS

Topic II - RAIDD affects the IFN-I Production

The Method section was adapted from the published manuscript in Cellular Physiology and Biochemistry 2016;39(4):1271-80. doi: 10.1159/000447832. Epub 2016 Sep 8. and it is entitled as

RAIDD mediates TLR3 and IRF7 driven type I interferon production

Authors: Sathish Kumar Maney[#], Haifeng C. Xu[#], Jun Huang, Aleksandra A. Pandyra, Christian Ehlting, Renan Aguilar-Valenzuela, Vitaly I. Pozdeev, David R. McIlwain, Albert Zimmermann, , Johannes Bode, Hartmut Hengel, Carsten J. Kirschning, Ira R. Kim, John Hiscott, Dirk Brenner Dieter Häussinger, Pamela S. Ohashi, Tak W. Mak, Karl S. Lang[+], and Philipp A. Lang[,+,*]

[+,#] equally contributed

Sathish K. Maney (SKM) contributed almost 35% to this study with experiments and manuscript preparation

Cell culture, Cloning, Plasmid preparation and Transfection:

Human RAIDD was amplified using 5‘-TGC GGC CGC_GGA GGC CAG AGA CAA ACA AGT-3‘and 5‘-TGT CGA CGA GGC ACC ATC ACT CCA ACA-

3‘.Amplified products were initially cloned into the pGEM-T-easy cloning vector, thereafter subcloned into the p3XFlag-CMV-7.1 vector using *Not*I and *Sal*I restriction enzymes. Human IKKε was amplfied using 5’-AAG CTG GCT AGC GTA TGC AGA GCA CAG CCA ATT A-3’ and 5’- GAG ACT AGG GTC AGC GAC ATC AGG AGG TGC TGG-3’ and cloned into pGEM-T-easy cloning vector, thereafter subcloned into pcDNA3.1/zeo with C-terminal HA-tag using *Nhe*I and *Psh*AI restriction enzymes.

Murine nucleotide sequence encoding RAIDD-C-term-HA was custom-synthesized by Gene script and cloned into pcDNA3.1/zeo (based on full ORF of NM_009950.2 with codon optimization for mouse expression). pBEN2-eYFP-IRF7A was obtained from CK. pUNO1-hIKKε was purchased from Invivogen (puno1-hikke). All the expression plasmids were amplified using promega maxi pre kit according to the manufactures instructions. Expression plasmids were transfected using lipofectamine 2000 or lipofectamine LTX (Invitrogen) in 293t cells or HEK TLR3 cell lines. 24h post transfection, cells were processed for further analysis. Unless otherwise indicated, cells were cultured in DMEM containing 10% FCS, L-Glutamine, Penicillin, and Streptomycin.

Stable Knockdown of RAIDD:

Lentiviral particles were generated by calcium phosphate transfection of sub-confluent (50-60%) 293TV cells with 10μg of shRNA (Origene), 5μg of pRSV-Rev and pMDLg/pRRE constructs. Lentiviral particles were collected 24 and 48 hours later, filtered through a 0.45μm filter and stored at -80C. Parental cells (293t cells or hektlr3 cells) were infected with lentiviral particles containing the indicated

shRNAs and cells were selected with puromycin (48h, 5μg/ml of puromycin). Two different specific RAIDD shRNA's were used in the experiments

IFN-I promoter assay:

IFNβ promoter assay (measured as previously described) [113], IFN4α promoter assay were measured as previously described [231]. Briefly, IFN luciferase promoter and reporters were transfected in the ratio of 10:1 in 293T cell lines or HEK TLR3 cell lines (Invivogen). 24h Post-transfection, reported gene activities were measured by dual luciferase reporter assay system (Promega).

Immmunoblotting & Immunoprecipitation:

Briefly, cells were lysed in PBS containing 1% TX-100 (Sigma), EDTA-free protease inhibitor cocktail (Sigma), Phospho stop (1 tablet/10mL). Immunoblots were probed with primary anti-RAIDD (abcam ab8426), anti-IRF7 (Cell Signaling 4920 or 13014), and β-ACTIN (Cell Signaling 5125). The pull-down was performed using MultiMACS HA/ GFP Isolation Kit or mAbs recognizing the FLAG.

Statistical analyses:

Data are expressed as mean ± S.E.M. Statistical significant differences between two different groups were analyzed using students t test. Statistical differences between several groups were tested using one-way ANOVA with additional Bonferroni or Dunnett's post-tests. Statistically significant differences between groups in experiments involving more than one analysis time point were calculated using two-way ANOVA (repeated measurements).

Chapter 5A- RESULTS

Topic I – Truncated iRhoms Promotes shedding of the TNF receptors

The following published manuscript in Science Signaling. 2015 Nov 3;8(401): ra109. doi: 10.1126/scisignal.aac5356 was adapted for the results section.

Deletions in the cytoplasmic domain of iRhom1 and iRhom2 promote shedding of the TNF receptor by the protease ADAM17

Sathish K. Maney,[#] David R. McIlwain,[#] Robin Polz,[#] Aleksandra A. Pandyra,[#] Balamurugan Sundaram, Dorit Wolff, Kazuhito Ohishi, Thorsten Maretzky, Matthew A. Brooke, Astrid Evers, Ananda A. Jaguva Vasudevan, Nima Aghaeepour, Jürgen Scheller, Carsten Münk, Dieter Häussinger, Tak W. Mak, Garry P. Nolan, David P. Kelsell, Carl P. Blobel, Karl S. Lang[+], and Philipp A. Lang[+],

- +,# equally contributed

Sathish K. Maney (SKM) contributed almost 18% to this study with experiments and manuscript preparation.

Truncation of iRhom2 or iRhom1 cytoplasmic domains triggers resistance against TNF-induced cell death

L-929 murine fibrosarcoma cells are highly sensitive to TNF-induced cell death through engagement of their cognate cell surface receptors [228-230]. cDNAs capable of conferring resistance to L-929 cell killing by TNF were identified from a mouse 3T3 cell-derived cDNA library through enrichment in a CPR screen [231]. Three different cDNAs were isolated following six successive rounds of infection, cell killing, and rescue of viral particles from surviving cells (Figure 10A). Sequencing revealed the identity of these hits as c-FLIP, an established negative regulator of TNF induced cell death [232], along with two cDNAs corresponding to nucleotides 249-2571 and 618-2571 of native iRhom1 (the latter referred to henceforth as iRhom1-ΔN) (Figure. 10B and Figure Supplementary 1A). The similarity of this result to the identification of an N-terminally truncated version of iRhom2 we previously reported using a separate CPR screen [229] and recent literature concerning mutations in the N-terminus of iRhom2 [151, 235] led us to investigate whether there was a selective advantage for removal of part of the extended cytoplasmic N-terminus, a hallmark feature of iRhoms [259].

Full-length and ΔN truncated iRhom proteins were detected at predicted molecular weights, and in similar abundance, in cells stably overexpressing tagged iRhom constructs (Figure 10C). We first compared the ability of cells overexpressing either full-length iRhom2-WT, iRhom2-ΔN or vector control to withstand exposure to recombinant TNF (Figure 10D). We observed only a slight reduction in cell death assessed by Annexin V and 7AAD staining for cells expressing iRhom2-WT, whereas iRhom2-ΔN cells had dramatically lower levels of Annexin V, 7AAD positive cells (Figure 10D). Interestingly, we found similar

effects when comparing cells expressing iRhom1-WT versus iRhom1-ΔN, which were also strongly resistant to TNF cytotoxicity (Figure 10E). Next, we confirmed these observations using a separate assay to measure cells remaining adherent following 48 hours of TNF treatment. Consistently, we observed a slight protection against TNF mediated cell death in iRhom2-WT expressing cells, but major protection was triggered by iRhom2-ΔN (Figure Supplementary 1B). Moreover, iRhom1-ΔN expressing cells were also protected against TNF induced cell death, compared to iRhom1-WT (Figure Supplementary 1C). Importantly, cells expressing full-length and ΔN iRhoms retained a similar capacity to undergo cell death resulting from other stimuli, such as staurosporine (Figure Supplementary 1D). These data indicate that deletion of part of the cytoplasmic domain of either iRhom1 or iRhom2 confers a selective advantage over their full length counterparts in TNF resistance.

Figure 10

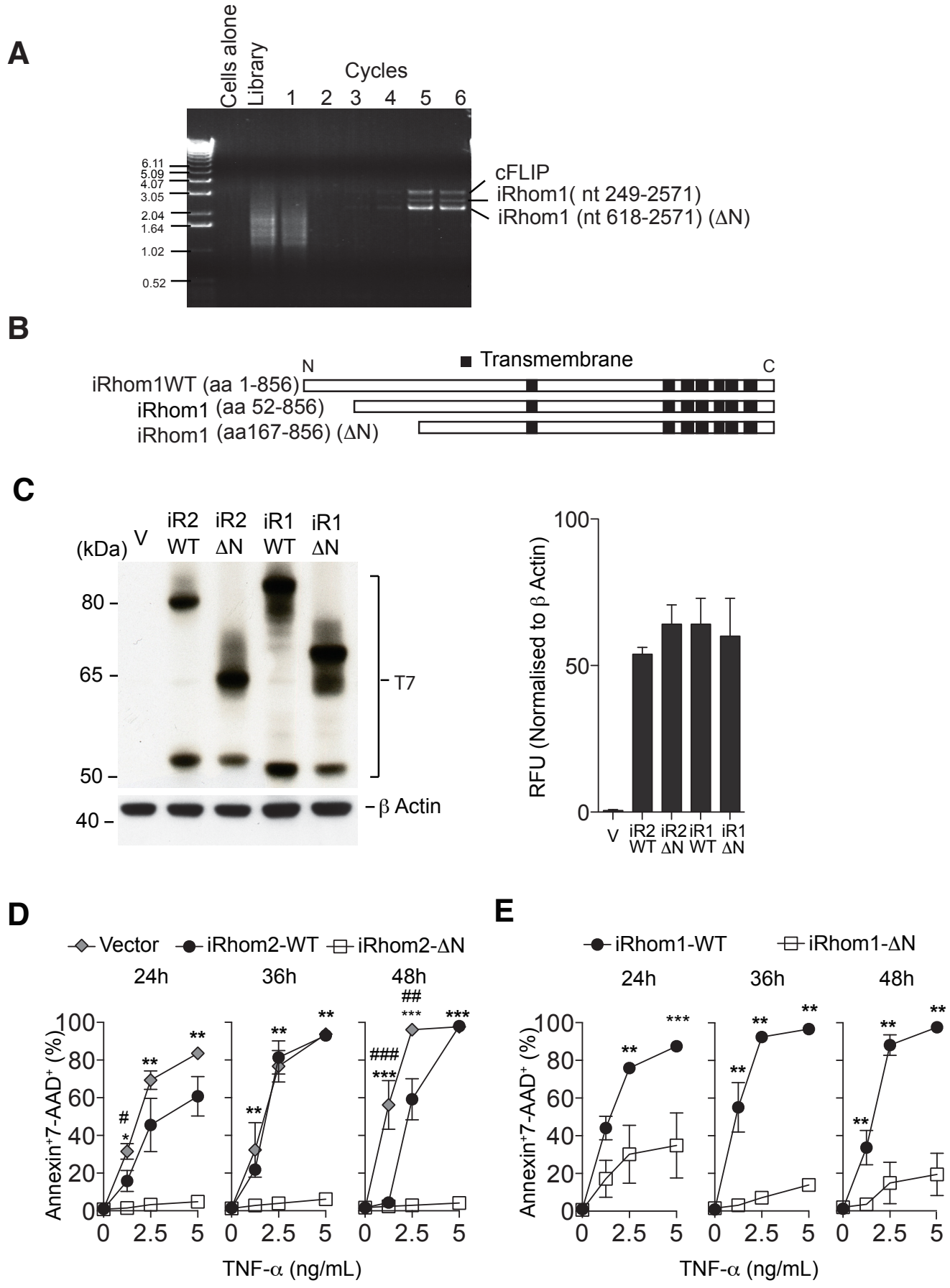
A
Cells alone
Library
Cycles
1 2 3 4 5 6
6.11
5.09
4.07
3.05
2.04
1.64
1.02
0.52
cFLIP
iRhom1(nt 249-2571)
iRhom1 (nt 618-2571) (ΔN)
B
N
Transmembrane
C
iRhom1WT (aa 1-856)
iRhom1 (aa 52-856)
iRhom1 (aa167-856) (ΔN)
C
(kDa)
V
iR2 WT
iR2 ΔN
iR1 WT
iR1 ΔN
80
65
50
40
T7
β Actin
RFU (Normalised to β Actin)
100
50
0
V
iR2 WT
iR2 ΔN
iR1 WT
iR1 ΔN
D
Vector
iRhom2-WT
iRhom2-ΔN
24h
36h
48h
Annexin+7-AAD+ (%)
TNF-α (ng/mL)
E
iRhom1-WT
iRhom1-ΔN
24h
36h
48h
Annexin+7-AAD+ (%)
TNF-α (ng/mL)

Figure10: N-truncated iRhom1-ΔN confers TNF resistance as identified by CPR screening.

(A) PCR results from each round in the CPR screen (see Methods) showing enrichment for cFLIP and two short versions of iRhom1 in TNF-resistant cells. **(B)** Systematic representation of wild-type (WT) and short versions of iRhom1 identified by CPR relative to their predicted transmembrane domain structures. **(C)** Immunoblotting and densitometry for T7 in lysates from L-929 cells expressing a control vector, or T7-tagged wild-type (WT) or ΔN iRhom1 (iR1) or iRhom2 (iR2) (n=3). **(D and E)** Cell death, assessed by Annexin V binding and 7-AAD staining using flow cytometry, in 10^5 L-929 cells transfected as indicated and treated with recombinant TNF for up to 48 hours. (n≥ 5). Data are mean ± S.E.M. from the number of experiments (n) indicated; * $p<0.05$, ** $p<0.01$, *** $p<0.001$ against ΔN; # $p<0.05$, ## $p<0.01$ against vector.

Supplementary Figure 1

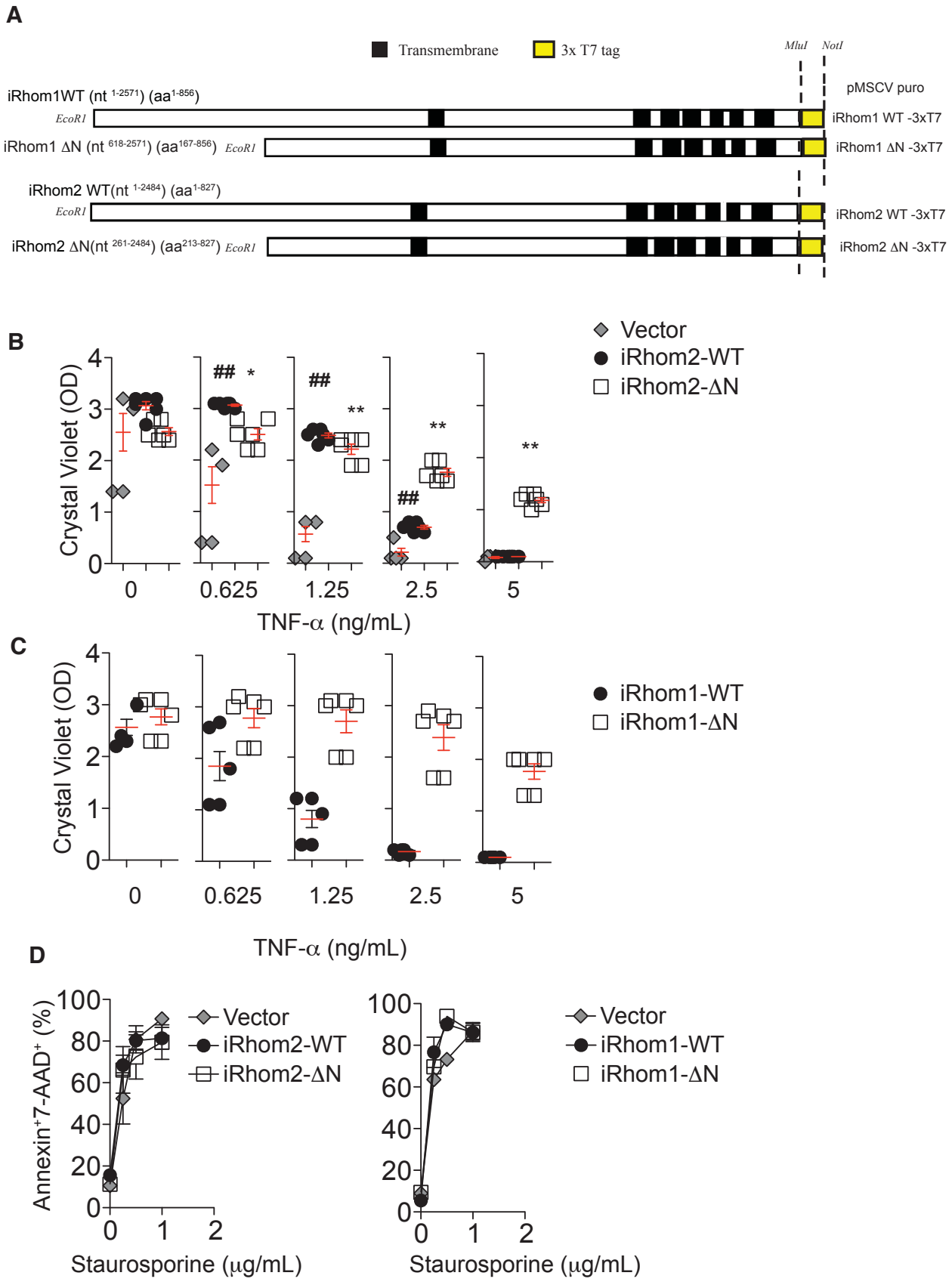

Figure Supplementary 1: Cloning of CPR screen identified iRhom versions.

(**A**) Diagram of cloning strategy used to generate iRhom1-WT, iRhom2-WT, and CPR screen-identified iRhom1-ΔN and iRhom2-ΔN constructs using EcoRI and NotI digestion into a modified version of MSCVpuro (Clontech) containing a C-terminal T7 tag vector. (see Materials and Methods). **(B and C)** 10^5 L-929 cells were treated with recombinant TNF for 48 hours followed by washing and crystal violet staining. Optical density values of crystal violet elution are shown for cells transduced with vector or (B) iRhom2-WT or iRhom2-ΔN , or (C) iRhom1-WT or iRhom1-ΔN (n=6) * $p<0.05$, ** = $p<0.01$, and *** = $p<0.001$; ### $p<0.001$ between iRhom2-WT and vector). **(D)** Cell death in cultures of 10^5 L-929 cells treated with staurosporine (0.5, 1 or 1.5 μg/ml) for 24 hours, assessed by Annexin V binding and 7-AAD staining using flow cytometry (Data are means n=6).

Truncated iRhoms curb TNFR signaling through release of TNF receptors

We next investigated the mechanism by which iRhom2-ΔN confers resistance towards TNF-induced cytotoxicity by examining the status of signaling downstream of the TNFRs. TNFR engagement in L-929 cells results in activation of both cell survival and cell death signaling pathways, causing activation of cell survival associated NF-κB and cleavage of cell death associated poly(ADP ribose) polymerase (PARP) [236-239]. When we examined PARP levels by immunoblot, we detected cleaved PARP in TNF-treated control cells (Figure 11A). However, PARP cleavage was reduced in cells expressing iRhom2-WT, and was not detected in cells expressing iRhom2-ΔN (Figure 11A). Next, we looked for hallmarks of TNF-mediated NF-κB activation [240], and we detect IκB-α phosphorylation and degradation as well as serine$^{(536)}$ phosphorylation of p65 in vector and iRhom2-WT expressing cells, but it was suppressed in iRhom2-ΔN expressing cells (Figure 11B). These findings indicate that TNFR signaling was blocked by iRhom2-ΔN upstream of both survival and death signaling branches [241].

To test whether surface TNFR abundance itself was affected by different iRhom2 isoforms, we used flow cytometry to measure TNFR abundance on the surface of L-929 cells transducted with vector, iRhom2-WT, or iRhom2-ΔN. TNFR1 and TNFR2 abundance was highly reduced on cells expressing iRhom2-ΔN or iRhom1-ΔN compared to cells expressing vector or either wild-type iRhom (Figure 11C and D). When we measured the concentration of soluble TNFRs in conditioned media from these cultures, we observed greater concentrations of soluble TNFR1 and TNFR2 in conditioned media from cells expressing iRhom2-ΔN or iRhom1-ΔN than in that from control cells or cells expressing either wild-type iRhom (Figure 11E and F). These effects were not associated with either

decreased *TNFR* transcript expression (Figure Supplementary 2A+B) or large differences in total cellular abundance of TNFRs (Figure Supplementary 2C-E).

Together, the data indicate that the blockade in TNFR signaling after ΔN-iRhom expression was caused by reduced surface abundance and enhanced shedding of TNFRs. Previous work suggested that shedding of TNFRs was responsible for iRhom2-mediated resistance towards TNF by blocking TNFR signaling [147,152]. We now show that this shedding mechanism is not only true for truncated iRhom2 but also for truncated iRhom1. Furthermore, we confirm that TNFR signaling is blocked by ΔN-iRhom expression by showing that both downstream cell survival and cell death signaling responses are suppressed in these cells.

Figure 11

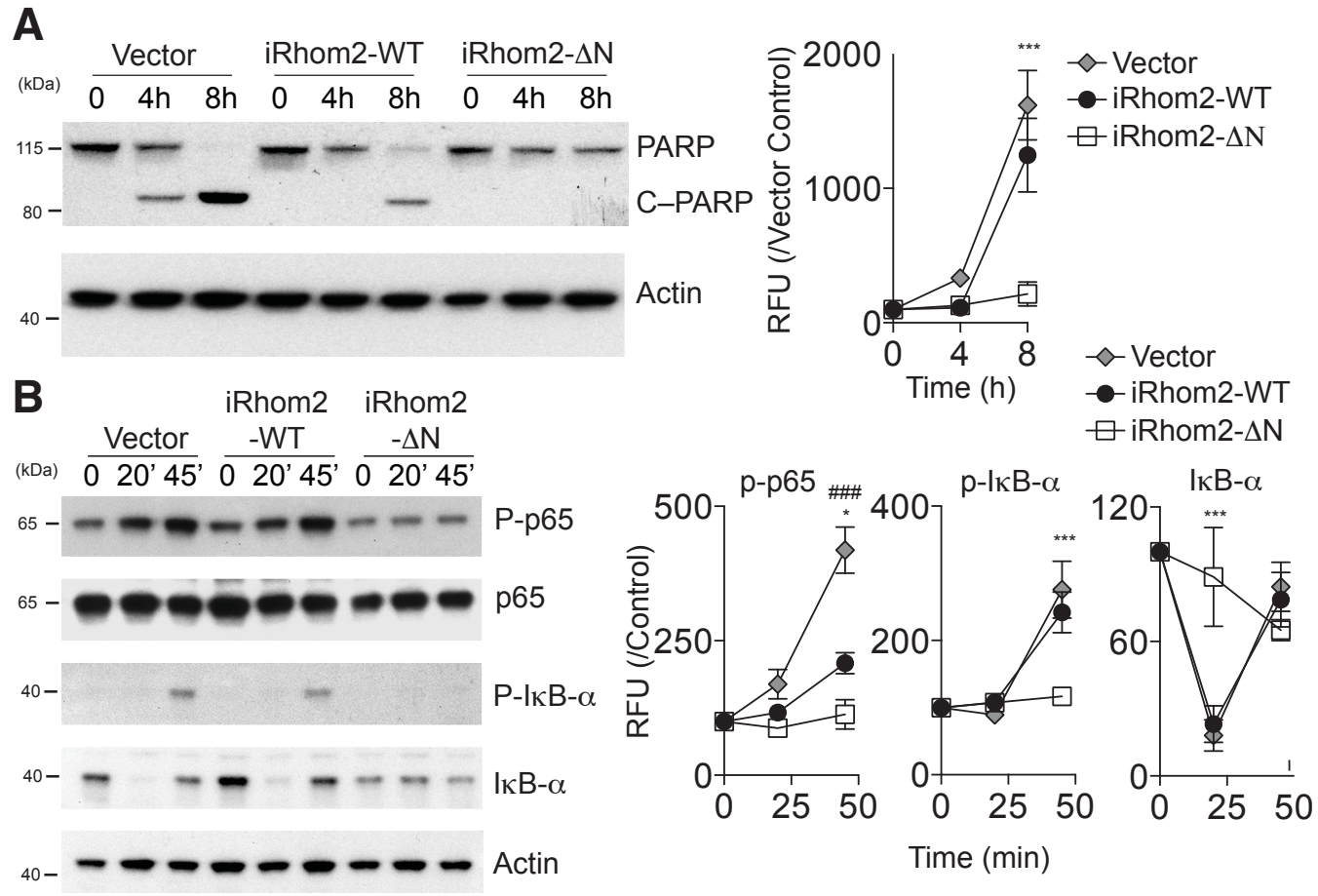
A
Vector
iRhom2-WT
iRhom2-ΔN
(kDa)
0 4h 8h 0 4h 8h 0 4h 8h
115
80
40
PARP
C–PARP
Actin
RFU (/Vector Control)
2000
1000
0
0 4 8
Time (h)
***
Vector
iRhom2-WT
iRhom2-ΔN
B
Vector
iRhom2 -WT
iRhom2 -ΔN
(kDa)
0 20' 45' 0 20' 45' 0 20' 45'
65
65
40
40
40
P-p65
p65
P-IκB-α
IκB-α
Actin
p-p65
p-IκB-α
IκB-α
RFU (/Control)
500
250
0
400
200
120
60
###
*
***
0 25 50
Time (min)
C
Vector
iRhom2-WT
iRhom2-ΔN
Mean Fluorescence Intensity (arbitrary units x 1000)
3
2
1
0
25
20
15
10
5
#
***
##
**
TNFR1
TNFR2
D
Vector
iRhom1-WT
iRhom1-ΔN
30
20
10
E
TNFR1 (pg/ml)
800
400
1000
500
F
1200
600

Figure 11: iRhom2-ΔN induces TNFR shedding.

(A and B) Immunoblotting and densitometry for PARP (A) or total and phosphorylated NF-κB pathway proteins (B) in lysates from L-929 cells overexpressing a vector control, iRhom2-WT or iRhom2-ΔN and exposed to recombinant TNF (2.5 ng/ml) for up to 8 hours (A) or 45 minutes (B). (n=3, normalized to control and actin). **(C and D)** Flow cytometry analysis of TNFR1 and TNFR2 surface abundance on L929 cells overexpressing wild-type or truncated iRhom2 (C) or iRhom1 (D). (n=5 or 6, respectively). **(E and F)** Amount of TNFR1 and TNFR2 in supernatants from 10^5 L929 cells expressing wild-type or truncated iRhom2 **(E)** or iRhom1 **(F)**. (n=5). Data are mean ± S.E.M. from the number of experiments (n) indicated; * $p<0.05$, ** $p<0.01$, *** $p<0.001$ against ΔN; # $p<0.05$, ## $p<0.01$, ### $p<0.001$ against vector.

Supplementary Figure 2

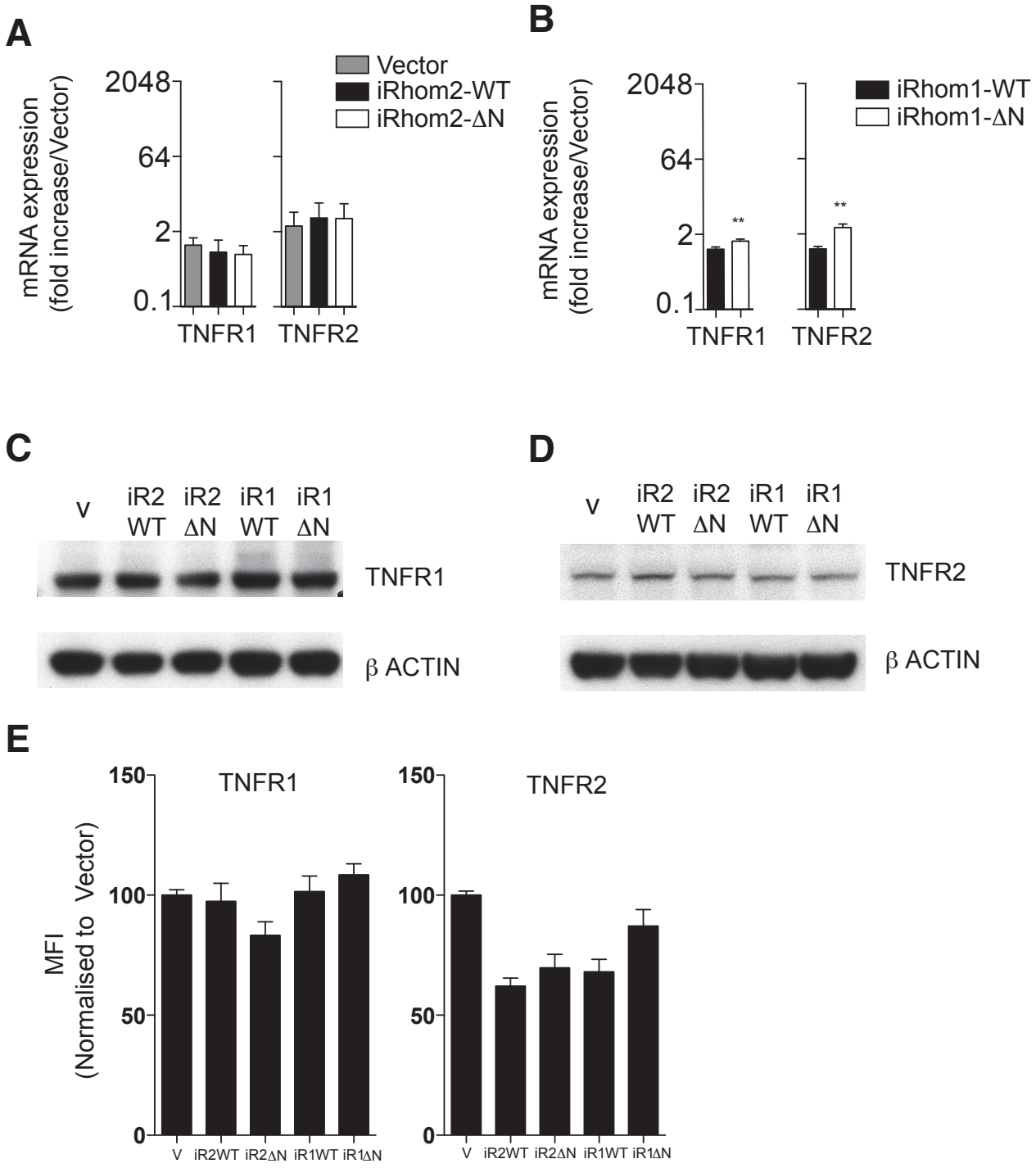

Figure Supplementary 2: TNFR1 and TNFR2 abundance in iRhom expressing cells.

(A and B) RNA expression of *TNFR1* (left panel) and *TNFR2* (right panel) in L929 cells expressing (A) iRhom2-WT or iRhom2-ΔN, or (B) iRhom1-WT, or iRhom1-ΔN (n=6 experiments, ** $p<0.01$ between iRhom2-WT and iRhom2-ΔN). **(C and D)** TNFR1 (C) and TNFR2 (D) abundance by Western blotting the whole cell lysates from L929 cells expressing vector control or wild-type (WT) or ΔN mutants of iRhom1 (iR1) or iRhom2 (iR2) (n=3). **(E)** TNFR1 and TNFR 2 abundance using flow cytometery analysis of permeabilized L929 cells transfected as in (C and D) (TNFR1n= 11 and TNFR2 n= (9-11)). Data are means ± SD.

iRhom-regulated TNFR shedding depends on ADAM17

TNFRs are cleaved from the cell surface by membrane proteases such as ADAM17 [242, 243] (Figure Supplementary 3A). To investigate whether increased TNFR shedding into the supernatant of iRhom-ΔN expressing cells was dependent on metalloproteases in L-929 cells, we investigated shedding in the presence of several ADAM family inhibitors. Increased release of TNFRs into the supernatant of iRhom2-ΔN expressing cells relative to control or wild-type iRhom2 was blocked by the broad spectrum metalloprotease inhibitor marimastat (Figure 12A). Furthermore, shedding induced by iRhom2-ΔN or iRhom1-ΔN was unaffected by an ADAM10 selective inhibitor, GI254023X (GI), but was abolished by an inhibitor of both ADAM10 and ADAM17, GW280264X (GW) (Figure 12B and C). Consistently, culturing iRhom2-ΔN expressing cells with marimastat restored the ability of recombinant TNF to trigger cell death to a similar extent as that observed in cells expressing wild-type iRhom2 (Figure. 12D). TNF itself had little effect on TNFR shedding (Figure Supplementary 3B and C).

To firmly establish that ΔN-iRhoms exert their effects through ADAM17, we stably expressed either a scrambled control or one of two ADAM17-specific shRNA (Figure 13A) in L-929 cells transduced with vector, iRhom2-WT, and iRhom2-ΔN. Surface TNFR1 and TNFR2 abundance was reduced in cells expressing iRhom2-ΔN or iRhom1-ΔN relative to wild-type or vector-transduced controls, however these effects were rescued by ADAM17 silencing (Figure 13B and Figure Supplementary 4A and B), suggesting that truncated iRhoms enhance ADAM17-dependent shedding. Next, we examined whether ADAM17 silencing would disrupt the survival advantage of ΔN-iRhoms against TNF. As expected,

knocking down of ADAM17 abolished the survival advantage caused by expression of ΔN-iRhoms conferred in response to TNF (Figure 13C and D).

Together, the data indicate that TNFR shedding and TNF resistance phenotypes associated with expression of N-terminally truncated iRhoms can be blocked by knockdown or inhibition of ADAM17, establishing ADAM17 as a mechanism through which iRhoms mediate their effects on TNF signaling *invitro*.

Figure 12

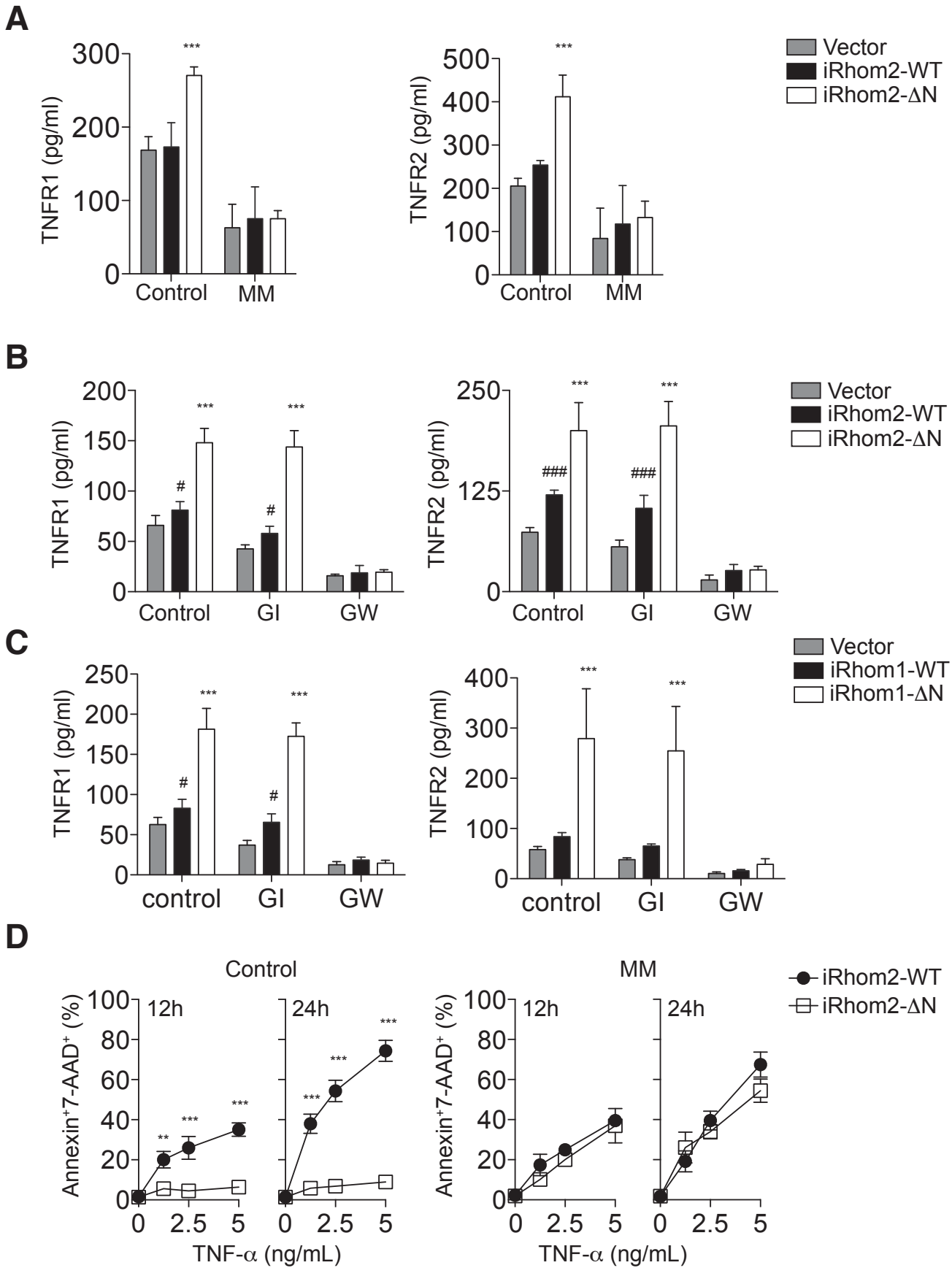
A
TNFR1 (pg/ml)
300
200
100
0
***
Control
MM
TNFR2 (pg/ml)
500
400
300
200
100
0
***
Control
MM
Vector
iRhom2-WT
iRhom2-ΔN
B
TNFR1 (pg/ml)
200
150
100
50
0
#
***
#
***
Control
GI
GW
TNFR2 (pg/ml)
250
125
0
###
***
###
***
Control
GI
GW
Vector
iRhom2-WT
iRhom2-ΔN
C
TNFR1 (pg/ml)
250
200
150
100
50
0
#
***
#
***
control
GI
GW
TNFR2 (pg/ml)
400
300
200
100
0
***
***
control
GI
GW
Vector
iRhom1-WT
iRhom1-ΔN
D
Control
MM
Annexin+7-AAD+ (%)
100
80
60
40
20
0
12h
24h
**
***
***
***
***
***
0
2.5
5
TNF-α (ng/mL)
iRhom2-WT
iRhom2-ΔN

Figure 12: Effects of ΔN iRhoms can be blocked by ADAM17 inhibitors.
(A and B) Abundance of TNFR1 and TNFR2 in the culture supernatants from 10^5 L-929 cells expressing wild-type or truncated iRhom2 cultured in presence or absence of **(A)** marimastat (MM, 20 μM) or **(B)** GI or GW (each 3 μM) for 6 hours. (n=5 or 6, respectively). **(C)** As in **(B)** in10^5 L-929 cells expressing wild-type or truncated iRhom1. **(D)** Cell death as a percentage of Annexin7^+-AAD^+ cells in cultures (n=3) of 10^5 L-929 cells expressing wild-type or truncated iRhom2 treated with recombinant TNF in the presence or absence of marimastat (MM, 20 μM). Data are mean ± S.E.M. from the number of experiments (n) indicated; ** $p<0.01$, *** $p<0.001$ against wild-type; # $p<0.05$, ### $p<0.001$ against vector.

Supplementary Figure 3

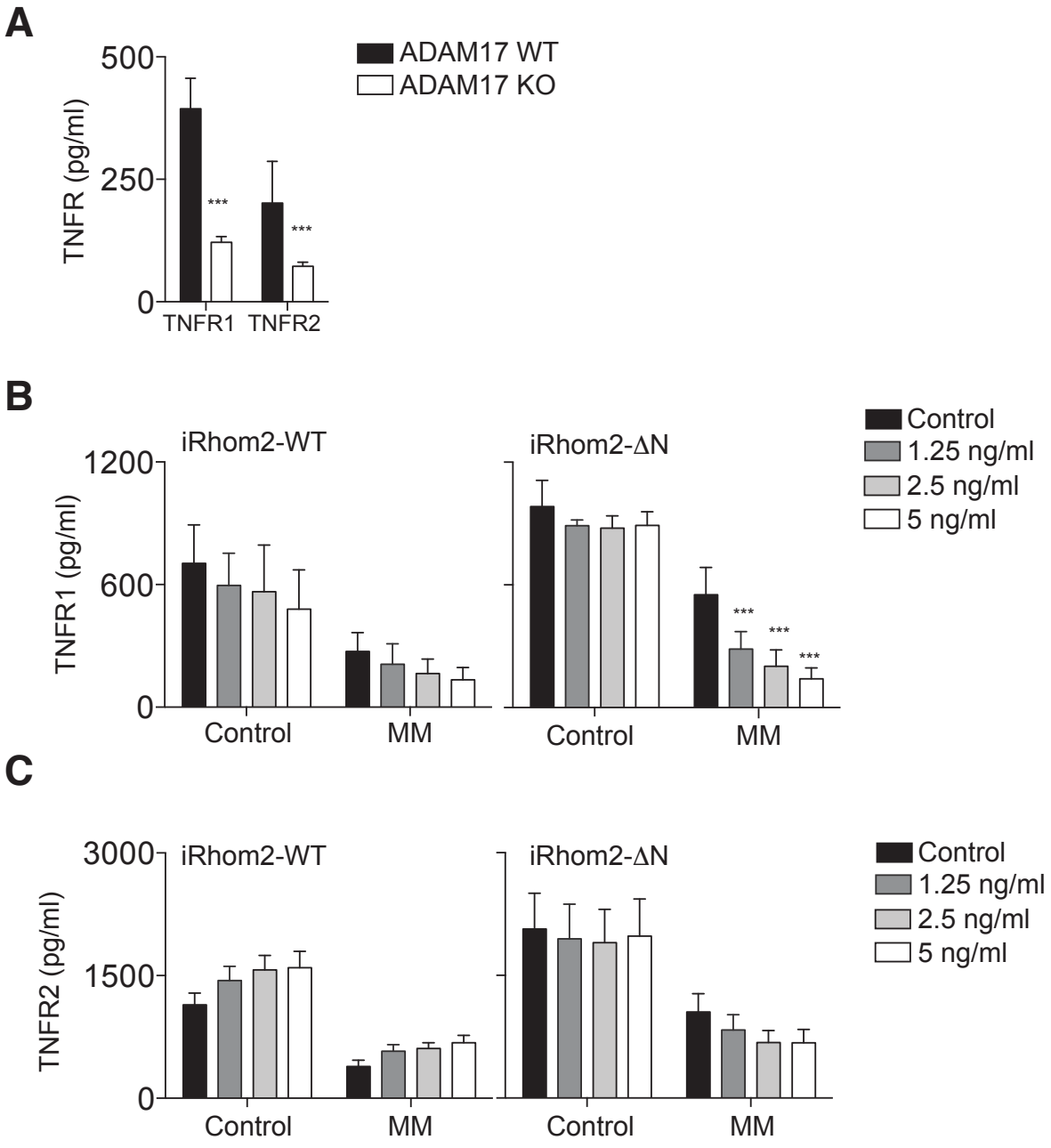

Figure Supplementary 3: ADAM17 mediates cleavage of TNFRs.

(A) TNFR1 and TNFR2 concentrations were determined in the supernatant of control and ADAM17-deficient imEFs (n=6 experiments). Data are means ± SEM *** $p < 0.001$ **(B and C)** TNFR1 (B) and TNFR2 (C) abundance in cultures of 10^5 L-929 cells expressing different versions of iRhom2 treated with recombinant TNF in the presence or absence of marimastat (MM, 20 μM), assessed by TNFR ELISA (n=6). Data are means ± SD; *** $p < 0.001$.

Figure 13

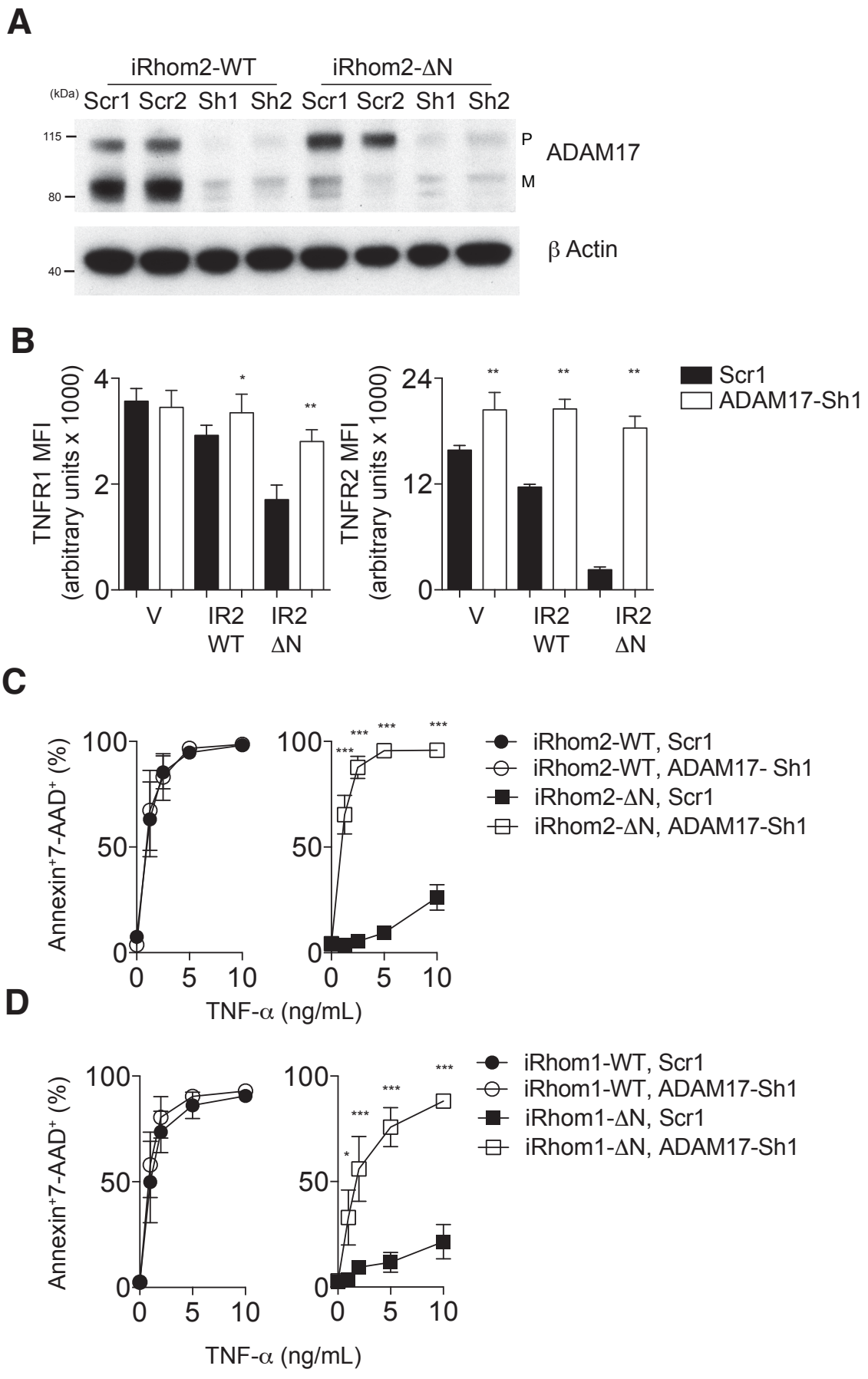
A
iRhom2-WT
iRhom2-ΔN
(kDa)
Scr1 Scr2 Sh1 Sh2 Scr1 Scr2 Sh1 Sh2
115
80
P
M
ADAM17
40
β Actin
B
TNFR1 MFI (arbitrary units x 1000)
TNFR2 MFI (arbitrary units x 1000)
V
IR2 WT
IR2 ΔN
Scr1
ADAM17-Sh1
C
Annexin+7-AAD+ (%)
TNF-α (ng/mL)
iRhom2-WT, Scr1
iRhom2-WT, ADAM17- Sh1
iRhom2-ΔN, Scr1
iRhom2-ΔN, ADAM17-Sh1
D
Annexin+7-AAD+ (%)
TNF-α (ng/mL)
iRhom1-WT, Scr1
iRhom1-WT, ADAM17-Sh1
iRhom1-ΔN, Scr1
iRhom1-ΔN, ADAM17-Sh1

Figure 13: Stable knockdown of ADAM17 prevents increased TNFR shedding and resistance to TNF.

(A) Immunoblot for pro (P) and mature (M) ADAM17 in lysates from L929 cells expressing full-length and ΔN iRhom2 transfected with either a scrambled control (Scr1) or an *ADAM17*-targeted shRNA (ADAM17-Sh1). Blot is representative of 3 experiments. **(B)** Surface abundance of TNFR1 and TNFR2 as determined by flow cytometry on L-929 cells expressing a vector control, full-length (WT) iRhom2 or iRhom2-ΔN in the presence of either control or ADAM17 shRNA (n=6). **(C and D)** Cell death as a proportion of Annexin7^{+}-AAD^{+} cells in cultures of 10^5 L-929 cells stably expressing full-length or ΔN iRhom2 (**C**) or iRhom1 (**D**) and either scrambled or ADAM17 shRNA treated with recombinant TNF for 48hours. (n=4 or 6, respectively). Data are mean ± S.E.M. from the number of experiments (n) indicated; * $p<0.05$, *** $p<0.001$.

Supplementary Figure 4

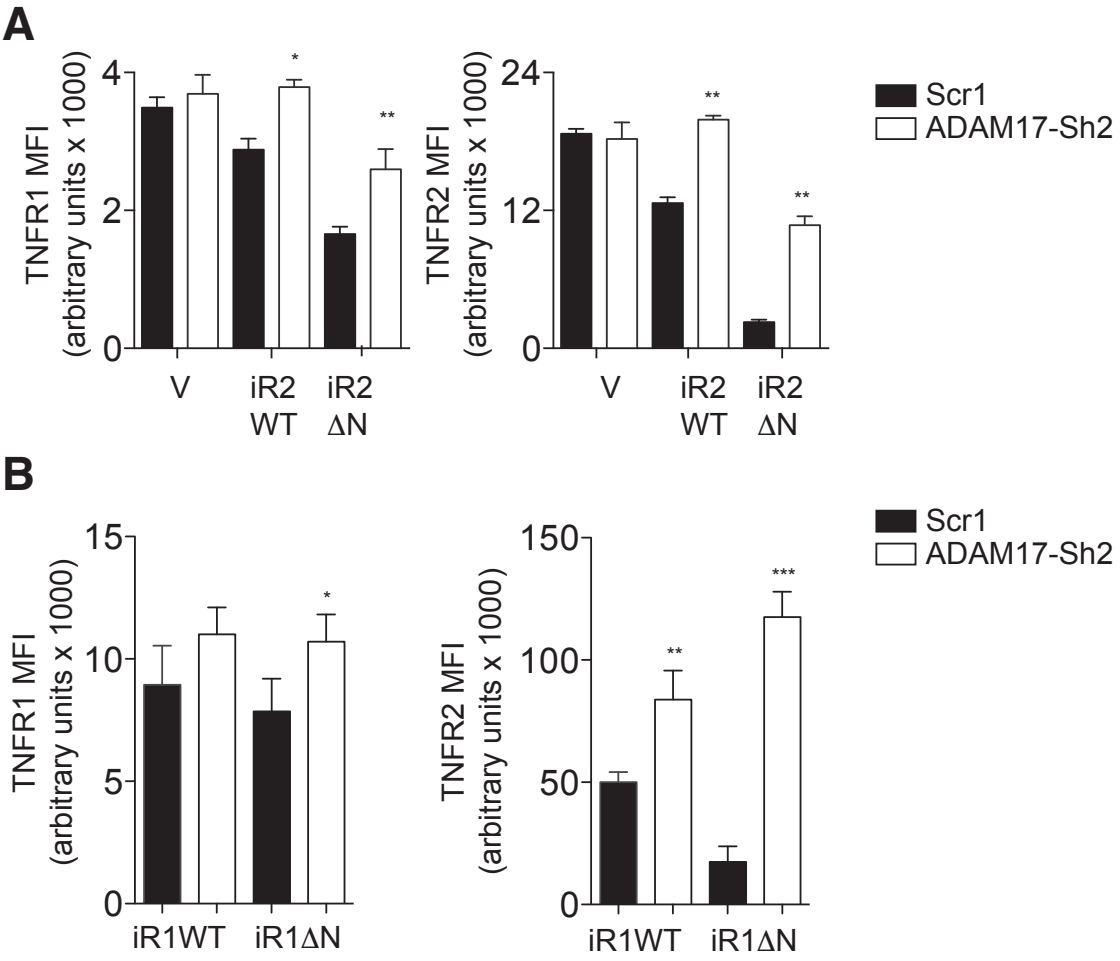

Figure Supplementary 4: Stable knockdown of ADAM17 prevents ΔN iRhom-dependent TNFR shedding. (A) Surface abundance of TNFR1 and TNFR2 determined by flow cytometry in L929 cells expressing a vector control (V), full length iRhom2 (WT) or iRhom2-ΔN in the presence of either scrambled shRNA (Scr1) or shRNA against *ADAM17* (Sh2) (n=6). **(B)** Surface abundance of TNFR1 (n=6) and TNFR2 (n=4) determined by flow cytometry in L929 cells expressing a full length iRhom1 or iRhom1-ΔN in presence of either scrambled (Scr1) or *ADAM17* shRNA. Data are means ± SD; * = $p<0.05$, ** = $p<0.01$, *** = $p<0.001$.

Truncation of the cytoplasmatic tail results in enhanced presence of iRhom2 at the cell surface

We next asked how wild-type iRhoms and their ΔN counterparts might differentially affect ADAM17 activity[147, 152, 244]. Binding of iRhom2 to ADAM17 is thought to be important for ADAM17 maturation and activation. When we pulled down either wild-type or truncated iRhom2, we detected ADAM17 in both immunoprecipitated lysates (Figure 14A). Reciprocally, when ADAM17 was pulled down, both iRhom2-WT and iRhom2-ΔN were detected (Figure 14A). Similar data was obtained in iRhom1-WT and iRhom1-ΔN expressing cells (Figure Supplementary 5A). These data indicated that both isoforms of iRhom1 and iRhom2 are capable of binding ADAM17, consistent with previous reports [147,153].

When we enriched for cell surface proteins, we noticed a larger proportion of iRhom2-ΔN was present in surface fractions versus intracellular fractions and relative to wild-type iRhom2 (Figure 14B). These findings were further confirmed by T7 surface antibody staining and flow cytometry, where the Mean fluorescent Intensity (MFI) for iRhom2-ΔN was significantly higher than that for wild-type iRhom2 (Figure 14C). Consistently, immunofluorescence of tagged iRhom2 revealed greater staining intensity for iRhom2-ΔN versus wild-type iRhom2 on formalin fixed cells, differences which were not apparent after 1% triton permeabilization (Figure 14D). Furthermore, in permeabilized cells, sub-cellular localization of both wild-type and ΔN-iRhoms in the proximity of Golgi marker GM130 (Figure Supplementary 5B). Increased surface localization of iRhom2-ΔN compared with wild-type iRhom2 persisted after ADAM17 knockdown and in ADAM17 knockout fibroblasts (Figure 14E and F) [139], indicating that ADAM17 is not strictly required for iRhom2-ΔN trafficking.

Truncated iRhom2 and wild-type Rhom2 did not exhibit significantly differenence in the rates of protein degradation after inhibition of protein synthesis with cycloheximide, as measured by immunoblotting (Figure Supplementary 5C). This argues against a role for differential protein stability affecting iRhom2 surface abundance. Increased surface abundance of iRhom2-ΔN is also unlikely to be the result of greater RNA expression, as transcript abundance was comparable between iRhom2-ΔN and wild-type iRhom2 (Figure Supplementary 5D). We detected mature ADAM17 on the cell surface of cells expressing vector, wild-type iRhom2, or iRhom2-ΔN (Figure Supplementary 5E). However, a puzzling overall reduction in the total quantity of mature ADAM17 was observed in immunoblots of cells expressing iRhom-ΔN (Figure 14A and Figure Supplementary 5A and E), an effect that was prevented by marimastat treatment (Figure Supplementary 5F). These data indicate that ΔN-iRhoms are capable of binding to ADAM17 in a similar manner to that of wild-type iRhoms, and that the specific effects of iRhom2-ΔN may be related to its enhanced abundance at the cell surface.

Figure 14

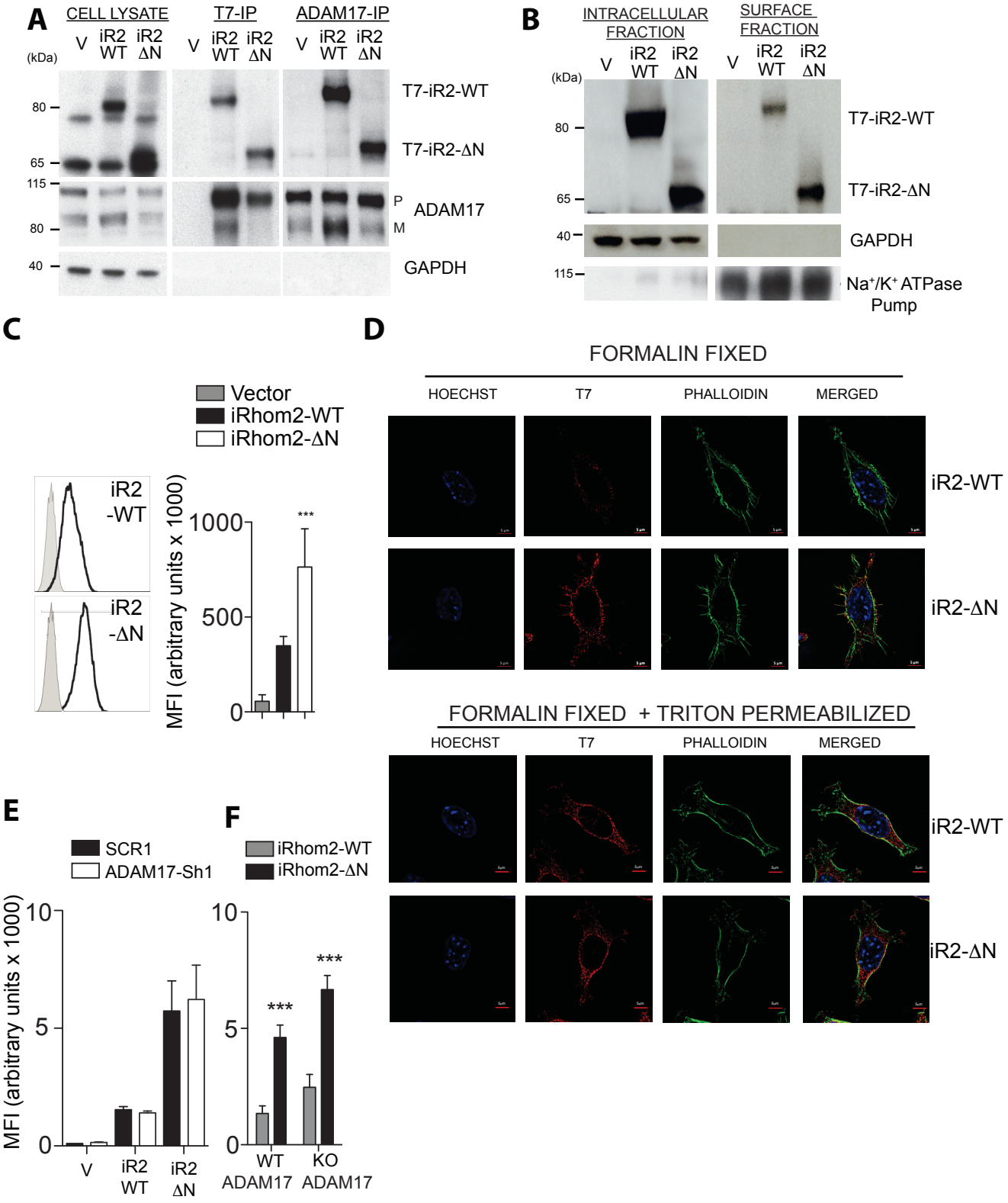
A
CELL LYSATE
T7-IP
ADAM17-IP
V
iR2 WT
iR2 ΔN
(kDa)
80
65
115
80
40
T7-iR2-WT
T7-iR2-ΔN
P
M
ADAM17
GAPDH
B
INTRACELLULAR FRACTION
SURFACE FRACTION
(kDa)
80
65
40
115
T7-iR2-WT
T7-iR2-ΔN
GAPDH
Na+/K+ ATPase Pump
C
Vector
iRhom2-WT
iRhom2-ΔN
iR2 -WT
iR2 -ΔN
MFI (arbitrary units x 1000)
1000
500
0
***
D
FORMALIN FIXED
HOECHST
T7
PHALLOIDIN
MERGED
iR2-WT
iR2-ΔN
FORMALIN FIXED + TRITON PERMEABILIZED
HOECHST
T7
PHALLOIDIN
MERGED
iR2-WT
iR2-ΔN
E
SCR1
ADAM17-Sh1
MFI (arbitrary units x 1000)
10
5
0
V
iR2 WT
iR2 ΔN
F
iRhom2-WT
iRhom2-ΔN
10
5
0
***
***
WT ADAM17
KO ADAM17

Figure 14: Truncation of the cytoplasmatic tail results in increased surface expression of iRhom2.

(A) Immunoprecipitation (IP) for T7 or ADAM17 followed by immunoblotting for the same in lysates from L-929 cells stably expressing T7-tagged wild-type or truncated iRhom2. P, pro and M, mature ADAM17. Blot is representative of 3 experiments. **(B)** Immunoblotting for iRhom2 using a T7 antibody in intracellular and cell surface fractions from L-929 cells stably expressing wild-type or truncated iRhom2. Blot is representative of 3 experiments. **(C)** Surface abundance of iRhom2, determined using an antibody against T7, on stably transfected L929 cells (n=8). **(D)** Immunocytochemistry for iRhom2 using T7-antibodies (Cy3), Phalloidin-FITC and Hoechst staining in stably transfected L-929 cellsfixed and/or permeabilized as indicated. (n≤3 experiments) **(E)** Flow cytometry analysis of mean fluorescence intensity (MFI) of the surface abundance of iRhom2 on unpermeabilized stably transfected L-929 cells expressing either scrambled or ADAM17 shRNA (E; n≤4 experiments) or immortalized wild-type or *Adam17* knockout MEFs (F; n=12 experiments). (Data are mean ± S.E.M. from the number of experiments (n) indicated; *** $p<0.001$.

Supplementary Figure 5

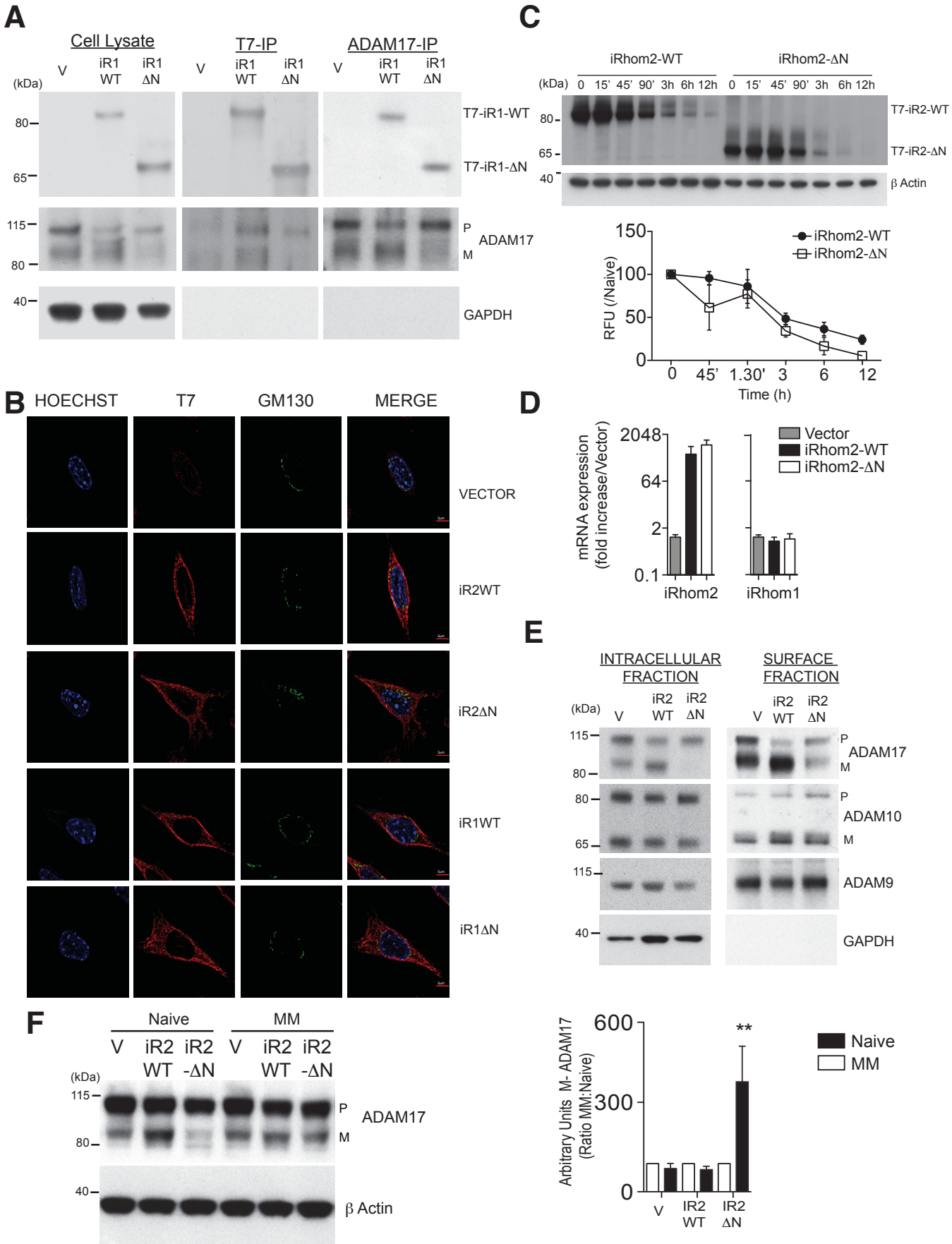

Figure Supplementary 5: Localization patterns of truncated iRhoms and association with ADAM17.

(A) L-929 cells stably expressing iRhom1-WT (T7-tagged), iRhom1-ΔN (T7-tagged), or a vector plasmid were lysed followed by immunoprecipitation (IP) using T7 or ADAM17 antibodies. Immunoblots of lysates enriched using T7 or ADAM17 antibodies are shown, with GAPDH as a control. Bands representing pro-(P) and mature-(M) ADAM17 are indicated. Blots are representative of 3 experiments. **(B)** L929 cells expressing vector control, iRhom2-WT, iRhom2-ΔN, iRhom1-WT or iRhom1-ΔN were fixed and permeabilized before staining for T7(Cy3) and GM130 (Cy2) along with Hoechst (n=3). **(C)** 10^5 L-929 cells expressing different versions of iRhom2 were treated with cycloheximide (100 µg/mL) for the indicated time points. Whole cell lysates were probed for T7-tagged-iRhom2-WT or -iRhom2-ΔN expression levels by immmunblotting and were quantified by densitometry (n=3). **(D)** iRhom2 and iRhom1 mRNA expression levels were determined in L929 cells expressing a vector control, iRhom2-WT, and iRhom2-ΔN (n=5). **(E)** Surface proteins from L-929 cells expressing full length iRhom2, iRhom2-ΔN, or a vector were enriched followed by immunoblotting for intracellular and surface fractions for ADAM17 (P = proform; M = mature form), ADAM10 (P = proform; M = mature form), and ADAM9; GAPDH served as loading control. Blots are representative of 3. **(F)** L929 cells overexpressing a vector control, iRhom2-WT or iRhom2-ΔN were exposed to marimastat. Immunoblot of ADAM17 is shown before and after marimastat treatment (left panel). Bands representing pro-(P) and mature-(M) ADAM17 are indicated. Right, data are mean densitometry values ± SD of 3 blots; ** $p<0.01$ between MM-treated and naïve cells).

N-terminal iRhom mutations increase constitutive activity of ADAM17

ADAM17 can be rapidly activated in response to stimuli including PMA [245, 246]. We therefore wondered whether the effects of ΔN-iRhoms might influence the rapid activation of ADAM17. When we stimulated L-929 cells with PMA, we observed an expected increase in TNFR1 and TNFR2 shedding from cells expressing either vector or wild-type iRhom2 (Figure Supplementary 6A). In contrast, we did not detect PMA-induced TNFR shedding from cells expressing iRhom2-ΔN (Figure Supplementary 6A), and the amount of TNFRs in the stimulated iRhom2-dN expressing cells was not increased when compared to wild-type iRhom2 expressing cells (Figure Supplementary 6A) In all cases, PMA-stimulated TNFR shedding was blocked by marimastat (Figure Supplementary 6A), or GW, which both inhibit ADAM17, but not by the ADAM10-selective inhibitor GI (Figure 15A). The data indicate that truncated iRhoms may induce a constitutively active TNFR shedding state, resembling PMA-stimulated shedding state in control cells (Figure 15B).

To investigate these effects in a different cellular context we co-expressed wild-type or truncated iRhom2 or as control, an unrelated cytoplasmic protein [mitotic arrest deficient 2 (MAD2)] along with the iRhom2-selective AP-tagged ADAM17 substrate KitL2 in *iRhom2*$^{-/-}$ immortalized mouse embryonic fibroblasts (iMEFs) [147, 155]. To improve the detection of potential differences in shedding, we took advantage of the reversible nature of ADAM17 inhibition with marimastat to block shedding overnight, enabling uncleaved substrate to accumulate, and then observed constitutive shedding immediately after washout of the inhibitor. Compared to control cells, only cells expressing iRhom2-ΔN exposed overnight to marimastat exhibted greatly enhanced shedding of KitL2 (Figure 15C). In a separate experiment, we used an irreversible inhibitor of ADAM17 (DPC), which selectively

binds to active ADAM17. Thus, if ADAM17 is not activated while cells are exposed to DPC, ADAM17 can be fully activated after the inhibitor has been removed; however, if ADAM17 is activated in the presence of DPC, ADAM17 will not be able to recover activity after the inhibitor is removed [245]. Incubation of cells expressing iRhom2-ΔN with DPC for as little as 30 minutes prevented the increased KitL2 shedding even after the inhibitor was removed, whereas cells expressing wild-type iRhom2 required overnight exposure to DPC to exhibit ADAM17 inactivation (Figure Supplementary 6B). These data suggest that ADAM17 is constitutively in a more active state in the iRhom2-ΔN setting.

Dominantly acting familial mutations in the N-terminal cytoplasmatic tail of iRhom2 cause a cancer susceptibility disorder called tylosis with esophageal cancer (TOC) [151, 247]. These mutations increase constitutive ADAM17 activity in keratinocytes [248]. Compared to overexpression of wild-type murine iRhom2 in iRhom1 and 2 double knockout iMEFs, expression of a construct bearing mouse homologues of two causative iRhom2$^{I156T/P159L}$ TOC mutations caused increased constitutive TGF-α shedding (Figure 15D). Finally, we examined human immortalized keratinocyte cell lines TYLK 1 and TYLK2 derived from TOC patients bearing heterozygous mutation in iRHOM2 $^{(I186T/WT)}$ [151, 247] and control keratinocyte cell lines (K17). Significantly higher amounts of constitutive TNFR1 shedding into culture supernatants was detected from cells generated from TOC patients compared to cells derived from healthy controls (Figure 15E), shedding which could be blocked by the ADAM17 inhibitor TMI-005. This data is consistent with enhanced ADAM17-dependent shedding of amphiregulin, TGF-α and HB-EGF that is observed in TOC patient derived keratinocytes [249].

These results indicate that ADAM17 activity is enhanced by N-terminal iRhom mutations and may provide an explanation for why cells that have ΔN iRhom proteins have a selective advantage over their wild-type counterparts in promoting resistance to TNF-induced cell death.

Figure 15

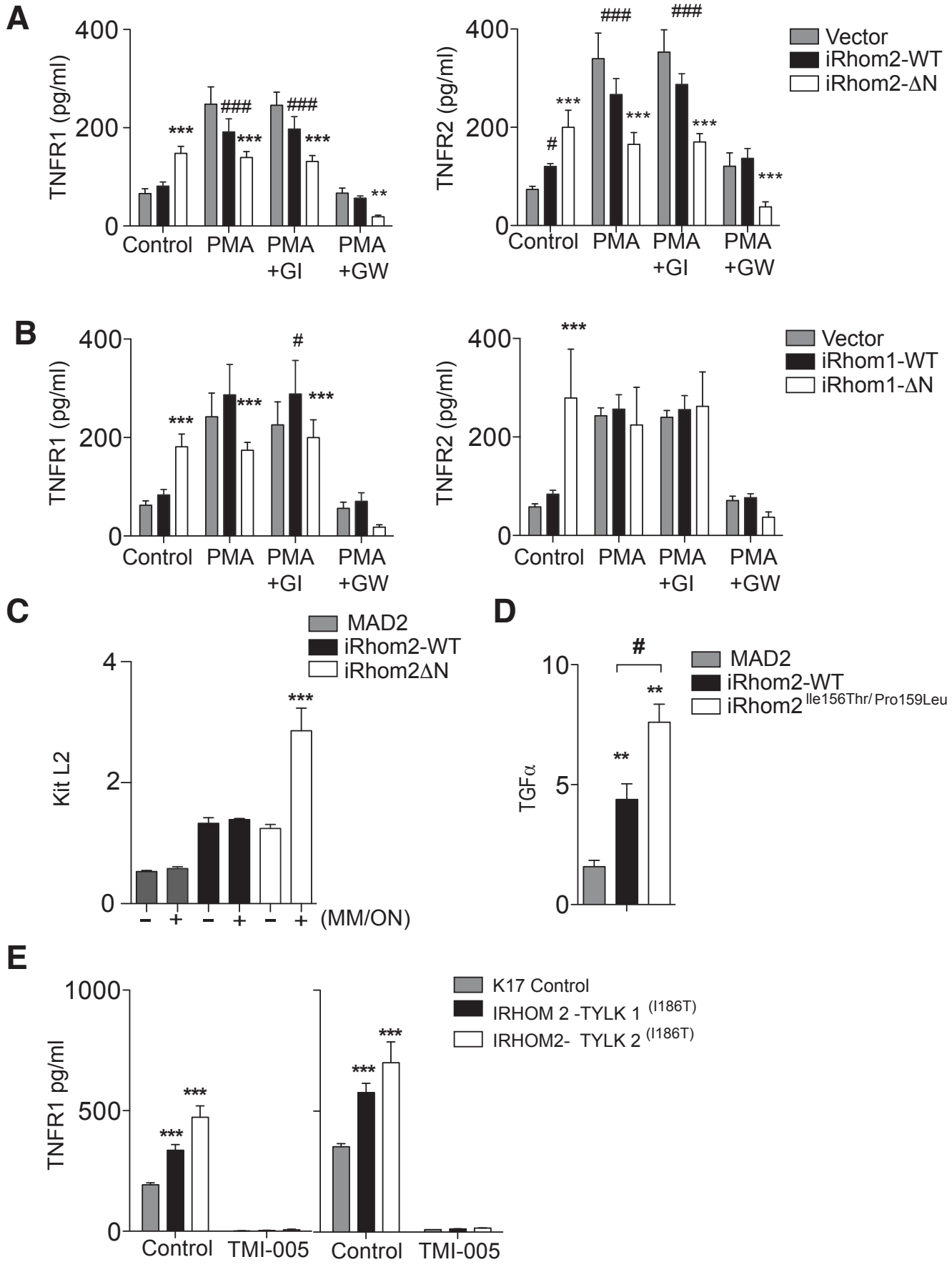
A
TNFR1 (pg/ml)
400
200
0
Control
PMA
PMA +GI
PMA +GW
***
###
**
TNFR2 (pg/ml)
#
Vector
iRhom2-WT
iRhom2-ΔN
B
TNFR1 (pg/ml)
TNFR2 (pg/ml)
Vector
iRhom1-WT
iRhom1-ΔN
C
Kit L2
4
2
0
MAD2
iRhom2-WT
iRhom2ΔN
(MM/ON)
D
TGFα
10
5
0
MAD2
iRhom2-WT
iRhom2 Ile156Thr/ Pro159Leu
E
TNFR1 pg/ml
1000
500
0
K17 Control
IRHOM 2 -TYLK 1 (I186T)
IRHOM2- TYLK 2 (I186T)
Control
TMI-005

Figure 15: N-terminal mutations in iRhom2 trigger constitutive activity of ADAM17.

(A and B) TNFR1 and TNFR2 in conditioned media 10^5 L-929 cells expressing wild-type or ΔN iRhom2 (A) or iRhom1 (B) cultured with PMA (100 ng/ml) in the presence (where indicated) of GI or GW (each 3 μM) (n=6). **(C)** KitL2 shedding in immortalized MEFs genetically lacking iRhom2 transfected with AP-tagged KitL2 along with MAD2 (control), iRhom2WT, or iRhom2-ΔN, and (where indicated, +) preincubated with marimastat overnight (MM/ON), followed by washout of the inhibitor (n=3). **(D)** TGF-α shedding from immortalized MEFs genetically lacking iRhom1 and iRhom2 and transfected with AP-tagged TGF-α along with MAD2 (control), murine wild-type iRhom2 or iRhom2$^{I156T + P159L}$ (n≥5). **(E)** Concentration of soluble TNFR1 in supernatants from 2 x 10^5 healthy donar (K17 cells) or tylosis patient with mutation in IRHOM2 $^{(I186T/WT)}$ [TYLK1 and TYLK2 donor human keratinocytes treated with vehicle (DMSO) or TMI-005 ADAM17 inhibitor for 24 (left) or 48 (right) hours. Data are mean ± S.E.M. from the number of experiments (n) indicated; * p<0.05, ** p<0.01, *** p<0.001 against wild-type (A and B) or MAD2 (D and E); # p<0.05 against vector (A and B) or mutant construct (D and E).

Supplementary Figure 6

A

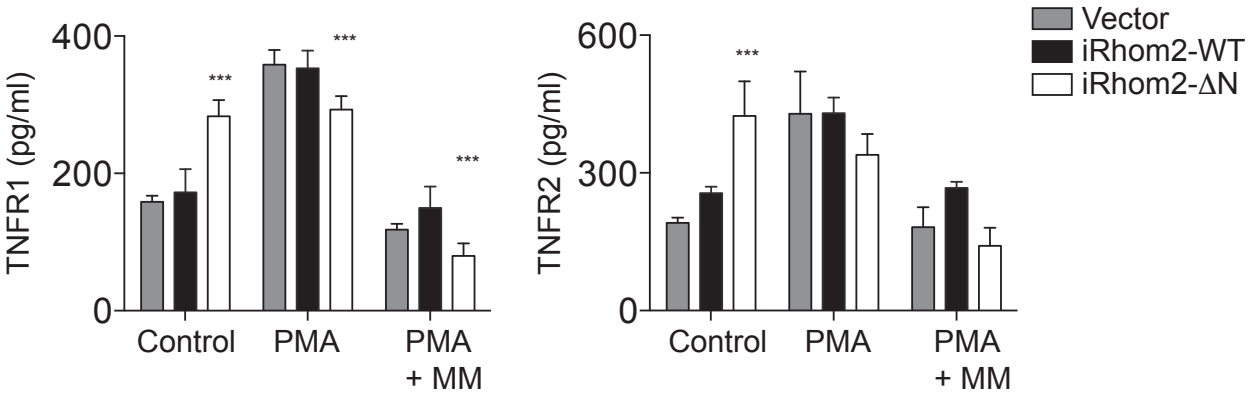

B

iRhom2$^{-/-}$mEFs/WT-iR2/KitL2-AP

1st	MMP pre-treatment	O/N		O/N		1hr		30min		0min	
2nd	1min washout	+	+	+	+	+	+	+	+	+	+
3rd	120min experiment	Ctrl	PMA	Ctrl	PMA	Ctrl	PMA	Ctrl	PMA	Ctrl	PMA

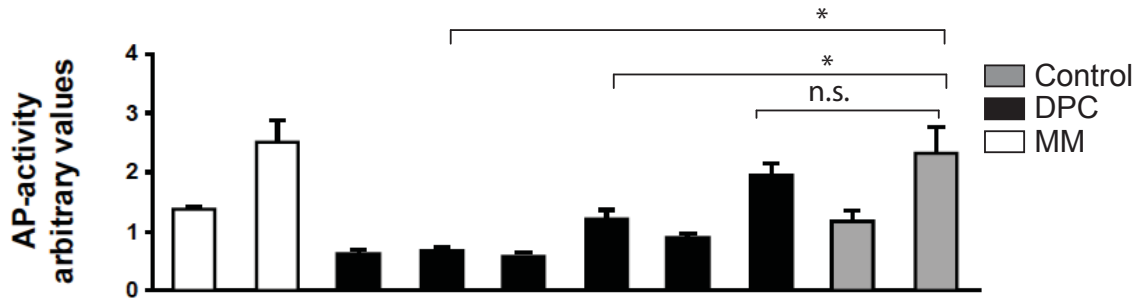

iRhom2$^{-/-}$mEFs/ ΔN- iR2/KitL2-AP

1st	MMP pre-treatment	O/N		O/N		1hr		30min		0min	
2nd	1min washout	+	+	+	+	+	+	+	+	+	+
3rd	120min experiment	Ctrl	PMA	Ctrl	PMA	Ctrl	PMA	Ctrl	PMA	Ctrl	PMA

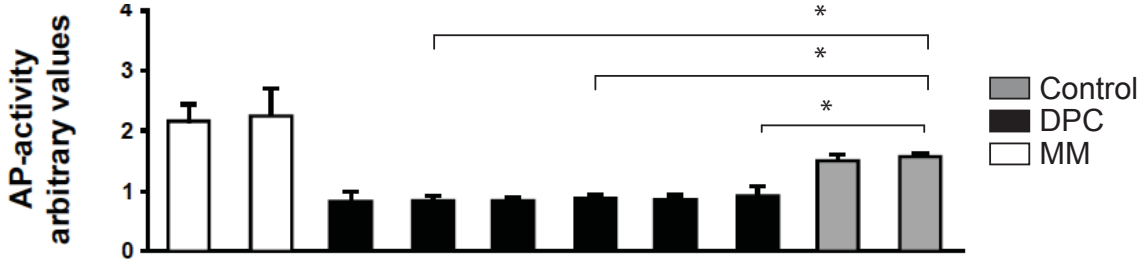

Figure Supplementary 6: Increased ADAM17 activity associated with N-terminal truncated iRhom2.

(A) TNFR1 ($n \geq 4$) and TNFR2 in supernatants from 10^5 L-929 cells expressing full length (WT) or -ΔN iRhom2 cultured with PMA (100 ng/ml) in the presence or absence of marimastat (MM, 20 μM) (*** $p<0.001$ compared to WT). **(B)** Mouse embryonic fibroblasts lacking iRhom2 (*iRhom2*$^{-/-}$ mEFs) were transfected with either iRhom2-WT (top panel) or iRhom2-ΔN (lower panel) and KitL2-AP. Following treatment with the irreversible ADAM17 inhibitor DPC, or the reversible ADAM17 inhibitor MM for indicated time points (O/N = over night), cells were washed and PMA dependent shedding of KitL2-AP was determined (n=3).

CHAPTER 5B – RESULTS

Topic II - RAIDD affects the IFN-I Production

The Results section was adapted from the submitted manuscript for publication (June 2016) to Cellular Physiology and Biochemistry (2016MS388), and it is entitled as

RAIDD mediates TLR3 and IRF7 driven type I interferon production

Authors: Sathish Kumar Maney,[#] Haifeng C. Xu,[#] Jun Huang, Aleksandra A. Pandyra, Christian Ehlting, Renan Aguilar-Valenzuela, Vitaly I. Pozdeev, David R. McIlwain, Albert Zimmermann, , Johannes Bode, Hartmut Hengel, Carsten J. Kirschning, Ira R. Kim, John Hiscott, Dirk Brenner, Dieter Häussinger, Pamela S. Ohashi, Tak W. Mak, Karl S. Lang,[+] and Philipp A. Lang.[+]

+,# equally contributed

Sathish K. Maney (SKM) contributed almost 35% to this study with experiments and manuscript preparation.

RAIDD is critical for IFN-I production after TLR3 stimulation.

IFN-I is induced by activation of PRRs including Toll like receptors (TLRs) [76]. Particularly, TLR3 can induce production of IFN-I following stimulation with its agonist PolyI:C [250]. To analyze the impact of RAIDD during TLR3 mediated IFN-I production, we generated HEK TLR3 transgenic cells, which stably express scramble (scrRNA) or shRNA against RAIDD (Figure 16A). When we challenged these cells with Poly I:C, they showed uniform expression of RAIDD at various time points (Figure 16A). In order to investigate the presence or absence of TLR3 mediated IFN-I activation signals, we used IFN4α promoter driven luciferase. When compared to untreated cells, Poly I:C treatment showed IFN-I activation evident by the expression of luciferase. However, cells lacking RAIDD expression showed significantly reduced activation of IFN-I after Poly I:C treatment (Figure 16B). Next, we examined the Poly I:C driven nuclear translocation of IRF7, which remains one of the molecular hallmark during IFN-I activation[123]. RAIDD deficient cells showed impaired expression and nuclear translocation of IRF7, when compared to scramble control cells (Figure 16C). Next, we checked the impact of RAIDD on other dsRNA sentinel receptors such as (MDA5) [37] and its potent adaptor molecule (IPS1) [111] no notable difference in the activation of IFN-I was observed, either in presence or absence of RAIDD expression (Figure 16D & E). Taken together, these data suggest that RAIDD specifically affects the TLR 3 mediated IFN-I activation.

Figure 16

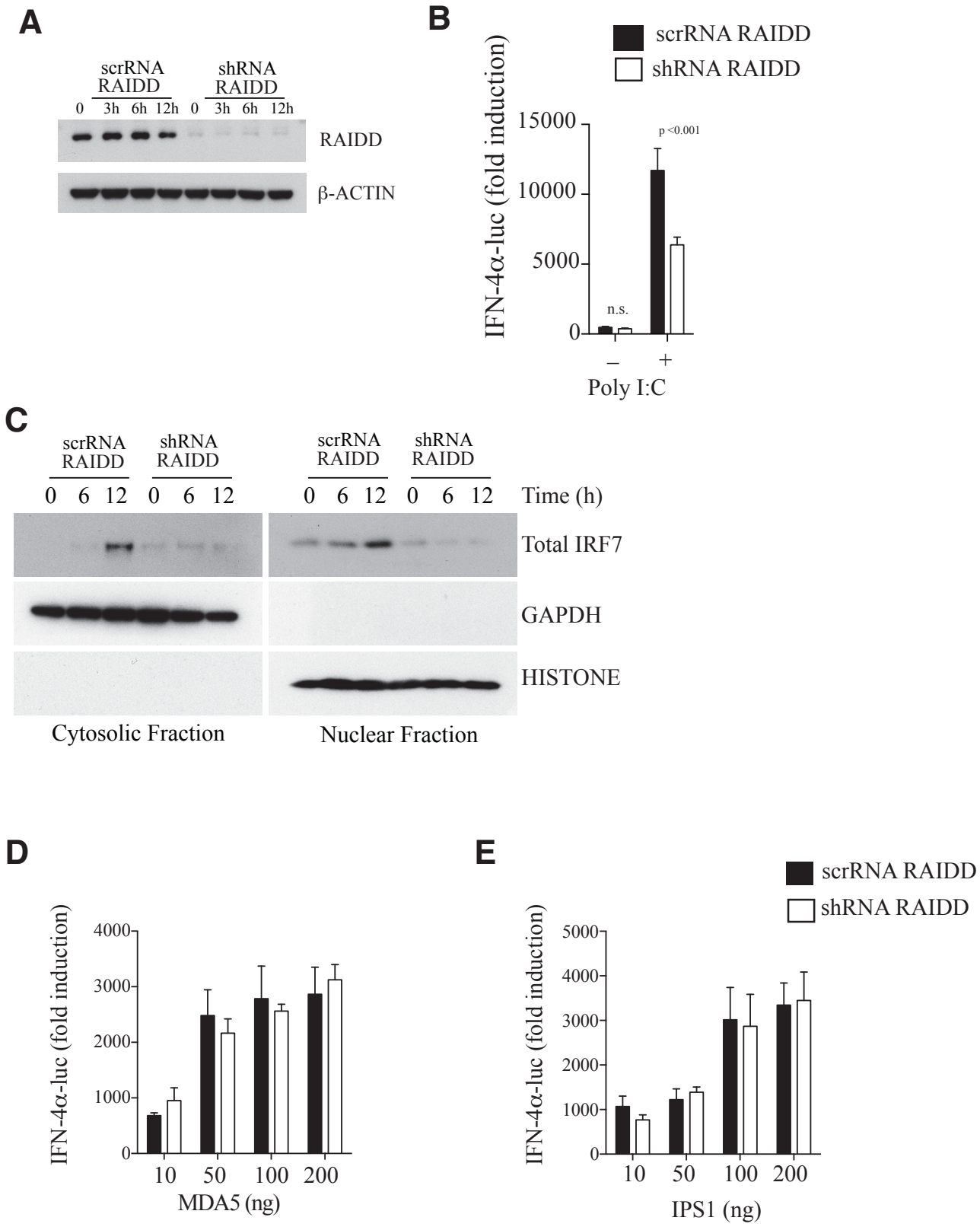
A
scrRNA RAIDD
shRNA RAIDD
0 3h 6h 12h 0 3h 6h 12h
RAIDD
β-ACTIN
B
scrRNA RAIDD
shRNA RAIDD
IFN-4α-luc (fold induction)
15000
10000
5000
0
p <0.001
n.s.
–
+
Poly I:C
C
scrRNA RAIDD
shRNA RAIDD
scrRNA RAIDD
shRNA RAIDD
0 6 12 0 6 12 0 6 12 0 6 12
Time (h)
Total IRF7
GAPDH
HISTONE
Cytosolic Fraction
Nuclear Fraction
D
IFN-4α-luc (fold induction)
4000
3000
2000
1000
0
10 50 100 200
MDA5 (ng)
E
scrRNA RAIDD
shRNA RAIDD
IFN-4α-luc (fold induction)
5000
4000
3000
2000
1000
0
10 50 100 200
IPS1 (ng)

Figure 16: RAIDD is critical for IFN-I production after TLR3 agonist treatment.

(A) Whole cell lysates were prepared from HEK TLR3 cells expressing scrRNA and shRNA RAIDD were treated with PolyI:C (25mg/ml) at indicated time points and probed for RAIDD and β ACTIN. (One representative of n=3 is shown) **(B)** HEK TLR3 cell lines, stably transduced with scramble or RAIDD-targeting shRNA, were transfected with IFN4α luciferase promoter and Renilla constructs (10:1), and IFN4α promoter activity was measured after 6h of PolyI:C (25mg/ml) treatment. Luciferase activity as normalized to Renilla luciferase activity was shown (n=6 is shown) (**C)** HEK TLR3 cytosolic and nuclear fractions were prepared after the treatment with PolyI:C (25mg/ml) at indicated time points and probed for IRF7, HISTONE H3, and GAPDH (one representative of n=3 is shown). **(D)** IFN4α promoter luciferase activities were measured after transient transfection of indicated concentration of IPS1 (n=6 is shown) and MDA5 (n=6 is shown) (24h post-transfection) from 293t cells stably expressing the scramble and shRNA of RAIDD.

RAIDD triggers IRF7 mediated IFN-I transcription.

Next, we investigated whether RAIDD may interact with IFN-I transcription factors. Co-immunoprecipitated RAIDD-HA showed interaction with endogenous IRF7; however, no interaction with the closely related IRF3 could be detected (Figure 17A). These results were validated by reciprocal co-immunoprecipitation using IRF7-YFP to pull down endogenous RAIDD from the IRF7-YFP precipitated lysates (Figure 17B). This interaction could be enriched when both molecules were co-expressed (Figure 17A and B). Further, RAIDD-HA did not interact with TRAF6 (Figure 17A) but in sharp contrast to enriched IRF7, which showed interaction as expected (Figure 17B). The immunoprecipitation of RAIDD-HA or IRF7-YFP showed no sign of interaction with IκBα (Figure 17A and B). These results indicate that RAIDD affects IFN-I activation, likely through a mechanism involving a direct molecular interaction with IRF7. Next, we tested the physiological impact of IRF7 and RAIDD association. Hence, we expressed IRF7 in the RAIDD deficient 293T cells and examined IFN-I activation through luciferase expression driven by IFN4α promoters. Consistent with the molecular interaction, IRF7 mediated IFN-I activation was significantly reduced in the RAIDD deficient cells when compared to scrRNA control (Figure 17C). Notably, IRF7 mediated IFN production is diminished in RAIDD deficient cells but not completely abrogated (Figure 17C), indicating a RAIDD independent activation of IRF7. Moreover, RAIDD was dispensable for IRF3 mediated IFN-I activation (Figure 17D). Together, these data suggest that RAIDD interacts with IRF7 to promote IFN-I transcription.

Figure 17

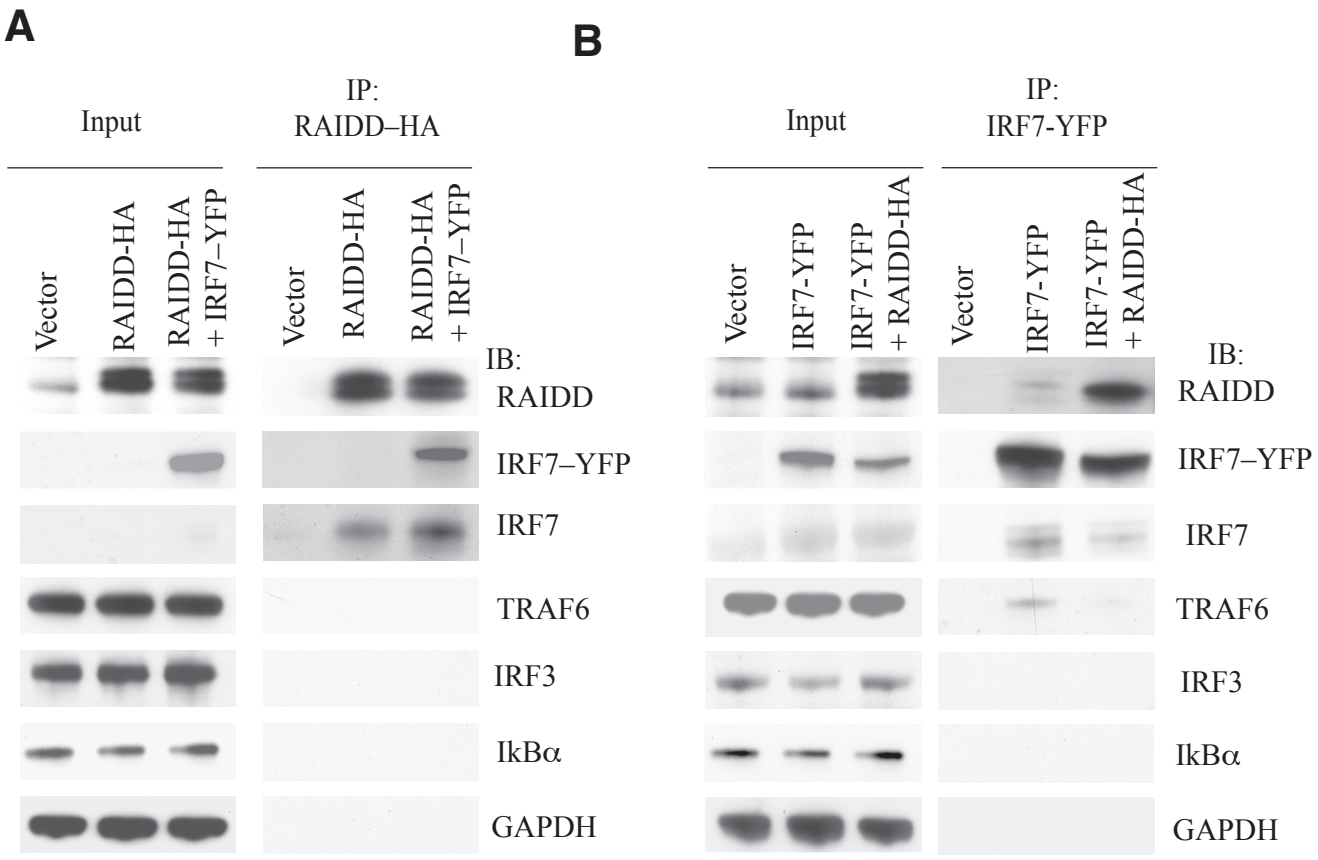
A
Input
IP:
RAIDD–HA
Vector
RAIDD-HA
RAIDD-HA
+ IRF7–YFP
Vector
RAIDD-HA
RAIDD-HA
+ IRF7–YFP
IB:
RAIDD
IRF7–YFP
IRF7
TRAF6
IRF3
IkBα
GAPDH
B
Input
IP:
IRF7-YFP
Vector
IRF7-YFP
IRF7-YFP
+ RAIDD-HA
Vector
IRF7-YFP
IRF7-YFP
+ RAIDD-HA
IB:
RAIDD
IRF7–YFP
IRF7
TRAF6
IRF3
IkBα
GAPDH

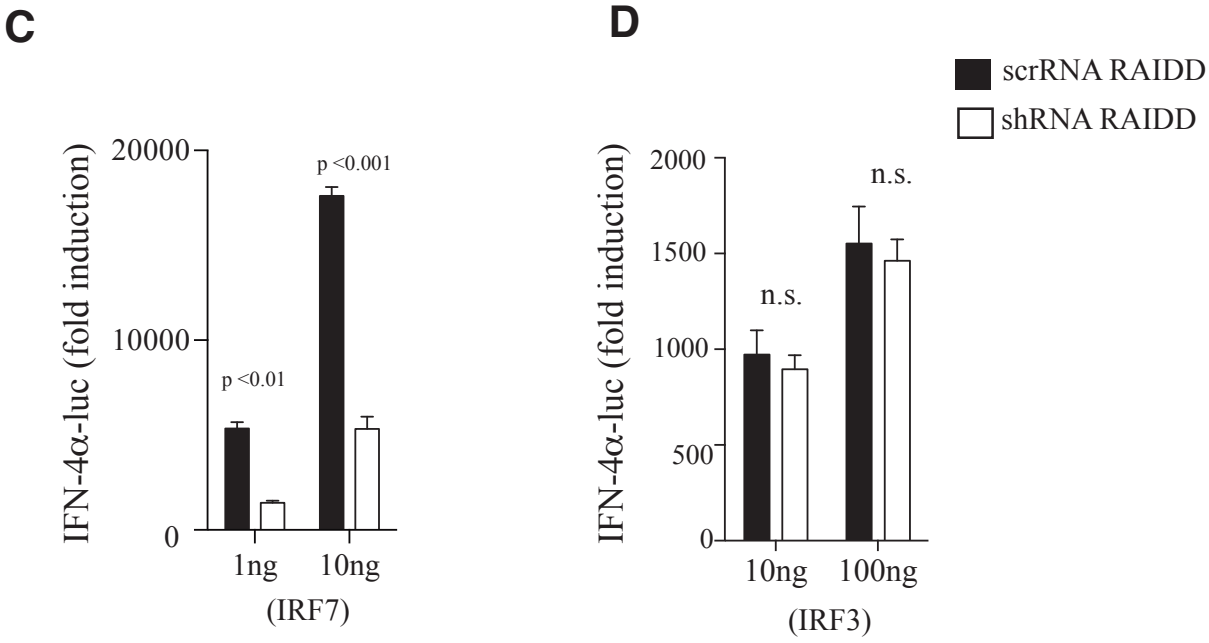
C
IFN-4α-luc (fold induction)
20000
10000
0
p <0.001
p <0.01
1ng
10ng
(IRF7)
D
scrRNA RAIDD
shRNA RAIDD
IFN-4α-luc (fold induction)
2000
1500
1000
500
0
n.s.
n.s.
10ng
100ng
(IRF3)

Figure 17: RAIDD interacts with IRF7 and synergizes with IRF7 in IFN-I activation.

(A,B) 293t cells were transfected with RAIDD-HA, IRF7-YFP, or EGFP control plasmids. Whole cell lysates were blotted directly after immunoprecipitation for RAIDD-HA using an anti-HA antibody **(A),** or immunoprecipitation for IRF7-YFP using an anti-YFP antibody **(B)**. Blotting was performed using anti-RAIDD, anti-IRF7, anti-TRAF6, anti-IRF3, anti-IκBa or GAPDH antibodies as indicated (one representative of n=3 experiments shown) (Error bars indicate SEM). **(C,D)** 293t cells stably expressing scrRNA control or shRNA RAIDD were transiently transfected with IRF7 **(**One representative of n=3 is shown) **(C)** or IRF3 (n=6 is shown) **(D)** together with IFN4α luciferase promoter and Renilla plasmids. Dual luciferase activity was measured at 24h post transfection.

RAIDD triggers IKKε but not TBK1 mediated IFN-4α activation

We further investigated the mechanism by which RAIDD affects IRF7 activation. Due to defects noticed in nuclear translocation of IRF7 in RAIDD deficient 293T cells (Figure 18C) we hypothesized that RAIDD may connect IRF7 to its phosphorylating kinases TBK1 or IKKε [209]. Accordingly, we expressed TBK1 or IKKε in RAIDD competent cells. Strikingly, when compared to scramble controls, we found IKKε driven IFN-I promoter activation was reduced in cells with RAIDD deficiency (Figure 18A), whereas this was not the case for TBK1 (Figure 18B). The increasing concentration of RAIDD with TBK1 also failed to enhance the basal induction of IFN-4α luciferase (Figure 18C). These data indicate, that IKKε but not TBK1 is able to mediate transcriptional activation of IFN4α and IKKε requires the RAIDD to mediate its effects.

Figure 18

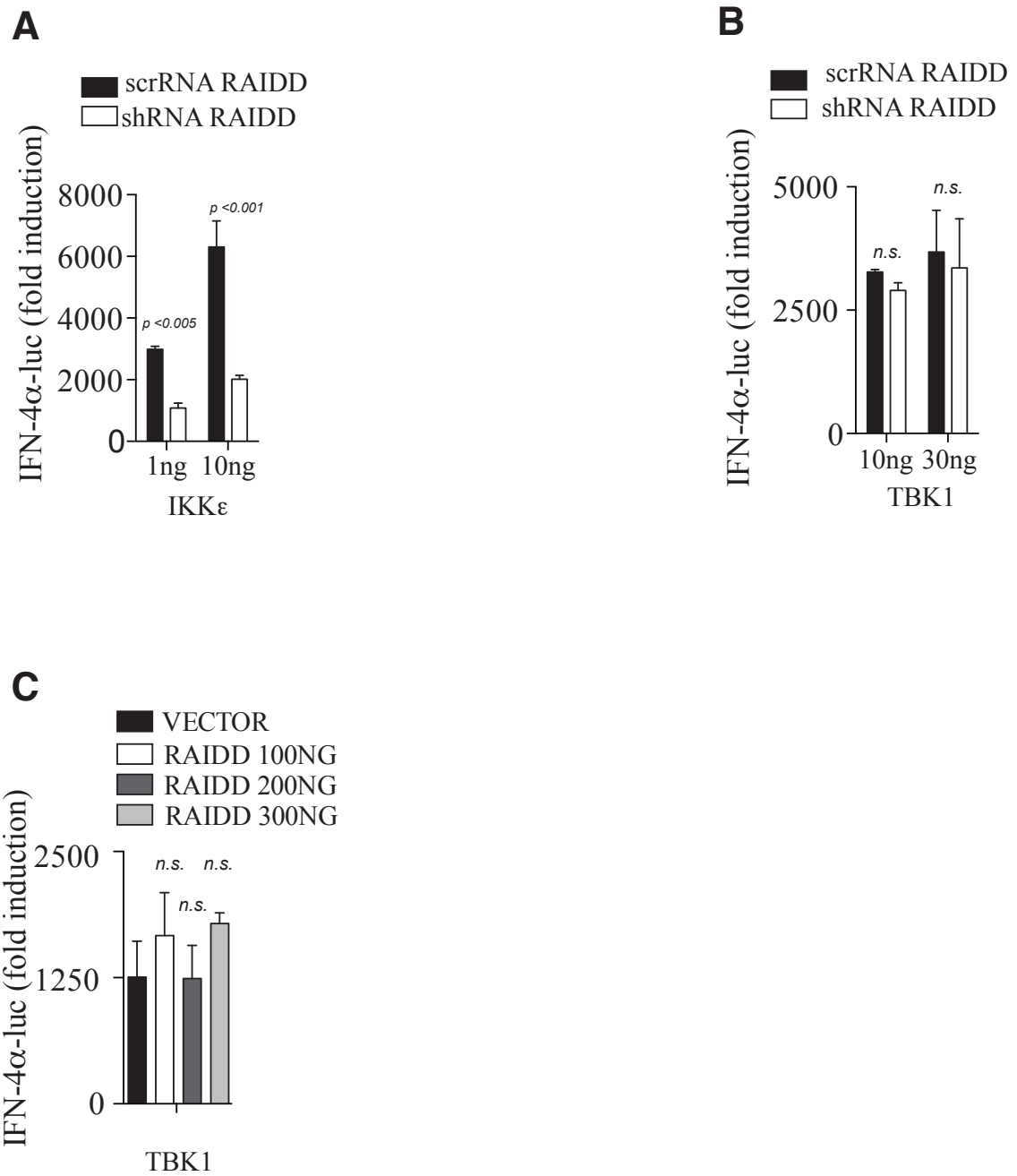
A
scrRNA RAIDD
shRNA RAIDD
IFN-4α-luc (fold induction)
8000
6000
4000
2000
0
p <0.001
p <0.005
1ng 10ng
IKKε
B
scrRNA RAIDD
shRNA RAIDD
IFN-4α-luc (fold induction)
5000
2500
0
n.s.
n.s.
10ng 30ng
TBK1
C
VECTOR
RAIDD 100NG
RAIDD 200NG
RAIDD 300NG
IFN-4α-luc (fold induction)
2500
1250
0
n.s.
n.s.
n.s.
TBK1

Figure 18: RAIDD triggers IKKε mediated IFN4α activation but not the TBK1.

(A,B) 293t cells stably expressing scrRNA or shRNA of RAIDD were transiently transfected with IKKε (10ng/ul) or TBK1 (30ng/ul). together with the indicated luciferase promoter and measured for IFN4α luciferase activity 24h post transfection. (**A) (**One representative of n=3 is shown) and **(B) (**n=6 is shown**). (C)** 293t cells were transiently transfected with increasing concentration of RAIDD together with same molecules of TBK1 (30ng/ml). IFN4α luciferase activities were measured at 24h post transfection (n=6 is shown).

Full-Length RAIDD drives activation of IFN-I

To investigate which domains of RAIDD trigger the IKKε mediated IFN-I activation, we generated deletion constructs of RAIDD, lacking the DD or the CARD (Figure 19A). We observed that the full-length RAIDD showed a significant increase of the IFN-I activation, while neither the CARD nor the DD alone promoted IFN-I transcription (Figure 19B and C). Notably expression of a mutant DD or CARD reduced the effects of full-length RAIDD in this setting, indicating that both domains are indeed needed to exert its effects on IFN-I activation (Figure 19B and C). In support of the previous finding, the different forms of RAIDD have no significant impact on TBK1 mediated IFN-I activation (Figure 19B).

Figure 19

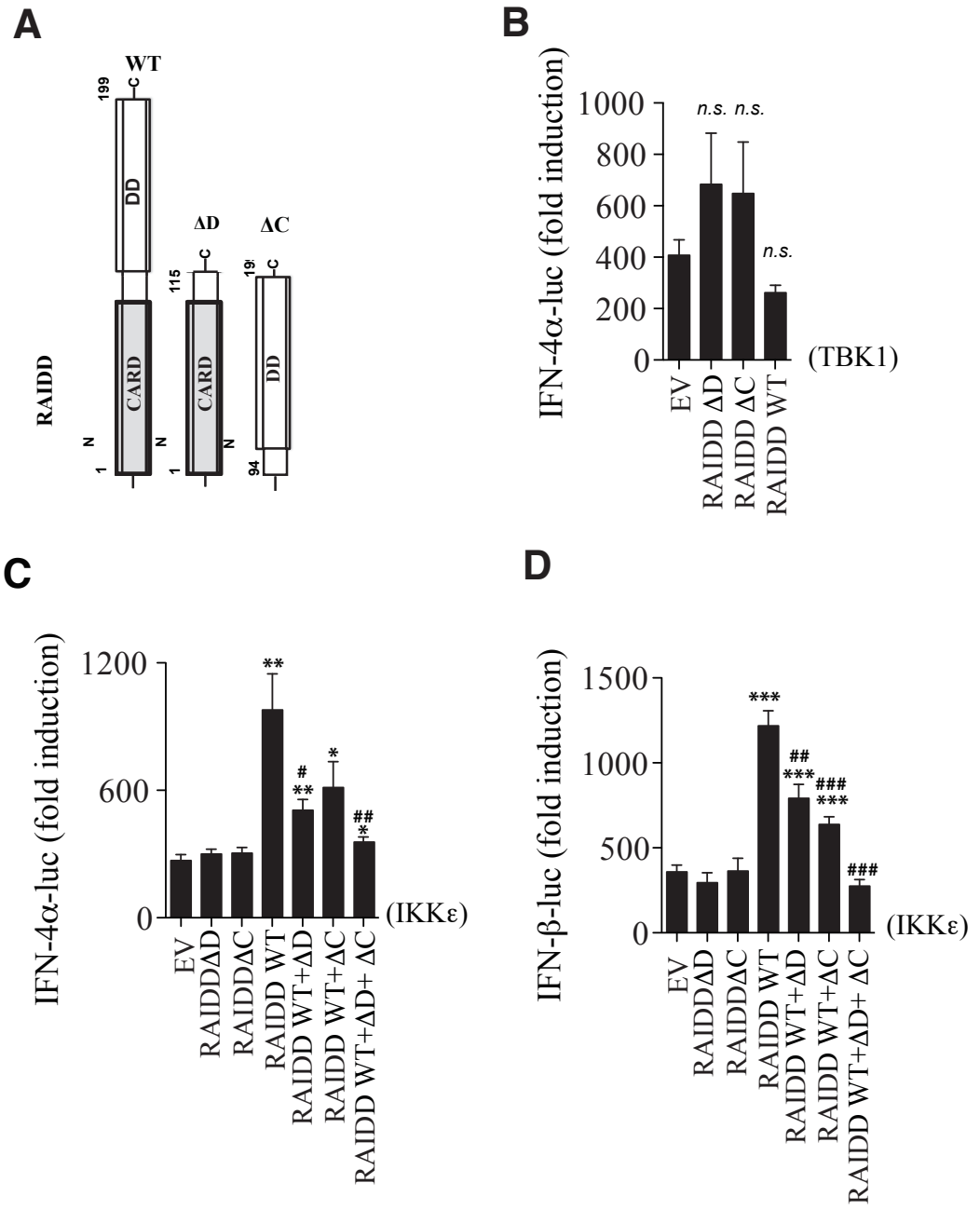
A
WT
199
C
DD
ΔD
ΔC
115
C
19
C
RAIDD
CARD
CARD
DD
N
1
N
1
N
94
B
IFN-4α-luc (fold induction)
1000
800
600
400
200
0
n.s.
n.s.
n.s.
(TBK1)
EV
RAIDD ΔD
RAIDD ΔC
RAIDD WT
C
IFN-4α-luc (fold induction)
1200
600
0
**
#
**
*
##
*
(IKKε)
EV
RAIDDΔD
RAIDDΔC
RAIDD WT
RAIDD WT+ΔD
RAIDD WT+ΔC
RAIDD WT+ΔD+ ΔC
D
IFN-β-luc (fold induction)
1500
1000
500
0
***
##
***
###
***
###
(IKKε)
EV
RAIDDΔD
RAIDDΔC
RAIDD WT
RAIDD WT+ΔD
RAIDD WT+ΔC
RAIDD WT+ΔD+ ΔC

Figure 19: Full length RAIDD enhances IKKε mediated IFN-I activation.

(A) A diagram illustrating the constructs of RAIDD, Death domain truncated RAIDD (DD), and CARD Domain truncated RAIDD (DC) is shown. **(B-D)** 293t cells were transfected with Empty Vector (EV), RAIDD (DC), RAIDD (DD), and Full length RAIDD along with TBK1 (n=6 is shown) **(B)** and IKKε (n=6 is shown) **(C, D)**. At 24h after transfection, IFN4α **(B,C)** and IFNβ **(D)** luciferase activities were measured.

RAIDD Coordinates the IKKε and IRF7 activation driven IFN –I Production

To further investigate the molecular interaction of RAIDD, we co-expressed IKKε together with empty vectors or CARD or DD or full-length RAIDD and examined for the protein-protein interaction. Although the various mutants of RAIDD were uniformly expressed, only the full-length RAIDD showed interaction with IKKε (Figure 20A). Consistently, the reciprocal immunoprecipitation also showed interaction of IKKε only with full length RAIDD but not with the one of the mutants (Figure 20B). Next, we examined the synergetic effects of these components and co-expressed empty vectors or CARD or DD or full length RAIDD together with IKKε + IRF7 following analysis of luciferase activity driven by IFN4α and IFNβ promoters. We observed significant IFN-I activation only in the presence of the full length RAIDD in sharp contrast to both deletion mutants (Figure 20C and D). We therefore hypothesized that intact RAIDD triggered IKKε and IRF7 mediated induction of IFN-I. Taken together, our data shows that RAIDD interacts with IRF7 and IKKε to coordinate IKKε mediated IRF7 activation and IFN-I production.

Figure 20

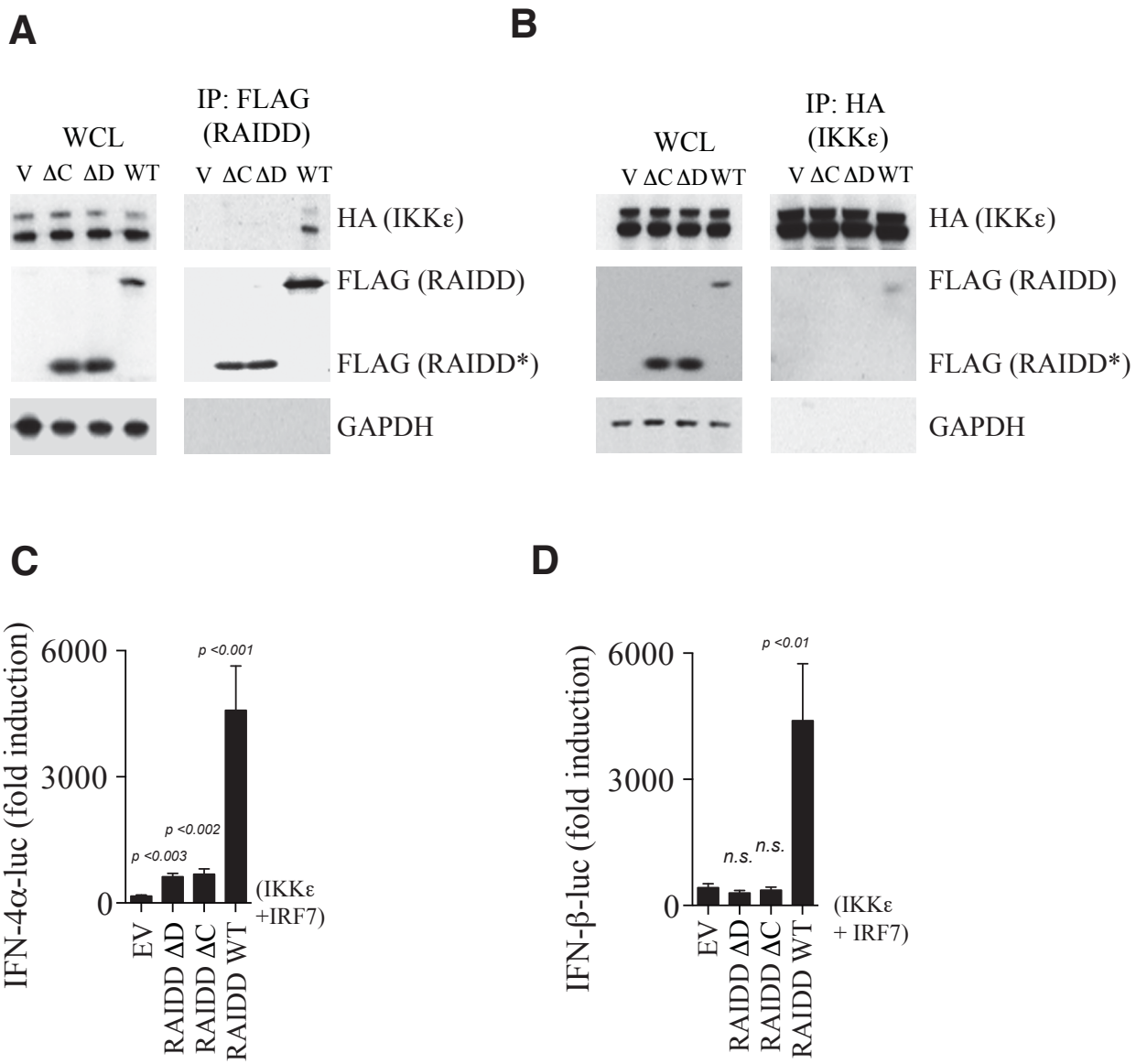
A
B
WCL
V ΔC ΔD WT
IP: FLAG
(RAIDD)
V ΔC ΔD WT
HA (IKKε)
FLAG (RAIDD)
FLAG (RAIDD*)
GAPDH
WCL
V ΔC ΔD WT
IP: HA
(IKKε)
V ΔC ΔD WT
HA (IKKε)
FLAG (RAIDD)
FLAG (RAIDD*)
GAPDH
C
D
IFN-4α-luc (fold induction)
6000
3000
0
p <0.001
p <0.002
p <0.003
EV
RAIDD ΔD
RAIDD ΔC
RAIDD WT
(IKKε
+IRF7)
IFN-β-luc (fold induction)
6000
3000
0
p <0.01
n.s.
n.s.
EV
RAIDD ΔD
RAIDD ΔC
RAIDD WT
(IKKε
+ IRF7)

Figure 20: Full length RAIDD interacts with RAIDD and drives the IFN-I mediated by IKKε and IRF7.

(A) 293t cells were lysed followed by immunoprecipitation (IP) using anti-FLAG (RAIDD) **(A)** or anti-HA (IKKε) **(B)** antibodies. Immunoblots were probed using anti-FLAG or anti-HA antibodies, along with anti-GAPDH as control (one representative of 3 experiments is shown). **(C, D)** 293t cells were transfected with Empty Vector (EV), RAIDD (ΔC), RAIDD (ΔD), and Full length RAIDD along with IKKε and IRF7. After 24h, cells were lysed and analyzed for IFN4α **(C)** (n=6 is shown) and IFNβ **(D)** (n=6 is shown) luciferase activities.

Chapter 6 - DISCUSSION:

Innate immune response plays a critical role in pathogen recognition and subsequent production of effector modulators such as TNF or IFN-I to control invading pathogens [12-14]. Here, we have characterized two adaptor proteins, iRhoms and RAIDD that play a crucial role in innate immunity.

The rhomboid proteases iRhom1 and 2 are considered inactive proteases [232, 233]. The removal of conserved cytoplasmic domains of iRhoms did not alter the functions. Nevertheless, their abundance and widespread expression strongly indicate that iRhoms should have an essential function. Earlier studies showed that, similar to flies, mammalian iRhoms could promote ERAD of EGF [234], but the physiological significance of this remains unclear. Knockout mouse studies suggested a differential role but also equally important role of mammalian iRhoms [70, 148]. The iRhom2 deficient murine models indicate that iRhom2 regulation is restricted to the hematopoietic compartment [70, 148, 168]. Further analysis shows that iRhom2 KO mice have intensive immunological defects. The iRhom2-deficient mice showed defects in ADAM17 activation and as the consequence is showed impaired TNF response to bacterial infection [70, 148]. In turn, iRhom2 expression was correlated with TNF-driven inflammatory arthritis in patients [235].

Similar to iRhom2, iRhom1 knockout mice also showed defects in ADAM17 activation in brain tissues, where iRhom2 expression is low [167]. Both iRhom1 and 2 reported to have similar interaction with ADAM17 [166, 167]. Notably, iRhom1-deficient mice showed a viability difference when compared with two knockout models. Earlier mouse models revealed that iRhom1-deficient mice were considered as embryonically lethal [166], whereas the more recent models showed they are

viable [167]. Furthermore, it was argued that extensive deletion of exons in the earlier models might be the cause for lethality, which requires further investigation. The iRhom1/2 double knockout mice showed the phenocopy of ADAM17-deficient mice. Furthermore, the characterization of iRhom1/2 double knockout mice [166, 167] or siRNA knockdown experiment [236] suggests that the primary role of iRhom1 and 2 is to regulate ADAM17. Overall, these data strongly indicate that for ADAM17 activity the iRhoms (iRhom1 or iRhom 2, or both) are highly indispensable [166, 167].

Based on a CPR screening, we investigated the role of iRhom1 or iRhom2, which lacks part of their extended N-terminal cytoplasmic domains. These truncated iRhoms triggered activation of ADAM17 and conceptually resistance to TNF-induced cytotoxicity. The hyperactivation of ADAM17 led to shedding of cell surface TNF receptors. Further, we observed a functional similarity between iRhom1 and iRhom2, suggesting the importance of the iRhom N-terminal cytoplasmic domain. Mechanistically, we found that WT iRhoms and truncated iRhoms showed similar interaction with ADAM17 and this indicates that the N-terminal cytoplasmic domain is dispensable for the interaction with ADAM17. Loss of the N-terminal cytoplasmic tail of iRhoms results in enriched plasma membrane localization. We speculate that membrane localization of mutant iRhoms might be an important factor for driving ADAM17 activity.

On the other hand, the conserved cytoplasmic N-terminal domain is very critical for the actions of both iRhom1 and iRhom2. Inherited dominant N-terminal mutations in human iRhom2 lead to esophageal cancer [228]. TOC-derived cell lines suggest

that these mutations could manipulate ADAM17 activity. It could have a direct impact on the consequence of neoplasia as observed in TOC keratinocytes, either by the constitutive shedding of EGFR ligands which is strongly implicated in cancer [229] or by shedding of TNFRs as an evasion mechanism for tumor cells from TNF-mediated tumor control. Similarly, the elevated expression of ADAM17 is also known to be associated with breast, ovarian, kidney, colon, and prostate cancers [230].

Furthermore, similar defects were also reported in murine models that lack the N-terminus of iRhom2, which exhibited severe hair loss and skin [231-234]. Moreover, the mice bearing both cub and Uncv allele displayed abnormalities that could be correlated with the deregulation of ADAM17 substrates. In case of both cub and Uncv, they showed an apparent decrease in expression of mature ADAM17 and it is reported to be the consequence of hyperactive ADAM17 [233, 234] [235]. We also observed similar apparent reduction in the mature form of ADAM17 in truncated iRhom cell lysates with increased activity of ADAM17.

Subsequently, this could be rescued by blocking ADAM17 function either chemically via marimastat or through specific molecular targets (ADAM17 shRNA). Moreover, the inhibition of ADAM17 using marimastat in iRhom2-ΔN-expressing cells provides the evidence of hyperactive ADAM17. Also our results associated with the N-terminal iRhom mutations with the activation of ADAM17 and might explain why familial human mutations in the N-terminus of iRhom2 can cause tissue overgrowth and oesophageal cancer.

In addition, ADAM17 is one of the components of innate immunity, which regulates EGFR and TNFR signaling pathways, and controls cell growth, cell death, oncogenesis, and immunity. Although many cell surface proteins are regulated by ADAM17 activity, the precise mechanisms involved in this regulation are poorly understood [154]. In addition to TNF and TNFR shedding, the iRhoms were reported to promote shedding of distinct ADAM17 substrates. iRhom2 regulates ADAM17 to shed epiregulin, EphB4, Kit ligand 2, heparin-binding EGF-like growth factor. TGFα shedding appears to be influenced by iRhom1 and iRhom2 [168].

Our data indicate that the N-terminal cytoplasmic tail of iRhom1 and 2 adaptor protein showed constitutive shedding of ADAM17 substrates for TNFRs, Kit ligand 2 and TGFα, thereby influencing the innate immune response. Taken together, this study shows that truncated iRhoms participate in ADAM17 mediated shedding mechanism on TNFRs which could protect cells from TNFα-induced apoptosis. Our data highlight the potential of iRhoms as a novel drug target for therapeutic interventions during inflammatory mediated diseases.

In a parallel study, another adaptor protein from the DD superfamily protein named RAIDD regulates the IFN-I signaling. DD superfamily proteins are known to exist as a single interacting domain or combined with two functional interacting domains, which are known to regulate multiple signaling cascades. The impact of DD superfamily is well known in the mammalian IL-1 receptor and Toll-like receptor (TLR) pathways [241]. In addition to the mammalian system, the expression of the DD superfamily proteins was reported in viruses in order to evade the host's innate

antiviral cytoxicity response [261]. The integration of DED-containing sequences in herpes virus and both DED-containing and PYD-containing sequences in poxviruses was acquired to interfere with the host apoptotic and inflammatory response against viral infection [261, 262].

In addition to TIR-containing adapters TIR-containing protein TIRAP, the IL-1 receptor and most Toll-like receptors recruits MyD88 [219]. MyD88 has both a DD and a TIR domain, and it recruits IRAKs (which include IRAK1, IRAK2, IRAKM and IRAK4) via a DD interaction. IRAKs are composed of a DD and a Ser/Thr kinase domain [219, 263]. Consequently IRAKs recruits TRAF6 for NFκB activation [264]. In Drosophila, the toll like receptor pathway is crucial for mediating anti-fungal immune responses [28] and for dorsoventral patterning [264, 265]. Similar to toll-like receptor pathway, the assembly of Tube and Pelle in Drosophila is mediated through the DD interactions. Pelle was considered as the functional ortholog of IRAK and Tube of MyD88 [267]. Therefore, the characterization of the DD superfamily is crucial to understand the fundamental principle of innate immunity. In our study we found that the deletion of either the death domain (DD) or the caspase recruitment domain (CARD) of RAIDD could not rescue IKKε and IRF7-mediated IFN-I, whereas intact RAIDD expression could reverse it.

We report for the first time that another DD superfamily protein, RAIDD, coordinates TLR3-driven IFN-I production during innate immunity. RAIDD is the only protein in the human and mouse genomes that contains both DD and a CARD [224, 239]. RAIDD was described to be expressed in almost all tissues; except the

brain, lung and kidneys, which had reduced expression [224]. This protein has been repeatedly suggested to regulate programmed cell death pathways. The interaction of RAIDD was reported to be associated with PIDD (p53-induced death domain protein) and caspase-2 to form a PIDDosome complex [225, 226]. This complex was observed to be important during the DNA damage or lethal heat shock response. Recent findings argued against this complex formation [268] and indicate other essential roles for RAIDD in signaling cascades.

In support of that, RAIDD was reported to sequester the B-cell CLL/Lymphoma 10 (BCL10) and it negatively regulates NFκB-dependent cytokine and chemokine expression in T cells [223]. Furthermore, a similar interaction was observed in endothelial cells under inflammatory conditions [269]. In our study, we found that RAIDD shows molecular interaction with IRF7. After TLR3 stimulation, a knockdown of RAIDD impaired nuclear translocation of IRF7, suggesting an interaction of RAIDD and IRF7 at the protein level.

Activation of IRF7 is required for the IFN I transcription. TLR3, 4,7,8,9 [249], and cytosolic RLRs, [115-117], are known to activate the IRF 7 for the production of type I IFNs. Recent studies have identified the surprising roles of TLR2 and 8 in cell-specific activation of IRFs for production of type I IFNs [270-272]. The internalized TLR2 activates IRF1, 3 and 7 in inflammatory monocytes and bone marrow-derived macrophages [270]. In our study, we found RAIDD deficiency particularly affects down stream activation of TLR3 but not RLR-mediated IFN-I production.

Adaptor molecules such as TRIF are essential for TLR3 and 4 signaling. MyD88 is essential for TLR2/7/8/9, and IRAK1/4 [128, 130] TRAF6 (for TLR7, 8 and 9 and RIG-I) [133, 222] and TRAF3 (for TLR3 and 4, RIG-I, and nucleotide-binding oligomerization domain-2) [112, 115-117] mediated signaling. The recruitment of all these adaptor proteins culminates in the activation of IKKε and TBK1. Both TBK1 and IKKε can phosphorylate IRF3/7 transcription factors. Furthermore, IRF7 phosphorylation was reported to be negatively regulated by the recently identified factor Pellino3 through the interaction with TRAF6 [252].

However, since we did not observe binding of RAIDD to TRAF6, we speculate that RAIDD triggers activation and nuclear translocation of IRF7 through a Pellino3 independent mechanism. Moreover, the 2-5´-oligoadenylate synthetase (OAS) family member OASL1 has been shown to prevent IRF7 mRNA translation and consequently IFN-I production [251]. Notably, the transcription factor ELF4 can enhance IRF3 and IRF7 binding followed by phosphorylation of TBK1 [273]. However, we observed no difference in TBK1-mediated IFN4α promoter activity following the knockdown of RAIDD. Our data indicate an alternative mechanism in which RAIDD connects IRF7 to the upstream kinase IKKε thereby increasing IFN-I production. We identified RAIDD as a crucial adaptor protein for innate immune activation. We have delineated an unexpected TBK1-independent signaling pathway that feeds via IKKε to IRF7 activation. Consequently, our data show that this pathway is crucial for IFN-I production. In conclusion, the doctoral research has provided a body of scientific evidence that supports the pivotal role of iRhom1 and 2 and RAIDD in innate immune response and its function.

Chapter 7 - LIST OF PUBLICATION

1. Deletions in the cytoplasmic domain of iRhom1 and iRhom2 promote shedding of the TNF receptor by the protease ADAM17, **Maney SK**, *et al*., Sci Signal. 2015 Nov.

2. RAIDD Mediates TLR3 and IRF7 Driven Type I Interferon Production, **Maney SK**, *et al*., Cell Physiol Biochem. 2016 (accepted for publication).

3. CEACAM1 induces B-cell survival and is essential for protective antiviral antibody production, Khairnar V, Duhan V, **Maney SK**, *et al*., Nat Commun. 2015 Feb.

4. Deficiency of the B cell-activating factor receptor results in limited CD169+ macrophage function during viral infection, Xu HC, Huang J, Khairnar V, Duhan V, Pandyra AA, Grusdat M, Shinde P, McIlwain DR, **Maney SK**, *et al*., J Virol. 2015 May.

5. IRF4 and BATF are critical for $CD8^+$ T-cell function following infection with LCMV,Grusdat M, McIlwain DR, Xu HC, Pozdeev VI, Knievel J, Crome SQ, Robert-Tissot C, Dress RJ, Pandyra AA, Speiser DE, Lang E, **Maney SK**, *et al*.,Cell Death Differ. 2014 Jul.

6. Reactive oxygen species delay control of lymphocytic choriomeningitis virus, Lang PA, Xu HC, Grusdat M, McIlwain DR, Pandyra AA, Harris IS, Shaabani N, Honke N, **Maney SK**, *et al*., Cell Death Differ. 2013 Apr.

7. Tricin 4'-O-(erythro-β-guaiacylglyceryl) ether and tricin 4'-O-(threo-β-guaiacylglyceryl) ether isolated from Njavara (Oryza sativa L. var. Njavara), induce apoptosis in multiple tumor cells by mitochondrial pathway, Mohanlal S, **Maney SK,** *et al.* JNat Med. 2013 Jul.

8. iRhom2 regulation of TACE controls TNF-mediated protection against Listeria and responses to LPS. McIlwain DR, Lang PA, Maretzky T, Hamada K, Ohishi K, **Maney SK**, *et al.,* Science. 2012 Jan.

9. Effect of apoptosis-inducing antitumor agents on endocardial endothelial cells, **Maney SK**,*et al*., Cardiovasc Toxicol. 2011,Sep.

10. Endoplasmic reticulum targeted Bcl2 confers long term cell survival through phosphorylation of heat shock protein 27, Chandrika BB, **Maney SK** *et al*., Int J Biochem Cell Biol. 2010 Dec.

11. Bax deficiency mediated drug resistance can be reversed by endoplasmic reticulum stress induced death signaling, Chandrika BB, **Maney SK**, *et al*., Biochem Pharmacol. 2010 Jun.

Chapter 8 - CURRICULUM VITAE

SATHISH KUMAR MANEY

Post Doctoral Fellow,
Molecular Medicine II,
Germany- 40225,
Citizenship – India,
DOB – 02.09.1984,

SCHOLARSHIP & AWARDS

- Awarded best poster presentation on GASL, HHU, Germany 2016.
- Qualified CSIR - Junior Research Scholarship, 2009.
- Recipient of IASc-INSA-NASI Summer Research Scholarship, 2007.
- Qualified Graduate Aptitude Test in Engineering (GATE) Scholarship, 2007 & 09.

TECHNICAL EXPERIENCE

- Primary cell culture- Dendritic cells (DC), Macrophages (MC), T & B cells.
- Genome Wide Screening using CRISPR Technology.
- Genetic Engineering of cells using lentiviral (shRNA& cDNA) or transient methods.
- Immmunoblotting, Co-immunoprecipitation and Fluorescent Microscopy.
- ELISA, Quantitative PCR, Microarray / RNA Seq Analysis.
- Interferon α, β, γ and NFκB etc., Promoter Binding Assay using Dual luciferase methods.
- Cell viability Assay - MTT, Clonogenic assay, Cell Cycle & ANNEXIN/ 7ADD Assay.
- Viral infection - LCMV, VSV, Listeria, RIPgp (type I diabetes) via I.P& I.V routes.
- Viral Quantification – Plaque Assay and Multicolor FACS staining and analysis.
- Sample collection – Blood, Brain, Spinal Cord, Spleen, Liver, Lymphnode etc.,
- Software Skills - Adobe Photoshop & Illustrator, Flowjo, Graphpad Prizm,
-

MENTORSHIP EXPERIENCES

Degree	Years	Subject	Institute
Master student	2008-2009	Heat shock protein regulation in cell Cycle.	RGCB, India
Master Student	2009-2010	Cell survival signaling during ER stress.	RGCB, India
Master Student	2014 - 2015	iRHOM2 regulation in TNFR Shedding	HHU, Germany

Chapter 9 - REFERENCES

1. *Introduction to Pathogens*
. 4th ed. Molecular biology of the cell, ed. B. Alberts. 2002, New York: Garland Science. xxxiv, 1464 p.
2. Iqbal, M.M., et al., *Spectrum of organisms causing peritonitis in peritoneal dialysis patients--experience from Bangladesh.* Adv Perit Dial, 2008. **24**: p. 40-3.
3. Fauci, A.S. and D.M. Morens, *The perpetual challenge of infectious diseases.* N Engl J Med, 2012. **366**(5): p. 454-61.
4. Ampel, N.M., *Plagues--what's past is present: thoughts on the origin and history of new infectious diseases.* Rev Infect Dis, 1991. **13**(4): p. 658-65.
5. Woolhouse, M. and E. Gaunt, *Ecological origins of novel human pathogens.* Crit Rev Microbiol, 2007. **33**(4): p. 231-42.
6. Cleaveland, S., M.K. Laurenson, and L.H. Taylor, *Diseases of humans and their domestic mammals: pathogen characteristics, host range and the risk of emergence.* Philos Trans R Soc Lond B Biol Sci, 2001. **356**(1411): p. 991-9.
7. Woolhouse, M.E. and S. Gowtage-Sequeria, *Host range and emerging and reemerging pathogens.* Emerg Infect Dis, 2005. **11**(12): p. 1842-7.
8. Keesing, F., et al., *Impacts of biodiversity on the emergence and transmission of infectious diseases.* Nature, 2010. **468**(7324): p. 647-52.
9. Morens, D.M., G.K. Folkers, and A.S. Fauci, *The challenge of emerging and re-emerging infectious diseases.* Nature, 2004. **430**(6996): p. 242-9.
10. Parrish, C.R., et al., *Cross-species virus transmission and the emergence of new epidemic diseases.* Microbiol Mol Biol Rev, 2008. **72**(3): p. 457-70.
11. Quinn, T.C., *Population migration and the spread of types 1 and 2 human immunodeficiency viruses.* Proc Natl Acad Sci U S A, 1994. **91**(7): p. 2407-14.
12. Janeway, C.A., Jr., *The immune system evolved to discriminate infectious nonself from noninfectious self.* Immunol Today, 1992. **13**(1): p. 11-6.
13. Medzhitov, R. and C.A. Janeway, Jr., *Innate immunity: the virtues of a nonclonal system of recognition.* Cell, 1997. **91**(3): p. 295-8.
14. Janeway, C.A., Jr., *Approaching the asymptote? Evolution and revolution in immunology.* Cold Spring Harb Symp Quant Biol, 1989. **54 Pt 1**: p. 1-13.
15. Akinbi, H.T., et al., *Bacterial killing is enhanced by expression of lysozyme in the lungs of transgenic mice.* J Immunol, 2000. **165**(10): p. 5760-6.
16. Cole, A.M., et al., *Cationic polypeptides are required for antibacterial activity of human airway fluid.* J Immunol, 2002. **169**(12): p. 6985-91.
17. Dubin, R.F., S.K. Robinson, and J.H. Widdicombe, *Secretion of lactoferrin and lysozyme by cultures of human airway epithelium.* Am J Physiol Lung Cell Mol Physiol, 2004. **286**(4): p. L750-5.
18. Nash, J.A., et al., *The peptidoglycan-degrading property of lysozyme is not required for bactericidal activity in vivo.* J Immunol, 2006. **177**(1): p. 519-26.
19. Singh, P.K., et al., *A component of innate immunity prevents bacterial biofilm development.* Nature, 2002. **417**(6888): p. 552-5.
20. Ganz, T., *Defensins: antimicrobial peptides of innate immunity.* Nat Rev Immunol, 2003. **3**(9): p. 710-20.
21. Klotman, M.E. and T.L. Chang, *Defensins in innate antiviral immunity.* Nat Rev Immunol, 2006. **6**(6): p. 447-56.

22. Nigro, E., et al., *An ancestral host defence peptide within human beta-defensin 3 recapitulates the antibacterial and antiviral activity of the full-length molecule.* Sci Rep, 2015. **5**: p. 18450.
23. Selsted, M.E. and A.J. Ouellette, *Mammalian defensins in the antimicrobial immune response.* Nat Immunol, 2005. **6**(6): p. 551-7.
24. Wilson, S.S., M.E. Wiens, and J.G. Smith, *Antiviral mechanisms of human defensins.* J Mol Biol, 2013. **425**(24): p. 4965-80.
25. Kolev, M., G. Le Friec, and C. Kemper, *Complement--tapping into new sites and effector systems.* Nat Rev Immunol, 2014. **14**(12): p. 811-20.
26. Fujita, T., *Evolution of the lectin-complement pathway and its role in innate immunity.* Nat Rev Immunol, 2002. **2**(5): p. 346-53.
27. Zipfel, P.F. and C. Skerka, *Complement regulators and inhibitory proteins.* Nat Rev Immunol, 2009. **9**(10): p. 729-40.
28. Branger, J., et al., *Role of Toll-like receptor 4 in gram-positive and gram-negative pneumonia in mice.* Infect Immun, 2004. **72**(2): p. 788-94.
29. Ghosh, S., M.J. May, and E.B. Kopp, *NF-kappa B and Rel proteins: evolutionarily conserved mediators of immune responses.* Annu Rev Immunol, 1998. **16**: p. 225-60.
30. Isaacs, A., R.A. Cox, and Z. Rotem, *Foreign nucleic acids as the stimulus to make interferon.* Lancet, 1963. **2**(7299): p. 113-6.
31. Lemaitre, B., et al., *The dorsoventral regulatory gene cassette spatzle/Toll/cactus controls the potent antifungal response in Drosophila adults.* Cell, 1996. **86**(6): p. 973-83.
32. Medzhitov, R., P. Preston-Hurlburt, and C.A. Janeway, Jr., *A human homologue of the Drosophila Toll protein signals activation of adaptive immunity.* Nature, 1997. **388**(6640): p. 394-7.
33. Miettinen, M., et al., *IFNs activate toll-like receptor gene expression in viral infections.* Genes Immun, 2001. **2**(6): p. 349-55.
34. Rotem, Z., R.A. Cox, and A. Isaacs, *Inhibition of virus multiplication by foreign nucleic acid.* Nature, 1963. **197**: p. 564-6.
35. Brint, E.K., et al., *ST2 is an inhibitor of interleukin 1 receptor and Toll-like receptor 4 signaling and maintains endotoxin tolerance.* Nat Immunol, 2004. **5**(4): p. 373-9.
36. Iwasaki, A. and R. Medzhitov, *Toll-like receptor control of the adaptive immune responses.* Nat Immunol, 2004. **5**(10): p. 987-95.
37. Kato, H., K. Takahasi, and T. Fujita, *RIG-I-like receptors: cytoplasmic sensors for non-self RNA.* Immunol Rev, 2011. **243**(1): p. 91-8.
38. Kawai, T. and S. Akira, *Innate immune recognition of viral infection.* Nat Immunol, 2006. **7**(2): p. 131-7.
39. Keating, S.E., M. Baran, and A.G. Bowie, *Cytosolic DNA sensors regulating type I interferon induction.* Trends Immunol, 2011. **32**(12): p. 574-81.
40. Dorner, T. and A. Radbruch, *Antibodies and B cell memory in viral immunity.* Immunity, 2007. **27**(3): p. 384-92.
41. Cancro, M.P. and J.F. Kearney, *B cell positive selection: road map to the primary repertoire?* J Immunol, 2004. **173**(1): p. 15-9.
42. Crotty, S., et al., *Cutting edge: long-term B cell memory in humans after smallpox vaccination.* J Immunol, 2003. **171**(10): p. 4969-73.
43. Amanna, I.J., M.K. Slifka, and S. Crotty, *Immunity and immunological memory following smallpox vaccination.* Immunol Rev, 2006. **211**: p. 320-37.

44. Ahmed, R. and D. Gray, *Immunological memory and protective immunity: understanding their relation.* Science, 1996. **272**(5258): p. 54-60.
45. Bachmann, M.F., et al., *Maintenance of memory CTL responses by T helper cells and CD40-CD40 ligand: antibodies provide the key.* Eur J Immunol, 2004. **34**(2): p. 317-26.
46. Anderson, S.M., L.G. Hannum, and M.J. Shlomchik, *Memory B cell survival and function in the absence of secreted antibody and immune complexes on follicular dendritic cells.* J Immunol, 2006. **176**(8): p. 4515-9.
47. Vieira, P. and K. Rajewsky, *Persistence of memory B cells in mice deprived of T cell help.* Int Immunol, 1990. **2**(6): p. 487-94.
48. Zinkernagel, R.M. and H. Hengartner, *Protective 'immunity' by pre-existent neutralizing antibody titers and preactivated T cells but not by so-called 'immunological memory'.* Immunol Rev, 2006. **211**: p. 310-9.
49. Wedemayer, G.J., et al., *Structural insights into the evolution of an antibody combining site.* Science, 1997. **276**(5319): p. 1665-9.
50. Gray, D., et al., *B-T lymphocyte interactions in the generation and survival of memory cells.* Immunol Rev, 1996. **150**: p. 45-61.
51. Brehm, M.A., L.K. Selin, and R.M. Welsh, *CD8 T cell responses to viral infections in sequence.* Cell Microbiol, 2004. **6**(5): p. 411-21.
52. Banchereau, J., et al., *The CD40 antigen and its ligand.* Annu Rev Immunol, 1994. **12**: p. 881-922.
53. Homann, D., L. Teyton, and M.B. Oldstone, *Differential regulation of antiviral T-cell immunity results in stable CD8+ but declining CD4+ T-cell memory.* Nat Med, 2001. **7**(8): p. 913-9.
54. Goldrath, A.W. and M.J. Bevan, *Low-affinity ligands for the TCR drive proliferation of mature CD8+ T cells in lymphopenic hosts.* Immunity, 1999. **11**(2): p. 183-90.
55. Harrington, L.E., et al., *Recombinant vaccinia virus-induced T-cell immunity: quantitation of the response to the virus vector and the foreign epitope.* J Virol, 2002. **76**(7): p. 3329-37.
56. Goldrath, A.W. and M.J. Bevan, *Selecting and maintaining a diverse T-cell repertoire.* Nature, 1999. **402**(6759): p. 255-62.
57. Rudolph, M.G. and I.A. Wilson, *The specificity of TCR/pMHC interaction.* Curr Opin Immunol, 2002. **14**(1): p. 52-65.
58. Sprent, J. and C.D. Surh, *T cell memory.* Annu Rev Immunol, 2002. **20**: p. 551-79.
59. Mason, D., *A very high level of crossreactivity is an essential feature of the T-cell receptor.* Immunol Today, 1998. **19**(9): p. 395-404.
60. Decaestecker, E., et al., *Host-parasite 'Red Queen' dynamics archived in pond sediment.* Nature, 2007. **450**(7171): p. 870-3.
61. Deane, A.S., *Early Miocene catarrhine dietary behaviour: the influence of the Red Queen Effect on incisor shape and curvature.* J Hum Evol, 2009. **56**(3): p. 275-85.
62. Brockhurst, M.A., et al., *Running with the Red Queen: the role of biotic conflicts in evolution.* Proc Biol Sci, 2014. **281**(1797).
63. Tellier, A., S. Moreno-Gamez, and W. Stephan, *Speed of adaptation and genomic footprints of host-parasite coevolution under arms race and trench warfare dynamics.* Evolution, 2014. **68**(8): p. 2211-24.
64. Samson, J.E., et al., *Revenge of the phages: defeating bacterial defences.* Nat Rev Microbiol, 2013. **11**(10): p. 675-87.

65. Regules, J.A., et al., *A Recombinant Vesicular Stomatitis Virus Ebola Vaccine - Preliminary Report.* N Engl J Med, 2015.
66. Barry, M., *The tail end of guinea worm - global eradication without a drug or a vaccine.* N Engl J Med, 2007. **356**(25): p. 2561-4.
67. Ewer, K., et al., *A Monovalent Chimpanzee Adenovirus Ebola Vaccine Boosted with MVA.* N Engl J Med, 2016. **374**(17): p. 1635-46.
68. Jacobson, I.M., et al., *Telaprevir for previously untreated chronic hepatitis C virus infection.* N Engl J Med, 2011. **364**(25): p. 2405-16.
69. Kowdley, K.V., et al., *Phase 2b trial of interferon-free therapy for hepatitis C virus genotype 1.* N Engl J Med, 2014. **370**(3): p. 222-32.
70. Savolainen, T., *Tetanus following vaccination against variola.* Ann Med Exp Biol Fenn, 1950. **28**(2): p. 168-73.
71. Sherman, K.E., et al., *Response-guided telaprevir combination treatment for hepatitis C virus infection.* N Engl J Med, 2011. **365**(11): p. 1014-24.
72. Matzinger, P., *The danger model: a renewed sense of self.* Science, 2002. **296**(5566): p. 301-5.
73. Medzhitov, R. and C. Janeway, Jr., *Innate immunity.* N Engl J Med, 2000. **343**(5): p. 338-44.
74. Basset, C., et al., *Innate immunity and pathogen-host interaction.* Vaccine, 2003. **21 Suppl 2**: p. S12-23.
75. Broz, P. and D.M. Monack, *Newly described pattern recognition receptors team up against intracellular pathogens.* Nat Rev Immunol, 2013. **13**(8): p. 551-65.
76. Kawai, T. and S. Akira, *The role of pattern-recognition receptors in innate immunity: update on Toll-like receptors.* Nat Immunol, 2010. **11**(5): p. 373-84.
77. Medzhitov, R., *Recognition of microorganisms and activation of the immune response.* Nature, 2007. **449**(7164): p. 819-26.
78. O'Neill, L.A., D. Golenbock, and A.G. Bowie, *The history of Toll-like receptors - redefining innate immunity.* Nat Rev Immunol, 2013. **13**(6): p. 453-60.
79. Qian, C., J. Liu, and X. Cao, *Innate signaling in the inflammatory immune disorders.* Cytokine Growth Factor Rev, 2014. **25**(6): p. 731-8.
80. Gordon, S., *Pattern recognition receptors: doubling up for the innate immune response.* Cell, 2002. **111**(7): p. 927-30.
81. Chamaillard, M., et al., *An essential role for NOD1 in host recognition of bacterial peptidoglycan containing diaminopimelic acid.* Nat Immunol, 2003. **4**(7): p. 702-7.
82. Girardin, S.E., et al., *Nod1 detects a unique muropeptide from gram-negative bacterial peptidoglycan.* Science, 2003. **300**(5625): p. 1584-7.
83. Girardin, S.E., et al., *Nod2 is a general sensor of peptidoglycan through muramyl dipeptide (MDP) detection.* J Biol Chem, 2003. **278**(11): p. 8869-72.
84. Girardin, S.E., et al., *Peptidoglycan molecular requirements allowing detection by Nod1 and Nod2.* J Biol Chem, 2003. **278**(43): p. 41702-8.
85. Hugot, J.P., et al., *Association of NOD2 leucine-rich repeat variants with susceptibility to Crohn's disease.* Nature, 2001. **411**(6837): p. 599-603.
86. Inohara, N., et al., *Host recognition of bacterial muramyl dipeptide mediated through NOD2. Implications for Crohn's disease.* J Biol Chem, 2003. **278**(8): p. 5509-12.

87. Chin, A.I., et al., *Involvement of receptor-interacting protein 2 in innate and adaptive immune responses.* Nature, 2002. **416**(6877): p. 190-4.
88. Kasper, C.A., et al., *Cell-cell propagation of NF-kappaB transcription factor and MAP kinase activation amplifies innate immunity against bacterial infection.* Immunity, 2010. **33**(5): p. 804-16.
89. Kim, Y.G., et al., *The cytosolic sensors Nod1 and Nod2 are critical for bacterial recognition and host defense after exposure to Toll-like receptor ligands.* Immunity, 2008. **28**(2): p. 246-57.
90. Legrand-Poels, S., et al., *Modulation of Nod2-dependent NF-kappaB signaling by the actin cytoskeleton.* J Cell Sci, 2007. **120**(Pt 7): p. 1299-310.
91. Meinzer, U., et al., *Yersinia pseudotuberculosis effector YopJ subverts the Nod2/RICK/TAK1 pathway and activates caspase-1 to induce intestinal barrier dysfunction.* Cell Host Microbe, 2012. **11**(4): p. 337-51.
92. Cui, S., et al., *The C-terminal regulatory domain is the RNA 5'-triphosphate sensor of RIG-I.* Mol Cell, 2008. **29**(2): p. 169-79.
93. Pichlmair, A., et al., *RIG-I-mediated antiviral responses to single-stranded RNA bearing 5'-phosphates.* Science, 2006. **314**(5801): p. 997-1001.
94. Takahasi, K., et al., *Nonself RNA-sensing mechanism of RIG-I helicase and activation of antiviral immune responses.* Mol Cell, 2008. **29**(4): p. 428-40.
95. Yoneyama, M., et al., *The RNA helicase RIG-I has an essential function in double-stranded RNA-induced innate antiviral responses.* Nat Immunol, 2004. **5**(7): p. 730-7.
96. Kato, H., et al., *Differential roles of MDA5 and RIG-I helicases in the recognition of RNA viruses.* Nature, 2006. **441**(7089): p. 101-5.
97. Yoneyama, M., et al., *Shared and unique functions of the DExD/H-box helicases RIG-I, MDA5, and LGP2 in antiviral innate immunity.* J Immunol, 2005. **175**(5): p. 2851-8.
98. Kowalinski, E., et al., *Structural basis for the activation of innate immune pattern-recognition receptor RIG-I by viral RNA.* Cell, 2011. **147**(2): p. 423-35.
99. Civril, F., et al., *The RIG-I ATPase domain structure reveals insights into ATP-dependent antiviral signalling.* EMBO Rep, 2011. **12**(11): p. 1127-34.
100. Jiang, F., et al., *Structural basis of RNA recognition and activation by innate immune receptor RIG-I.* Nature, 2011. **479**(7373): p. 423-7.
101. Luo, D., et al., *Structural insights into RNA recognition by RIG-I.* Cell, 2011. **147**(2): p. 409-22.
102. Gack, M.U., et al., *TRIM25 RING-finger E3 ubiquitin ligase is essential for RIG-I-mediated antiviral activity.* Nature, 2007. **446**(7138): p. 916-920.
103. Oshiumi, H., et al., *Riplet/RNF135, a RING finger protein, ubiquitinates RIG-I to promote interferon-beta induction during the early phase of viral infection.* J Biol Chem, 2009. **284**(2): p. 807-17.
104. Wu, B., et al., *Structural basis for dsRNA recognition, filament formation, and antiviral signal activation by MDA5.* Cell, 2013. **152**(1-2): p. 276-89.
105. Zeng, W., et al., *Reconstitution of the RIG-I pathway reveals a signaling role of unanchored polyubiquitin chains in innate immunity.* Cell, 2010. **141**(2): p. 315-30.
106. Berke, I.C., et al., *MDA5 assembles into a polar helical filament on dsRNA.* Proc Natl Acad Sci U S A, 2012. **109**(45): p. 18437-41.

107. Peisley, A., et al., *Cooperative assembly and dynamic disassembly of MDA5 filaments for viral dsRNA recognition.* Proc Natl Acad Sci U S A, 2011. **108**(52): p. 21010-5.
108. Sun, Q., et al., *The specific and essential role of MAVS in antiviral innate immune responses.* Immunity, 2006. **24**(5): p. 633-42.
109. Kumar, H., et al., *Essential role of IPS-1 in innate immune responses against RNA viruses.* J Exp Med, 2006. **203**(7): p. 1795-803.
110. Kato, H., et al., *Cell type-specific involvement of RIG-I in antiviral response.* Immunity, 2005. **23**(1): p. 19-28.
111. Kawai, T., et al., *IPS-1, an adaptor triggering RIG-I- and Mda5-mediated type I interferon induction.* Nat Immunol, 2005. **6**(10): p. 981-8.
112. Meylan, E., et al., *Cardif is an adaptor protein in the RIG-I antiviral pathway and is targeted by hepatitis C virus.* Nature, 2005. **437**(7062): p. 1167-72.
113. Seth, R.B., et al., *Identification and characterization of MAVS, a mitochondrial antiviral signaling protein that activates NF-kappaB and IRF 3.* Cell, 2005. **122**(5): p. 669-82.
114. Wu, J. and Z.J. Chen, *Innate immune sensing and signaling of cytosolic nucleic acids.* Annu Rev Immunol, 2014. **32**: p. 461-88.
115. Kawai, T. and S. Akira, *Toll-like receptor and RIG-I-like receptor signaling.* Ann N Y Acad Sci, 2008. **1143**: p. 1-20.
116. Beutler, B., *Not "molecular patterns" but molecules.* Immunity, 2003. **19**(2): p. 155-6.
117. Akira, S., S. Uematsu, and O. Takeuchi, *Pathogen recognition and innate immunity.* Cell, 2006. **124**(4): p. 783-801.
118. Brinkmann, M.M., et al., *The interaction between the ER membrane protein UNC93B and TLR3, 7, and 9 is crucial for TLR signaling.* J Cell Biol, 2007. **177**(2): p. 265-75.
119. Casrouge, A., et al., *Herpes simplex virus encephalitis in human UNC-93B deficiency.* Science, 2006. **314**(5797): p. 308-12.
120. Kim, Y.M., et al., *UNC93B1 delivers nucleotide-sensing toll-like receptors to endolysosomes.* Nature, 2008. **452**(7184): p. 234-8.
121. Hacker, H. and M. Karin, *Regulation and function of IKK and IKK-related kinases.* Sci STKE, 2006. **2006**(357): p. re13.
122. Hacker, H., et al., *Specificity in Toll-like receptor signalling through distinct effector functions of TRAF3 and TRAF6.* Nature, 2006. **439**(7073): p. 204-7.
123. Honda, K., et al., *Spatiotemporal regulation of MyD88-IRF-7 signalling for robust type-I interferon induction.* Nature, 2005. **434**(7036): p. 1035-40.
124. Oganesyan, G., et al., *Critical role of TRAF3 in the Toll-like receptor-dependent and -independent antiviral response.* Nature, 2006. **439**(7073): p. 208-11.
125. Tseng, P.H., et al., *Different modes of ubiquitination of the adaptor TRAF3 selectively activate the expression of type I interferons and proinflammatory cytokines.* Nat Immunol, 2010. **11**(1): p. 70-5.
126. Grell, M., et al., *The transmembrane form of tumor necrosis factor is the prime activating ligand of the 80 kDa tumor necrosis factor receptor.* Cell, 1995. **83**(5): p. 793-802.
127. Aversa, G., J. Punnonen, and J.E. de Vries, *The 26-kD transmembrane form of tumor necrosis factor alpha on activated CD4+ T cell clones provides a*

costimulatory signal for human B cell activation. J Exp Med, 1993. **177**(6): p. 1575-85.
128. Lou, J., et al., *Direct cell/cell contact with stimulated T lymphocytes induces the expression of cell adhesion molecules and cytokines by human brain microvascular endothelial cells.* Eur J Immunol, 1996. **26**(12): p. 3107-13.
129. Macchia, D., et al., *In vitro infection with HIV enables human CD4+ T cell clones to induce noncognate contact-dependent polyclonal B cell activation.* J Immunol, 1991. **146**(10): p. 3413-8.
130. Parry, S.L., et al., *Contact with T cells modulates monocyte IL-10 production: role of T cell membrane TNF-alpha.* J Immunol, 1997. **158**(8): p. 3673-81.
131. Schmid, E.F., et al., *Both tumor necrosis factor receptors, TNFR60 and TNFR80, are involved in signaling endothelial tissue factor expression by juxtacrine tumor necrosis factor alpha.* Blood, 1995. **86**(5): p. 1836-41.
132. Xu, J., et al., *Essential role of the TNF-TNFR2 cognate interaction in mouse dendritic cell-natural killer cell crosstalk.* Blood, 2007. **109**(8): p. 3333-41.
133. Aggarwal, B.B., *Signalling pathways of the TNF superfamily: a double-edged sword.* Nat Rev Immunol, 2003. **3**(9): p. 745-56.
134. Aggarwal, B.B., S.C. Gupta, and J.H. Kim, *Historical perspectives on tumor necrosis factor and its superfamily: 25 years later, a golden journey.* Blood, 2012. **119**(3): p. 651-65.
135. Aggarwal, B.B., et al., *Human tumor necrosis factor. Production, purification, and characterization.* J Biol Chem, 1985. **260**(4): p. 2345-54.
136. Faustman, D. and M. Davis, *TNF receptor 2 pathway: drug target for autoimmune diseases.* Nat Rev Drug Discov, 2010. **9**(6): p. 482-93.
137. Bell, J.H., et al., *Role of ADAM17 in the ectodomain shedding of TNF-alpha and its receptors by neutrophils and macrophages.* J Leukoc Biol, 2007. **82**(1): p. 173-6.
138. Black, R.A., et al., *A metalloproteinase disintegrin that releases tumour-necrosis factor-alpha from cells.* Nature, 1997. **385**(6618): p. 729-33.
139. Horiuchi, K., et al., *Cutting edge: TNF-alpha-converting enzyme (TACE/ADAM17) inactivation in mouse myeloid cells prevents lethality from endotoxin shock.* J Immunol, 2007. **179**(5): p. 2686-9.
140. Moss, M.L., et al., *Cloning of a disintegrin metalloproteinase that processes precursor tumour-necrosis factor-alpha.* Nature, 1997. **385**(6618): p. 733-6.
141. Gooz, M., *ADAM-17: the enzyme that does it all.* Crit Rev Biochem Mol Biol, 2010. **45**(2): p. 146-69.
142. Khokha, R., A. Murthy, and A. Weiss, *Metalloproteinases and their natural inhibitors in inflammation and immunity.* Nat Rev Immunol, 2013. **13**(9): p. 649-65.
143. Gonzales, P.E., et al., *Inhibition of the tumor necrosis factor-alpha-converting enzyme by its pro domain.* J Biol Chem, 2004. **279**(30): p. 31638-45.
144. Lee, M.H., et al., *The C-terminal domains of TACE weaken the inhibitory action of N-TIMP-3.* FEBS Lett, 2002. **520**(1-3): p. 102-6.
145. Schlondorff, J., J.D. Becherer, and C.P. Blobel, *Intracellular maturation and localization of the tumour necrosis factor alpha convertase (TACE).* Biochem J, 2000. **347 Pt 1**: p. 131-8.

146. Wisniewska, M., et al., *Structural determinants of the ADAM inhibition by TIMP-3: crystal structure of the TACE-N-TIMP-3 complex.* J Mol Biol, 2008. **381**(5): p. 1307-19.
147. McIlwain, D.R., et al., *iRhom2 regulation of TACE controls TNF-mediated protection against Listeria and responses to LPS.* Science, 2012. **335**(6065): p. 229-32.
148. Freeman, M., *Rhomboid proteases and their biological functions.* Annu Rev Genet, 2008. **42**: p. 191-210.
149. Freeman, M., *Rhomboids: 7 years of a new protease family.* Semin Cell Dev Biol, 2009. **20**(2): p. 231-9.
150. Freeman, M., *Rhomboids, signalling and cell biology.* Biochem Soc Trans, 2016. **44**(3): p. 945-50.
151. Blaydon, D.C., et al., *RHBDF2 mutations are associated with tylosis, a familial esophageal cancer syndrome.* Am J Hum Genet, 2012. **90**(2): p. 340-6.
152. Adrain, C., et al., *Tumor necrosis factor signaling requires iRhom2 to promote trafficking and activation of TACE.* Science, 2012. **335**(6065): p. 225-8.
153. Christova, Y., et al., *Mammalian iRhoms have distinct physiological functions including an essential role in TACE regulation.* EMBO Rep, 2013. **14**(10): p. 884-90.
154. Li, X., et al., *iRhoms 1 and 2 are essential upstream regulators of ADAM17-dependent EGFR signaling.* Proc Natl Acad Sci U S A, 2015. **112**(19): p. 6080-5.
155. Maretzky, T., et al., *iRhom2 controls the substrate selectivity of stimulated ADAM17-dependent ectodomain shedding.* Proc Natl Acad Sci U S A, 2013. **110**(28): p. 11433-8.
156. Trinchieri, G., *Type I interferon: friend or foe?* J Exp Med, 2010. **207**(10): p. 2053-63.
157. Hertzog, P.J. and B.R. Williams, *Fine tuning type I interferon responses.* Cytokine Growth Factor Rev, 2013. **24**(3): p. 217-25.
158. Pestka, S., C.D. Krause, and M.R. Walter, *Interferons, interferon-like cytokines, and their receptors.* Immunol Rev, 2004. **202**: p. 8-32.
159. Goubau, D., S. Deddouche, and C. Reis e Sousa, *Cytosolic sensing of viruses.* Immunity, 2013. **38**(5): p. 855-69.
160. Iwasaki, A., *A virological view of innate immune recognition.* Annu Rev Microbiol, 2012. **66**: p. 177-96.
161. Paludan, S.R. and A.G. Bowie, *Immune sensing of DNA.* Immunity, 2013. **38**(5): p. 870-80.
162. Levy, D.E. and J.E. Darnell, Jr., *Stats: transcriptional control and biological impact.* Nat Rev Mol Cell Biol, 2002. **3**(9): p. 651-62.
163. Stark, G.R. and J.E. Darnell, Jr., *The JAK-STAT pathway at twenty.* Immunity, 2012. **36**(4): p. 503-14.
164. MacMicking, J.D., *Interferon-inducible effector mechanisms in cell-autonomous immunity.* Nat Rev Immunol, 2012. **12**(5): p. 367-82.
165. Rusinova, I., et al., *Interferome v2.0: an updated database of annotated interferon-regulated genes.* Nucleic Acids Res, 2013. **41**(Database issue): p. D1040-6.
166. Schoggins, J.W., et al., *A diverse range of gene products are effectors of the type I interferon antiviral response.* Nature, 2011. **472**(7344): p. 481-5.

167. Yan, N. and Z.J. Chen, *Intrinsic antiviral immunity.* Nat Immunol, 2012. **13**(3): p. 214-22.
168. McNab, F., et al., *Type I interferons in infectious disease.* Nat Rev Immunol, 2015. **15**(2): p. 87-103.
169. Pavlovic, J., O. Haller, and P. Staeheli, *Human and mouse Mx proteins inhibit different steps of the influenza virus multiplication cycle.* J Virol, 1992. **66**(4): p. 2564-9.
170. Price, G.E., A. Gaszewska-Mastarlarz, and D. Moskophidis, *The role of alpha/beta and gamma interferons in development of immunity to influenza A virus in mice.* J Virol, 2000. **74**(9): p. 3996-4003.
171. Tumpey, T.M., et al., *The Mx1 gene protects mice against the pandemic 1918 and highly lethal human H5N1 influenza viruses.* J Virol, 2007. **81**(19): p. 10818-21.
172. Chakrabarti, A., B.K. Jha, and R.H. Silverman, *New insights into the role of RNase L in innate immunity.* J Interferon Cytokine Res, 2011. **31**(1): p. 49-57.
173. Dugan, J.W., et al., *Nucleotide oligomerization domain-2 interacts with 2'-5'-oligoadenylate synthetase type 2 and enhances RNase-L function in THP-1 cells.* Mol Immunol, 2009. **47**(2-3): p. 560-6.
174. Lohofener, J., et al., *The Activation Mechanism of 2'-5'-Oligoadenylate Synthetase Gives New Insights Into OAS/cGAS Triggers of Innate Immunity.* Structure, 2015. **23**(5): p. 851-62.
175. Pindel, A. and A. Sadler, *The role of protein kinase R in the interferon response.* J Interferon Cytokine Res, 2011. **31**(1): p. 59-70.
176. Brass, A.L., et al., *The IFITM proteins mediate cellular resistance to influenza A H1N1 virus, West Nile virus, and dengue virus.* Cell, 2009. **139**(7): p. 1243-54.
177. Sheehy, A.M., et al., *Isolation of a human gene that inhibits HIV-1 infection and is suppressed by the viral Vif protein.* Nature, 2002. **418**(6898): p. 646-50.
178. Daffis, S., et al., *2'-O methylation of the viral mRNA cap evades host restriction by IFIT family members.* Nature, 2010. **468**(7322): p. 452-6.
179. Pichlmair, A., et al., *IFIT1 is an antiviral protein that recognizes 5'-triphosphate RNA.* Nat Immunol, 2011. **12**(7): p. 624-30.
180. Zust, R., et al., *Ribose 2'-O-methylation provides a molecular signature for the distinction of self and non-self mRNA dependent on the RNA sensor Mda5.* Nat Immunol, 2011. **12**(2): p. 137-43.
181. Fernandez-Sesma, A., *The influenza virus NS1 protein: inhibitor of innate and adaptive immunity.* Infect Disord Drug Targets, 2007. **7**(4): p. 336-43.
182. Riegger, D., et al., *The nucleoprotein of newly emerged H7N9 influenza A virus harbors a unique motif conferring resistance to antiviral human MxA.* J Virol, 2015. **89**(4): p. 2241-52.
183. Zimmermann, P., et al., *The viral nucleoprotein determines Mx sensitivity of influenza A viruses.* J Virol, 2011. **85**(16): p. 8133-40.
184. Bach, E.A., M. Aguet, and R.D. Schreiber, *The IFN gamma receptor: a paradigm for cytokine receptor signaling.* Annu Rev Immunol, 1997. **15**: p. 563-91.
185. Hemmi, S., et al., *A novel member of the interferon receptor family complements functionality of the murine interferon gamma receptor in human cells.* Cell, 1994. **76**(5): p. 803-10.

186. Pestka, S., et al., *Interferons and their actions.* Annu Rev Biochem, 1987. **56**: p. 727-77.
187. Soh, J., et al., *Identification and sequence of an accessory factor required for activation of the human interferon gamma receptor.* Cell, 1994. **76**(5): p. 793-802.
188. Stark, G.R., et al., *How cells respond to interferons.* Annu Rev Biochem, 1998. **67**: p. 227-64.
189. Donnelly, R.P., et al., *The expanded family of class II cytokines that share the IL-10 receptor-2 (IL-10R2) chain.* J Leukoc Biol, 2004. **76**(2): p. 314-21.
190. Kotenko, S.V., et al., *IFN-lambdas mediate antiviral protection through a distinct class II cytokine receptor complex.* Nat Immunol, 2003. **4**(1): p. 69-77.
191. Taniguchi, T., et al., *IRF family of transcription factors as regulators of host defense.* Annu Rev Immunol, 2001. **19**: p. 623-55.
192. Savitsky, D., et al., *Regulation of immunity and oncogenesis by the IRF transcription factor family.* Cancer Immunol Immunother, 2010. **59**(4): p. 489-510.
193. Ning, S., J.S. Pagano, and G.N. Barber, *IRF7: activation, regulation, modification and function.* Genes Immun, 2011. **12**(6): p. 399-414.
194. Tamura, T., et al., *The IRF family transcription factors in immunity and oncogenesis.* Annu Rev Immunol, 2008. **26**: p. 535-84.
195. Nehyba, J., et al., *A novel interferon regulatory factor (IRF), IRF-10, has a unique role in immune defense and is induced by the v-Rel oncoprotein.* Mol Cell Biol, 2002. **22**(11): p. 3942-57.
196. Chen, W. and W.E. Royer, Jr., *Structural insights into interferon regulatory factor activation.* Cell Signal, 2010. **22**(6): p. 883-7.
197. Hiscott, J., *Triggering the innate antiviral response through IRF-3 activation.* J Biol Chem, 2007. **282**(21): p. 15325-9.
198. Takaoka, A., T. Tamura, and T. Taniguchi, *Interferon regulatory factor family of transcription factors and regulation of oncogenesis.* Cancer Sci, 2008. **99**(3): p. 467-78.
199. Gabriele, L. and K. Ozato, *The role of the interferon regulatory factor (IRF) family in dendritic cell development and function.* Cytokine Growth Factor Rev, 2007. **18**(5-6): p. 503-10.
200. Matsuyama, T., et al., *Targeted disruption of IRF-1 or IRF-2 results in abnormal type I IFN gene induction and aberrant lymphocyte development.* Cell, 1993. **75**(1): p. 83-97.
201. Honda, K., et al., *IRF-7 is the master regulator of type-I interferon-dependent immune responses.* Nature, 2005. **434**(7034): p. 772-7.
202. Lin, R., et al., *Virus-dependent phosphorylation of the IRF-3 transcription factor regulates nuclear translocation, transactivation potential, and proteasome-mediated degradation.* Mol Cell Biol, 1998. **18**(5): p. 2986-96.
203. Mori, M., et al., *Identification of Ser-386 of interferon regulatory factor 3 as critical target for inducible phosphorylation that determines activation.* J Biol Chem, 2004. **279**(11): p. 9698-702.
204. Panne, D., et al., *Interferon regulatory factor 3 is regulated by a dual phosphorylation-dependent switch.* J Biol Chem, 2007. **282**(31): p. 22816-22.

205. Suhara, W., et al., *Analyses of virus-induced homomeric and heteromeric protein associations between IRF-3 and coactivator CBP/p300.* J Biochem, 2000. 128(2): p. 301-7.
206. Fitzgerald, K.A., et al., *IKKepsilon and TBK1 are essential components of the IRF3 signaling pathway.* Nat Immunol, 2003. **4**(5): p. 491-6.
207. Hemmi, H., et al., *The roles of two IkappaB kinase-related kinases in lipopolysaccharide and double stranded RNA signaling and viral infection.* J Exp Med, 2004. **199**(12): p. 1641-50.
208. Perry, A.K., et al., *Differential requirement for TANK-binding kinase-1 in type I interferon responses to toll-like receptor activation and viral infection.* J Exp Med, 2004. **199**(12): p. 1651-8.
209. Sharma, S., et al., *Triggering the interferon antiviral response through an IKK-related pathway.* Science, 2003. **300**(5622): p. 1148-51.
210. Erlandsson, L., et al., *Interferon-beta is required for interferon-alpha production in mouse fibroblasts.* Curr Biol, 1998. **8**(4): p. 223-6.
211. Sato, M., et al., *Distinct and essential roles of transcription factors IRF-3 and IRF-7 in response to viruses for IFN-alpha/beta gene induction.* Immunity, 2000. **13**(4): p. 539-48.
212. Taniguchi, T. and A. Takaoka, *The interferon-alpha/beta system in antiviral responses: a multimodal machinery of gene regulation by the IRF family of transcription factors.* Curr Opin Immunol, 2002. **14**(1): p. 111-6.
213. Janeway, C.A., Jr. and R. Medzhitov, *Innate immune recognition.* Annu Rev Immunol, 2002. **20**: p. 197-216.
214. O'Neill, L.A. and A.G. Bowie, *The family of five: TIR-domain-containing adaptors in Toll-like receptor signalling.* Nat Rev Immunol, 2007. **7**(5): p. 353-64.
215. O'Neill, L.A., K.A. Fitzgerald, and A.G. Bowie, *The Toll-IL-1 receptor adaptor family grows to five members.* Trends Immunol, 2003. **24**(6): p. 286-90.
216. Uematsu, S., et al., *Interleukin-1 receptor-associated kinase-1 plays an essential role for Toll-like receptor (TLR)7- and TLR9-mediated interferon-{alpha} induction.* J Exp Med, 2005. **201**(6): p. 915-23.
217. Oshiumi, H., et al., *TICAM-1, an adaptor molecule that participates in Toll-like receptor 3-mediated interferon-beta induction.* Nat Immunol, 2003. **4**(2): p. 161-7.
218. Kawai, T., et al., *Interferon-alpha induction through Toll-like receptors involves a direct interaction of IRF7 with MyD88 and TRAF6.* Nat Immunol, 2004. **5**(10): p. 1061-8.
219. Fitzgerald, K.A., et al., *Mal (MyD88-adapter-like) is required for Toll-like receptor-4 signal transduction.* Nature, 2001. **413**(6851): p. 78-83.
220. Duan, H. and V.M. Dixit, *RAIDD is a new 'death' adaptor molecule.* Nature, 1997. **385**(6611): p. 86-9.
221. Shearwin-Whyatt, L.M., N.L. Harvey, and S. Kumar, *Subcellular localization and CARD-dependent oligomerization of the death adaptor RAIDD.* Cell Death Differ, 2000. **7**(2): p. 155-65.
222. Berube, C., et al., *Apoptosis caused by p53-induced protein with death domain (PIDD) depends on the death adapter protein RAIDD.* Proc Natl Acad Sci U S A, 2005. **102**(40): p. 14314-20.

223. Lin, Q., et al., *Cutting edge: the "death" adaptor CRADD/RAIDD targets BCL10 and suppresses agonist-induced cytokine expression in T lymphocytes.* J Immunol, 2012. **188**(6): p. 2493-7.
224. Manzl, C., et al., *Caspase-2 activation in the absence of PIDDosome formation.* J Cell Biol, 2009. **185**(2): p. 291-303.
225. Tu, S., et al., *In situ trapping of activated initiator caspases reveals a role for caspase-2 in heat shock-induced apoptosis.* Nat Cell Biol, 2006. **8**(1): p. 72-7.
226. Xue, L., et al., *iRhoms 1 and 2 are essential upstream regulators of ADAM17-dependent EGFR signaling.* Proc Natl Acad Sci U S A, 2015. **(In Press)**.
227. van Pesch, V. and T. Michiels, *Characterization of interferon-alpha 13, a novel constitutive murine interferon-alpha subtype.* J Biol Chem, 2003. **278**(47): p. 46321-8.
228. Vercammen, D., et al., *Inhibition of caspases increases the sensitivity of L929 cells to necrosis mediated by tumor necrosis factor.* J Exp Med, 1998. **187**(9): p. 1477-85.
229. Tsujimoto, M., Y.K. Yip, and J. Vilcek, *Tumor necrosis factor: specific binding and internalization in sensitive and resistant cells.* Proc Natl Acad Sci U S A, 1985. **82**(22): p. 7626-30.
230. Vanlangenakker, N., et al., *TNF-induced necroptosis in L929 cells is tightly regulated by multiple TNFR1 complex I and II members.* Cell Death Dis, 2011. **2**: p. e230.
231. Bhattacharya, D., et al., *Identification of gene function by cyclical packaging rescue of retroviral cDNA libraries.* Proc Natl Acad Sci U S A, 2002. **99**(13): p. 8838-43.
232. Irmler, M., et al., *Inhibition of death receptor signals by cellular FLIP.* Nature, 1997. **388**(6638): p. 190-5.
233. Hosur, V., et al., *Rhbdf2 mutations increase its protein stability and drive EGFR hyperactivation through enhanced secretion of amphiregulin.* Proc Natl Acad Sci U S A, 2014. **111**(21): p. E2200-9.
234. Liu, B., et al., *Proteomic analysis of differentially expressed skin proteins in iRhom2(Uncv) mice.* BMB Rep, 2015. **48**(1): p. 19-24.
235. Siggs, O.M., et al., *Genetic interaction implicates iRhom2 in the regulation of EGF receptor signalling in mice.* Biol Open, 2014. **3**(12): p. 1151-7.
236. Azijli, K., et al., *Non-canonical kinase signaling by the death ligand TRAIL in cancer cells: discord in the death receptor family.* Cell Death Differ, 2013. **20**(7): p. 858-68.
237. Kearney, C.J., et al., *Necroptosis suppresses inflammation via termination of TNF- or LPS-induced cytokine and chemokine production.* Cell Death Differ, 2015.
238. McIlwain, D.R., T. Berger, and T.W. Mak, *Caspase functions in cell death and disease.* Cold Spring Harb Perspect Biol, 2013. **5**(4): p. a008656.
239. Strelow, A., et al., *Overexpression of acid ceramidase protects from tumor necrosis factor-induced cell death.* J Exp Med, 2000. **192**(5): p. 601-12.
240. Legler, D.F., et al., *Recruitment of TNF receptor 1 to lipid rafts is essential for TNFalpha-mediated NF-kappaB activation.* Immunity, 2003. **18**(5): p. 655-64.

241. Micheau, O. and J. Tschopp, *Induction of TNF receptor I-mediated apoptosis via two sequential signaling complexes.* Cell, 2003. **114**(2): p. 181-90.
242. Peschon, J.J., et al., *An essential role for ectodomain shedding in mammalian development.* Science, 1998. **282**(5392): p. 1281-4.
243. Reddy, P., et al., *Functional analysis of the domain structure of tumor necrosis factor-alpha converting enzyme.* J Biol Chem, 2000. **275**(19): p. 14608-14.
244. Siggs, O.M., et al., *iRhom2 is required for the secretion of mouse TNFalpha.* Blood, 2012. **119**(24): p. 5769-71.
245. Le Gall, S.M., et al., *ADAM17 is regulated by a rapid and reversible mechanism that controls access to its catalytic site.* J Cell Sci, 2010. **123**(Pt 22): p. 3913-22.
246. Maretzky, T., et al., *Migration of growth factor-stimulated epithelial and endothelial cells depends on EGFR transactivation by ADAM17.* Nat Commun, 2011. **2**: p. 229.
247. Saarinen, S., et al., *Analysis of a Finnish family confirms RHBDF2 mutations as the underlying factor in tylosis with esophageal cancer.* Fam Cancer, 2012. **11**(3): p. 525-8.
248. Brooke, M.A., et al., *iRHOM2-dependent regulation of ADAM17 in cutaneous disease and epidermal barrier function.* Hum Mol Genet, 2014. **23**(15): p. 4064-76.
249. Kawai, T. and S. Akira, *Toll-like receptors and their crosstalk with other innate receptors in infection and immunity.* Immunity, 2011. **34**(5): p. 637-50.
250. Alexopoulou, L., et al., *Recognition of double-stranded RNA and activation of NF-kappaB by Toll-like receptor 3.* Nature, 2001. **413**(6857): p. 732-8.
251. Lee, M.S., et al., *OASL1 inhibits translation of the type I interferon-regulating transcription factor IRF7.* Nat Immunol, 2013. **14**(4): p. 346-55.
252. Siednienko, J., et al., *Pellino3 targets the IRF7 pathway and facilitates autoregulation of TLR3- and viral-induced expression of type I interferons.* Nat Immunol, 2012. **13**(11): p. 1055-62.
253. Nitoiu, D., S.L. Etheridge, and D.P. Kelsell, *Insights into desmosome biology from inherited human skin disease and cardiocutaneous syndromes.* Cell Commun Adhes, 2014. **21**(3): p. 129-40.
254. Hirsch, F.R., M. Varella-Garcia, and F. Cappuzzo, *Predictive value of EGFR and HER2 overexpression in advanced non-small-cell lung cancer.* Oncogene, 2009. **28 Suppl 1**: p. S32-7.
255. Mochizuki, S. and Y. Okada, *ADAMs in cancer cell proliferation and progression.* Cancer Sci, 2007. **98**(5): p. 621-8.
256. Leilei, Y., et al., *iRhom2 mutation leads to aberrant hair follicle differentiation in mice.* PLoS One, 2014. **9**(12): p. e115114.
257. Doedens, J.R. and R.A. Black, *Stimulation-induced down-regulation of tumor necrosis factor-alpha converting enzyme.* J Biol Chem, 2000. **275**(19): p. 14598-607.
258. Brenner D, Blaser H, Mak TW. Regulation of tumour necrosis factor signalling: live or let die. *Nature reviews Immunology* 2015, **15**(6)**:** 362-374.
259. Adrain C, Freeman M. New lives for old: evolution of pseudoenzyme function illustrated by iRhoms. Nature reviews Molecular cell biology 2012, 13(8): 489-498.

260. Park HH, Lo YC, Lin SC, Wang L, Yang JK, Wu H. The death domain superfamily in intracellular signaling of apoptosis and inflammation. Annual review of immunology 2007, 25: 561-586.
261. Hu S, Vincenz C, Buller M, Dixit VM. A novel family of viral death effector domain-containing molecules that inhibit both CD-95- and tumor necrosis factor receptor-1-induced apoptosis. *The Journal of biological chemistry* 1997, **272**(15)**:** 9621-9624.
262. Fitzgerald KA, Chen ZJ. Sorting out Toll signals. *Cell* 2006, **125**(5)**:** 834-836.
263. Johnston JB, Barrett JW, Nazarian SH, Goodwin M, Ricciuto D, Wang G*, et al.* A poxvirus-encoded pyrin domain protein interacts with ASC-1 to inhibit host inflammatory and apoptotic responses to infection. *Immunity* 2005, **23**(6)**:** 587-598.
264. Chen ZJ. Ubiquitin signalling in the NF-kappaB pathway. *Nature cell biology* 2005, **7**(8)**:** 758-765.
265. Lemaitre B, Nicolas E, Michaut L, Reichhart JM, Hoffmann JA. The dorsoventral regulatory gene cassette spatzle/Toll/cactus controls the potent antifungal response in Drosophila adults. *Cell* 1996, **86**(6)**:** 973-983.
266. Sun H, Bristow BN, Qu G, Wasserman SA. A heterotrimeric death domain complex in Toll signaling. *Proceedings of the National Academy of Sciences of the United States of America* 2002, **99**(20)**:** 12871-12876.
267. Letsou A, Alexander S, Orth K, Wasserman SA. Genetic and molecular characterization of tube, a Drosophila gene maternally required for embryonic dorsoventral polarity. *Proceedings of the National Academy of Sciences of the United States of America* 1991, **88**(3)**:** 810-814.
268. Peintner L, Dorstyn L, Kumar S, Aneichyk T, Villunger A, Manzl C. The tumor-modulatory effects of Caspase-2 and Pidd1 do not require the scaffold protein Raidd. *Cell death and differentiation* 2015, **22**(11)**:** 1803-1811.
269. Qiao H, Liu Y, Veach RA, Wylezinski L, Hawiger J. The adaptor CRADD/RAIDD controls activation of endothelial cells by proinflammatory stimuli. *The Journal of biological chemistry* 2014, **289**(32)**:** 21973-21983.
270 Barbalat R, Lau L, Locksley RM, Barton GM. Toll-like receptor 2 on inflammatory monocytes induces type I interferon in response to viral but not bacterial ligands. *Nature immunology* 2009, **10**(11)**:** 1200-1207.
271. Dietrich N, Lienenklaus S, Weiss S, Gekara NO. Murine toll-like receptor 2 activation induces type I interferon responses from endolysosomal compartments. *PloS one* 2010, **5**(4)**:** e10250.
272. Martinez J, Huang X, Yang Y. Toll-like receptor 8-mediated activation of murine plasmacytoid dendritic cells by vaccinia viral DNA. *Proceedings of the National Academy of Sciences of the United States of America* 2010, **107**(14)**:** 6442-6447.
273. You F, Wang P, Yang L, Yang G, Zhao YO, Qian F*, et al.* ELF4 is critical for induction of type I interferon and the host antiviral response. *Nature immunology* 2013, **14**(12)**:** 1237-1246.